HHS Public Access

Author manuscript

Adv Drug Deliv Rev. Author manuscript; available in PMC 2023 January 01.

Published in final edited form as:

Adv Drug Deliv Rev. 2022 January ; 180: 114043. doi:10.1016/j.addr.2021.114043.

Towards controlled drug delivery in brain tumors with microbubble-enhanced focused ultrasound

Scott Schoen Jr[1], **M. Sait Kilinc**[2], **Hohyun Lee**[1], **Yutong Guo**[1], **F. Levent Degertekin**[1], **Graeme F. Woodworth**[3,4,5], **Costas Arvanitis**[1,6]

[1]Woodruff School of Mechanical Engineering, Georgia Institute of Technology, Atlanta, GA 30332, USA

[2]School of Electrical and Computer Engineering, Georgia Institute of Technology, Atlanta, GA 30332, USA

[3]Department of Neurosurgery, University of Maryland School of Medicine, Baltimore, MD 21201, USA

[4]Department of Diagnostic Radiology and Nuclear Medicine, University of Maryland School of Medicine, College Park, MD 20742, USA

[5]Fischell Department of Bioengineering A. James Clarke School of Engineering, University of Maryland

[6]Coulter Department of Biomedical Engineering, Georgia Institute of Technology and Emory University, Atlanta, GA 30332, USA

Abstract

Brain tumors are particularly challenging malignancies, due to their location in a structurally and functionally distinct part of the human body – the central nervous system (CNS). The CNS is separated and protected by a unique system of brain and blood vessel cells which together prevent most bloodborne therapeutics from entering the brain tumor microenvironment (TME). Recently, great strides have been made through microbubble (MB) ultrasound contrast agents in conjunction with ultrasound energy to locally increase the permeability of brain vessels and modulate the brain TME. As we elaborate in this review, this physical method can effectively deliver a wide range of anticancer agents, including chemotherapeutics, antibodies, and nanoparticle drug conjugates across a range of preclinical brain tumors, including high grade glioma (glioblastoma), diffuse intrinsic pontine gliomas, and brain metastasis. Moreover, recent evidence suggests that this technology can promote the effective delivery of novel immunotherapeutic agents, including, immune check-point inhibitors and chimeric antigen receptor T cells, among others. With early clinical studies demonstrating safety and several Phase I/II trials testing the preclinical findings underway this technology is making firm steps towards shaping the future treatments of primary and metastatic brain cancer. By elaborating on its key components, including ultrasound systems

and MB technology along with methods for closed-loop spatial and temporal control of MB activity, we highlight how this technology can be tuned to enable new, personalized treatment strategies for primary brain malignancies and brain metastases.

Introduction

Brain tumors, including glioblastoma (GBM) – one of the most fatal forms, are among the most difficult to treat of all human tumors. While the reasons for these dismal outcomes are several, effective delivery of bloodborne drugs remains a major challenge. For effective delivery, the anticancer agent must cross the neurovascular unit (NVU), composed of a complex system of endothelial and brain cells (glia/microglia, pericytes, and neurons) [1,2], traffic through the dense extracellular matrix, avoid clearance, and be taken up by the cancer cells. The NVU functions to establish the blood brain barrier (BBB), which controls the transport of most agents and entities into and out of the central nervous system (CNS). Although the vasculature in most brain tumors is abnormally leaky and is frequently characterized by fenestrated or compromised endothelial cells and tight junctions (referred to as blood tumor barrier or BTB), its permeability is highly heterogeneous, and is occasionally similar to healthy brain [3,4]. As such, it is often considered a rate-limiting factor to the delivery of both small and large molecular weight anticancer agents in brain tumors [5,6]. Furthermore, malignant cells often invade into surrounding functional brain regions with an intact BBB [7], which shields them from treatment.

Beyond the vascular barriers, the tumor interstitial fluid pressure (although not as high in intracranial malignancies [8]) may impede (convective) mass transport across the vessel wall and into the interstitial space by diminishing the pressure gradients that mediate the flow from the blood into the tumor core. Apart from the physical barriers to bulk transport, changes in the function of the dynamic influx/efflux transporter system, which plays a key role in mediating drug resistance, at the vessel's luminal surface and cancer cell membrane may oppose both drug (i.e., chemotherapy) extravasation and cancer cell uptake [9]. Despite progress, these barriers that consistently hinder clinically effective treatment against primary brain malignancies and brain metastases [10–12], underscore the need for more robust drug delivery strategies and systems.

Low-intensity focused ultrasound (FUS) combined with ultrasound contrast agents called microbubbles (MBs) provides a physical method to transiently modulate the brain TME and NVU and improve the delivery of anticancer agents in the brain [13–15]. Beyond demonstrating safety and efficacy of MB-enhanced FUS (MB-FUS) drug combinations in the preclinical setting and establishing safety in the clinical setting, the rapid expansion of this technology is facilitated by numerous technological innovations including reliable MB formulations, ultrasound systems tailored for brain applications and novel methods to monitor and locally control the cerebrovascular MB dynamics. The integration of such innovations opens the possibility to make MB-FUS technology completely "tunable" and creates unique opportunities for targeted drug delivery with novel therapeutic agents. Beyond targeted drug delivery, this technology through the application of localized mechanical stress is offering the unique opportunity to modulate the immune tumor

microenvironment and improve immunotherapeutic trafficking and convert immunologically "cold" tumors into immunologically "hot" ones that are prone to generate prolonged anti-tumor immune responses [16].

In this review, we first assess the state of pre-clinical and clinical work towards leveraging MB-FUS to enhance drug delivery to brain tumors. Next, we discuss progress on the technical advancements underlying these applications, namely: the systems and the methods for accurate localization of the US beam into the brain and the technology for monitoring and controlling MB activity to ensure safe and effective drug delivery. Finally, we discuss future perspectives, including the combination of this technology with immunotherapy and how it might enhance liquid biopsy techniques for treatment monitoring and lead to improved outcomes in the therapeutically challenging brain tumors. To facilitate the reader, we provide the definitions of key terms in Box 1.

In this review, we will not discuss extensively the structure and function of the NVU and how tumor progression may affect the BBB; for detailed discussion on this topic, we refer the reader to a recent review by Arvanitis et al. [5]. Likewise, for detailed literature review in the numerous minimally invasive and noninvasive methods for drug delivery in brain tumors, we refer the reader to recent comprehensive reviews on the topic [5,17]. Similarly, for detailed discussion of MB-FUS BBB opening in healthy or diseased brains (beyond cancer), including FUS parameter optimization and safety studies we direct the reader to other reviews on the topic [13,18–20]. Herein, we will briefly review the key interactions of MB-FUS with the NVU to facilitate discussion for their implications on brain cancer therapy. Finally, given that ultrasound and MB physics and biophysics are large topics that span several decades of intense research [13,21], here we will focus on research that is primarily related to therapeutic delivery in brain tumors.

Microbubble-enhanced ultrasound targeted drug delivery in tumors

Encapsulated MBs are stabilized gas bubbles whose diameters are typically 1 to 4.5 μm and are typically administered by intravenous injection of 10-300 μL/kg of body weight (for the studies summarized in Table 1), with injection concentration of 10^7-10^9 MBs/ml. They were originally developed as vascular contrast agents to improve the acoustic contrast in diagnostic imaging [22,23]. However, when subjected to incident ultrasound bursts, these tiny gas-filled bubbles undergo high frequency vibrations (expand in peak negative and contract in peak positive pressures) that exert upon the cells that comprise the NVU circumferential or shear stresses (stretch, pull, or perturb; Figure 1). Cellular and molecular evidence suggests that these physical interactions can promote paracellular transport via transient reorganization of the tight junctions [24–27] and facilitate transcellular passage through vesicle (caveolae) transport [28,29]. When the ultrasound beam is focused, these changes in the NVU structure and function are localized in the focal region and can lead to a local increase in the vascular permeability for up to 24 hours post sonication [13,15,18], providing a window for targeted drug delivery in both space (focal region) and time (up to 24 hours), while allowing physiological brain function to resume thereafter [13]. Moreover, the sonications can be repeated numerous times over a long period without any apparent functional deficit and deliver agents to both white and grey matter structures [30].

Although at higher pressures (i.e., mechanical index near 0.5; Box 1), where MB oscillation becomes more potent at disrupting the BBB, MB collapse (inertial cavitation) that can lead to more abrupt changes in vessel wall porosity and microhemorrhage is also possible. While MB collapse can led to dramatic changes in NVU structure and function [31,32], several investigations have demonstrated that MB type, dose, and exposure settings can be optimized to limit undesired effects while tuning and controlling BBB opening [33–38].

These findings supported the assessment of this physical and tunable method to open the BBB/BTB in a range of brain tumors, including high grade glioma (GBM), gliosarcoma, diffuse intrinsic pontine gliomas (DIPG), medulloblastoma, and melanoma and breast brain metastasis, as well as deliver a wide range of anticancer agents, including chemotherapeutics, antibodies, nanoparticle drug conjugates, and viruses. Below and in Tables 1 and 2, we summarize the preclinical and clinical investigations to date, highlight the main findings, and discuss the challenges in attaining clinically effective drug delivery in primary and metastatic brain tumors. To summarize quantitatively current preclinical findings, we analyzed the fold increase in the delivery of anticancer agents and the percentage increase in median survival time (IST) as compared to drug-only treatments reported in the literature. The specific values used in our analysis are provided in Suppl. Table 1. While our analysis exclude cell-based therapeutics [39,40], this very promising therapeutic strategys is discussed separately at the end of this review (Perspectives section).

Preclinical investigations

Chemotherapy: Chemotherapy is currently a component of the standard of care for many tumors, including brain tumors. As such, chemotherapies are often the first drug class to be tested with any new drug delivery technology. The delivery of small molecular weight (194 – 690 Da; $\ll$ 1 nm) chemotherapeutic agents in the brain tumor microenvironment (TME) was found to be on average 3.9-fold (Median: 3.5-fold) higher under MB-FUS conditions (Figure 2; see also Suppl. Table 1). This improvement in delivery, which is substantial and has been demonstrated across a range of brain tumor models, has resulted in approximately 30% increase in median survival compared to chemotherapy treatment alone. Interestingly, larger molecules (> 400 Da) and higher doses provide better results [41,42], presumably due to the higher differential impact of the BBB/BTB opening on their transport and the higher drug penetration associated with the steeper drug gradients attained by the higher circulating dose (i.e., diffusive transport) [43].

While 30% IST can be significant in the clinical setting, a major challenge with chemotherapeutics, beyond their significant toxicities, is their rapid pharmacokinetics, which results in rapid clearance from the circulation and, subsequently, limited exposure for cancer cells. Although slower drug infusions and alternative dosing schemes can potentially mitigate this challenge, chemotherapy clearance from the TME can be augmented by drug efflux transporters, such as the Permeability-glycoprotein (Pgp), that can be over expressed on the BBB and cancer cell membrane as part of drug resistance mechanisms [5]. Interestingly, recent investigations suggested that MB-FUS can temporarily suppress Pgp expression in the vasculature of healthy mice, potentially providing an additional mechanism by which MB-FUS could enhance chemotherapy effects in brain tumors [44]. However,

other studies, also in the healthy brain (rat), demonstrated that the efflux transport of erlotinib, a small molecule tyrosine kinase inhibitor, persisted despite FUS-mediated BBB opening [45]. Further research is needed to determine whether the reported changes in the function of efflux transporters in the brain TME under MB-FUS are sufficiently strong to lead to meaningful increase in drug retention. Moreover, more detailed assessment of different drug administration protocols (e.g., bolus vs infusion) and drug combinations (e.g., with efflux transporter inhibitors targeting cancer cells [46]) are needed in order to refine current therapeutic strategies and inform the design of ongoing and new clinical investigations.

Antibody: Antibodies (Abs) provide a highly potent therapeutic technology with comparatively low toxicity profile [47,48]. With MB-FUS, an average 2.7-fold increase in Ab delivery (Median: 2-fold) has been reported for both primary and metastatic brain tumor models. Despite the smaller improvement in delivery compared to small molecular weight chemotherapies, the average increase in median survival with MB-FUS treatment across different tumor models is substantial (~32%) as compared to Ab delivery alone. While these findings highlight the potential of MB-FUS in combination with Abs to improve delivery and outcomes, recent investigations indicate that the improvement in the delivery of trastuzumab emtansine, a chemotherapy Ab conjugate, in a human $HER2^+$ (BT474) breast metastasis mice model, diminishes five days after administration [43]. This is possibly due to the Ab's long circulation time (5 days half-life) that surpasses by more than five-fold the expected duration of BBB opening post- sonication (up to 24 hours).

In recognition of the potential implications of Abs's long half-life in tumor accumulation, Kobus et al. hypothesized that multiple sonications (one per day for five days) can enhance the delivery of pertuzumab and bevacizumab and improve outcomes in human $HER2^+$ (MDA-MB-361) breast metastasis mice model [49]. Despite the use of a tumor model displaying low vascular permeability, the investigators observed no improvement in survival as compared to Abs only group. Unfortunately, the Abs delivery was not reported in this study, so it is not clear if the poor outcomes are related to the delivery, or to the *in vivo* effectiveness of these Abs in this tumor model. Interestingly and potentially counterintuitively, other investigations demonstrated improved anti-CD47 monoclonal Ab uptake in glioma-bearing (GL261) mice when it was administrated after the sonication (as compared to both post sonication and Ab only group) [50]. Likewise, recent investigations using fluorescently labeled anti-PD1 Ab observed enhanced and localized delivery to brain parenchyma, which was further enhanced with an additional sonication treatment performed immediately after the initial sonication, potentially supporting the above hypothesis [51]. Of note is that both antibodies target (or are believed to target) the microglia and both studies demonstrated that the improved delivery led to markedly improved survival [52,53]. While these findings are promising, better understanding of Ab penetration across the BBB and uptake from stromal and cancer cells following different sonication schemes and conditions and possibly different tumor models are needed to establish optimal treatment protocols and further support the evaluation of therapeutic Ab combinations with MB-FUS in the clinic.

Nanoparticle Drug Conjugates: While the improved drug delivery in brain TME under MB-FUS is primarily attributed to transient changes in the BBB permeability [13], recent studies have alluded to the ability of MB-FUS to also increase the interstitial fluid flow [43,54]. These observations both explained and underscored the potential of MB-FUS to improve the delivery of therapeutic nanoparticles (NPs) (i.e., driven by convective transport) across a range of brain tumor models. To date, on average 6.2-fold increase in NP and/or cargo delivery (Median: 3.7-fold) has been attained. This substantial improvement in delivery (highest among all anticancer agents) leads in approximately 37% increase in median survival. With NP administration before the sonication [55], closed-loop (sonication) control methods (see Real-time Control of Microbubble Dynamics that will take into account the impulse response function of the receivers, in addition to absolute calibration methods, will likely be critical moving forward.

Real-time Control of Microbubble Dynamics) [56], and nanoparticles in the range of 50 nm [57,58], resulting in the most robust delivery. While most studies have employed anionic NPs (−25 mV to −5 mV surface charge), recent investigations have suggested that cationic nanoparticles (~10 mV surface charge; 50 nm in size) can lead to increased NP delivery (10-fold or higher) and attain both high cancer cell uptake (60% of the delivered NPs) and payload delivery, in this case an siRNA targeting the smoothened activated sonic hedgehog subgroup of medulloblastoma [58].

Although the above findings are encouraging, it is important going forward to assess the NP and cargo delivery in absolute terms or as a fraction of the administered dose. Attaining delivery in the brain TME higher than 1% of the total dose is a reasonable benchmark for refining formulation designs and accelerating translation to the clinic [59]. Likewise, systems and methods to track the NP biodistributions, kinetics and their cargo during the sonication combined with methods to monitor the MB dynamics may reveal new treatment strategies, in addition to helping refine our understanding on the role of stable MB oscillation on NP delivery in the brain TME [43,60].

Magnetic Nanoparticle Drug Conjugates: NP magnetic actuation in combination with MB-FUS aims to improve both NP retention and penetration in the brain TME [61–63]. Although this approach has led to an average of 2.3-fold increase in NP delivery in different tumor models in rodents as compared to MB-FUS alone (Table 1), scaling it up might be challenging, as attaining strong magnetic fields deep in the brain, which is critical for exerting significant forces to small NPs (<50 nm), might be challenging. Despite these challenges the potential of this method to improve NP delivery in cortical tumors, including pediatric tumors, remains untapped.

Microbubble Drug Conjugates: This approach aims to combine targeted BBB opening with triggered drug release to improve drug delivery in the brain TME. While current findings are promising, the fast bubble kinetics (a few minutes) and the requirement to burst the bubble to release its cargo might affect the efficacy and safety, respectively, of this approach. Despite these concerns, this strategy has been shown to provide unique opportunities for delivering anti-angiogenic drugs in the brain TME and modulating the BBB phenotype [95,101].

Virus: While only a small number of studies have been performed in this direction, demonstrating on average 2.6-fold improvement in delivery [99,100], the increasing potential of viral therapy in mediating anticancer immunity [102], combined with the limited bioavailability of the virus in the brain TME, creates unique opportunities for synergies with MB-FUS. MB-FUS may also help address tradeoffs between virus size, which dictates its ability to accommodate larger transgenes [103], and its penetration across the BBB/BTB and into the TME.

Clinical investigations

In recognition of the potential impact of MB-FUS to improve the uptake and penetration of drugs in the brain and brain TME, multiple clinical trials have been initiated (Table 2). These clinical investigations have already demonstrated the safety and feasibility of MB-FUS across different centers and for different devices [104–106], supporting the application of this technology in combination with anticancer agents for the treatment of primary and metastatic brain tumors.

For the treatment of GBM, which is a tumor with urgent need for new treatments [107], MB-FUS has been combined with the current standard of care chemotherapy, temozolomide (TMZ). While the preclinical data revealed equivocal results with this combination [68,70] and dose-intensified TMZ protocols (without FUS) did not provide significant benefit in survival [108–112] (i.e., suggesting that the limited efficacy is not due to limited delivery), this combination coupled with information from surgical studies and analyses of molecules in the tumor is already generating important data to further assess safety and move from proof of principle investigations to clinically relevant treatment protocols [113].

An established chemotherapeutic agent that is not frequently used to treat brain tumors, but has supportive preclinical data for treating GBM, is carboplatin. Current Phase I/II clinical trials are establishing the safety of carboplatin combined with MB-FUS in patient with recurrent GBM and also provide early evidence of therapeutic efficacy [42,114]. This combination may also reveal if MB-FUS can re-purpose drugs with unfavorable PK/PD profiles. Albumin-bound paclitaxel (Abraxane) is another FDA approved anti-cancer drug that falls in this category partly due to its high toxicity and low penetration across the BBB/BTB [90]. Currently, Abraxane is being evaluated in a Phase I/II clinical trial with MB-FUS in recurrent GBM patients. Of note, the preclinical investigations of Abraxane plus MB-FUS did not demonstrate substantial improvement in survival [90], however the investigators posited that the BBB/BTB in the preclinical animal models used did not represent (i.e., they are leakier) the human BBB/BTB and anticipate that the combination will lead to high differential effect in clinical trials.

Several investigations are also looking to assess the ability of MB-FUS to improve the delivery of Abs and other drugs in the setting of metastatic brain tumors. While MB-FUS may certainly have a variety of potentially beneficial therapeutic effects in the context of brain metastasis, the impact of MB-FUS on BBB permeability is less clear. This is because brain metastases (i.e., even very small tumors) have a leaky BBB/BTB, which can be visualized early in their growth using contrast enhanced MRI, implying that the differential

effect of this combination might be less pronounced. However, the relationship between contrast enhanced MRI and Abs permeability still needs to be investigated in more detail.

Finally, fueled by promising preclinical studies [74], several investigators are planning to combine MB-FUS with current and new drugs for the treatment of the notoriously treatment-resistant pediatric brain tumor, diffuse intrinsic pontine glioma (DIPG). DIPG is characterized by highly infiltrative tumor cells within eloquent brain regions and minimal BBB/BTB leakiness. This constellation of features drastically lowers the therapeutic ratio for most agents and points to a clear need for new treatment strategies.

Moving forward, it will be important to quantify changes in serum-to-brain drug ratios or changes in brain concentration of drugs following MB-FUS, in addition to the overall goal of assessing overall patient survival. Such investigations should be enabled by advanced imaging (e.g., PET-MRI) of labelled therapeutics following MB-FUS treatments to indirectly quantify and track delivery enhancements. In addition, window of opportunity studies providing surgical specimens following drug MB-FUS combinations [113] will enable direct analyses of delivered agents as well as early evidence of biological effects and treatment responses that will support better patient stratification in Phase III trials.

Therapeutic US Technology

The aim of therapeutic US systems is to deliver the required acoustic energy at the tumor core and infiltrating margin while sparing healthy tissue. Although technically it is straightforward to focus the US beam deep in the tissue, it is particularly challenging to do so through the skull. This is because the skull, which comprises the highly porous trabecular bone (diploë) sandwiched by two cortical tables, induces significant losses (absorption, scattering, and reflection) and aberration (refraction and skull heterogeneity) to the US beam [115–117], which are especially severe in patients whose skulls have low ratios of diploe to cortical bone (i.e., skull density ratio – SDR < 0.45) [14,118]. The presence of the skull also makes it difficult to predict the focal pressure, which is critical for attaining MB activity at levels pertinent to safe and effective BBB opening. To mitigate these challenges, several approaches and systems have been developed (Figure 3 and Table 3) that are currently under clinical or preclinical evaluation for targeted drug delivery in the brain. While this review is primarily focused on the state of the art along with current challenges and future developments of this technology, for a historic perspective we direct the reader to other review papers and textbooks, which also include early approaches and designs of the systems described herein [14,119,120].

Targeting the Tumor

To reduce skull related losses, trans-skull US systems operate at much lower frequencies than other therapeutic and diagnostic US scanners (i.e., below 1 MHz). Additionally, they make extensive use of at least one of the following: intraoperative MRI, preoperative CT, and real-time mathematical modeling of sound propagation (i.e., aberration correction algorithms). The trans-skull MR guided focused ultrasound (MRgFUS) system, which builds on the technology originally developed for thermal ablation [121–123], and as such retains most of the functionality of these systems, is the most advanced system. Trans-skull

MRgFUS systems employ intraoperative MRI for localizing the tumor and registering the US system to patient's brain. Following target identification, preoperative CT datasets — from which the CT Hounsfield Units (HU) have been converted to density, attenuation, and speed of sound maps through semi-empirical models or measurements [116,117,124] — are registered to the MRI frame and used for *in situ* aberration correction. These corrections are determined using a range of methods, such as ray tracing and time-reversal processing [124–130]. In ray tracing, used for these current clinical systems [125,131], aberration caused by the skull to the beam is determined for each element, and appropriate time delays are applied to focus and steer the beam of the system to the desired location in the brain. The amplitude of the emitted signal can also be used account for the losses, although for frequencies below 500 kHz, this is less critical [115–117]. The trans-skull MRgFUS system used in the clinic (e.g., ExAblate) is a hemispherical phased array, composed of a thousand elements with central frequency at 220 kHz and can effectively to target noninvasively brain tumors at different locations with subwavelength precision [104,132]. The large aperture of these arrays enables very tight focusing (focal spot full width at half maximum is approximately 2 mm transverse and 7 mm in the axial direction [133,134]) and large beam steering. Multiple non-overlapping sonications (up to 32 sub-targeted 10 ms bursts at 1 Hz repetition frequency; 32 % duty cycle) can be performed to cover larger volume. While the targeting precision with these arrays and methods is considered excellent for most applications, developing arrays with more elements (i.e., ten thousand or more) remains an active area of research, as such arrays could lead to more effective (i.e., theoretical limit) aberration correction and beam steering. However, cost and engineering challenges need to be overcome to make these arrays a reality.

Despite the unique features of current MRgFUS systems, the use of intraoperative MRI, which is essential for monitoring thermo-ablative interventions via MR temperature imaging, is potentially not necessary for monitoring and promoting purely mechanical effects (i.e., those due to acoustic cavitation and/or stable MB oscillation). As a result, neuronavigational systems that employ neurosurgical stereotactic guidance, wherein targeting and aberration correction is based on the stereotactically registered FUS array to the patient's head and CT, respectively, have been proposed and are currently under evaluation in the clinic [106,135]. The main advantages of these systems are their lower operational cost, as they do not need intraoperative MRI, and portability. However, the targeting precision is similar to the standard stereotactic systems used in neurosurgery, and less than that of the MRgFUS systems (Table 3) [136]. While it is not clear what is the required targeting precision for targeted drug delivery in brain tumors, a potential challenge with this approach (and systems) is that it requires maintaining the registration during the treatment, which is not trivial, especially for larger treatment volumes (i.e., long treatment duration). To mitigate this challenge, multiple phased arrays attached to a 3D printed scaffold based on the CT scans of the patients have been proposed [137]. While these helmet-like constructs that conform to patient skull may provide a more robust solution to registration errors during the treatment, they do not solve this problem completely as the large area they cover might exaggerate small registration errors. Nevertheless, these approaches are very promising as they may provide systems with targeting, steering, and monitoring capabilities that do not rely on intraoperative MRI.

An alternative approach that may allow for real-time adjustments in the registration is based on intraoperative US imaging (US guided therapeutic US phased arrays) and fusion of the US images (e.g., of the skull) with diagnostic MRI and CT, and by extension of the therapeutic US phased array [138]. As we elaborate below, the use of US imaging arrays is also important for monitoring and controlling acoustic cavitation in the brain; hence addressing challenges associated with poor US image quality due to imaging with sparse arrays, which limits the registration accuracy with MR/CT images, may make this approach a viable and potentially very precise alternative for MB-FUS brain therapy.

While increasing the number of elements can improve performance, reducing the number of elements, and thus the electronics required to drive these arrays, can simplify the system and its use, while drastically reducing its cost. To this end, US implants based on the direct placement of the transducer on the dural surface via a small craniotomy used for tumor resection have been developed and successfully tested in the clinic [139]. Despite the simplicity of this system, which is amenable to the widespread use of this technology, a potential drawback of this approach is that is highly invasive and feasible only after tumor resection that may ultimately limit its use for non-resectable brain tumors. This limitation could be mitigated by single-element systems based on neuronavigational guidance [135], though skull aberrations may limit their performance. This challenge can potentially be addressed by employing a patient specific 3D printed acoustic lens for aberration correction [140–142]. While the use of lens limits the highest pressure that can be delivered to the focus, this approach does not require craniotomy and, for drug delivery applications, the required pressure levels are not very high (i.e., below 1 MPa peak negative). More research in this direction, potentially using metamaterials or other methods [143], along with addressing positioning challenges of the lens with respect to the skull is warranted.

An interesting potential approach to focus the beam through the skull is based on Lamb waves [144,145], whereby US waves generated by wedge shaped transducers can be guided through the skull, and when they leak out (i.e., the US is radiated as longitudinal waves in the brain) can focus the beam at the hard-to-target brain locations immediately below the skull [146]. Despite promising early findings, mostly based on numerical simulations, the focusing ability and efficacy of this method must be studied more rigorously and demonstrated experimentally.

Excitation Transducer Technology

Largely, US systems for targeting brain tumors have so far relied exclusively on piezoelectric transducers. Transducers based on piezoceramic materials have high mechanical impedance as compared to liquids and therefore can be tuned to generate large displacements over a narrow frequency band, which makes them natural sources for the low frequency, high pressure ultrasound transmission needed for trans-skull US [154,155]. While these characteristics are critical for thermal ablation, for BBB opening, where acoustic power output requirements are more than an order of magnitude lower, alternative technologies might be relevant and potentially more appropriate [15,156]. Most notably, recent developments in piezoelectric micromachined ultrasonic transducers (PMUTs) and capacitive micromachined ultrasonic transducers (CMUTs) indicate that these devices

could generate acoustic intensities suitable for BBB opening [157,158]. Furthermore, these micromachined devices, which are MR compatible, offer the advantage of integrated electronics supporting dense 2-D arrays with manageable cable count and improved control of acoustic wavefronts [158,159]. The latter can allow for dual mode operation, potentially allowing to design high performance MRgFUS and/or USgFUS systems for targeted drug delivery in brain tumors. These technologies are summarized in Table 3.

Microbubble Technology

Microbubbles are a key component of FUS mediated drug delivery in brain tumors. As we summarize in Table 4, the MB size (mean diameter and distribution), shell properties (thickness and composition), and gas core can vary considerably between commercially available formulations, which in turn can affect both their response to sonications and their half-life [160], and, by extension, their ability to modulate the BBB and brain TME. Additionally, while up to five times the typical clinical dose of MBs used for diagnostic imaging is considered safe [133], the optimal concentration and maximum tolerated dose for human therapies remains an open question [161]. While several studies have assessed the impact of MB properties on BBB permeability [162], no systematic investigations have been performed in brain tumors. Hence, current evidence, including the discussion below, can only be used to make inferences about the impact of MB properties in modulating the brain TME and the extent to which they can be tuned to attain specific responses.

The effect of MB size:

Commercial MBs are typically 1-4.5 μm in diameter, consist of a gas core encapsulated by a stabilizing shell and, have a mean half-life of less than 5 min (Table 4) [163]. While bubbles smaller than 1 μm are possible (termed nanobubbles [163]), bubbles larger than 8-10 μm are cleared very quickly, setting an upper limit on their effective size. Early investigators have indicated that larger MBs (4-6 μm in diameter) lead to larger BBB permeability increase that takes longer to return to baseline permeability [38,164–167]. Although the exact reason is not well understood, it is hypothesized that the mechanisms of action (and interaction) of the MBs on the vasculature, particularly in capillaries, (Figure 1) are more pronounced for larger bubbles. Interestingly, for larger MBs their resonance, which is largely governed by their size [168,169], is closer to frequencies used in the brain (below 2 MHz), making their oscillation more pronounced for a given focal pressure.

Investigations by McDannold et al. indicate that BBB opening is characterized by the Mechanical Index - MI (i.e., a higher pressure is required to open the BBB when a higher frequency is used; see Box 1) [170], suggesting that resonant effects are highly damped in the brain capillaries. Of note these investigations have been performed with commercial MBs that are characterized by reasonably high polydispersity [171]. The latter contributes to a wider range of behaviors within a MB population that may in turn overshadow resonant effects. More recently, Song et al. proposed the MB gas volume as a unified dose parameter of MB effects on BBB, with larger total volume leading to higher BBB leakiness [171,172]. Notably, this metric, which allows to take both the MB size and concentration into consideration, excludes resonant effects. Interestingly, recent investigations using

phospholipid MBs with different size and distribution, while controlling for MB gas volume, found that changes in BBB permeability and immune phenotype correlated with bubble size, highlighting the importance of MBs size towards attaining distinct changes in BBB phenotype [38]. However, when assessing the effect of size, accounting for circulation time is also critical [173].

The effect of MB shell: The MB shell, which stabilizes the MB by providing a diffusion barrier to the encapsulated gas, is typically composed of lipids, proteins, or polymers, and directly impacts their behavior, including circulation half-life (or dissolution) [160] and probability of inertial cavitation [174]. Trying to elucidate the role of MB shell properties on BBB opening, McDannold et al. demonstrated that MBs with shell made of human serum albumin (Optison) produced a larger BBB opening than phospholipid shell MBs (Definity®) under similar acoustic exposure. However, in their investigations they used the clinical dose of each formulation, which resulted in higher gas volume for Optison MBs [175]. This comparison (i.e., Optison vs Definity) has been repeated recently under the same gas volume (1.1–1.2 μL/mL), where the assessment of Evans blue leakage indicated higher BBB permeability with Optison MBs as compared to Definity [176]. Of note, in this study, the investigators tried to match the acoustic emissions between the two agents, which led to the use of higher pressure for Optison. Although the relevance of MB acoustic emissions to the observed changes in BBB permeability is an active area of research (see next section) and determining the focal pressure in rodents is always challenging [32], these findings suggest that the shell properties should be taken into consideration for predicting changes in BBB permeability. This is reinforced by investigations that employed MBs with the same shell material (Definity® and SonoVue®; both are made of phospholipid shell) that showed similar effects under the same exposure conditions and MB concentration [177].

Surface charge (or the addition of targeting ligands) could be used to further increase MB specificity and potency by maximizing their contact (or minimizing their distance) to the vessel wall through interactions between, for example, a positively charged (cationic) MB shell and the negatively charged cell membranes of the NVU [162]. However, shell charge can affect the clearance rate [178,179]. Although some studies have reported longer half-life for cationic MBs [180], it is important to balance their interaction and retention with the vessel wall and the brain TME, respectively.

The effect of MB gas:

The encapsulated gas is typically a heavy molecular weight, inert gas that is characterized by low diffusivity across the shell wall and low solubility in the surrounding medium, such as perfluoropropane (C_3F_8) or sulphur hexafluoride (SF_6) (also called 2nd generation MBs; 1st generation MBs used the higher diffusivity air), to improve the bubble half-life after injection [199–201]. Unless a reactive gas is encapsulated, the effect of gas core on the BBB opening should be fully described by the MB half-life, with longer half-lives leading to more robust BBB opening [202].

Additional research to link MB properties with specific changes in the structure and function of the NVU and brain TME and how they are related to the exerted strength of the circumferential and shear stresses will greatly facilitate the advancement of this

technology. Efforts to maximize the BBB permeability should also take into consideration that its magnitude enhancement correlates with the transcription of several key inflammatory mediators, including *Tnf, Icam1, Ccl5,* and *Il1b* [203], which imposes an upper limit for obtaining safe BBB opening, at least in healthy brains.

Monitoring and Control of Microbubble Activity

As we alluded to above, monitoring (detection, characterization, and localization) of the cavitation activity is essential for safe and effective treatment of brain tumors with MB-FUS. Before we describe the main components and approaches currently used in preclinical and clinical systems to guide this intervention, we will briefly introduce the origin of the signal used to detect and characterize cavitation during MB-FUS.

Acoustic Cavitation and Emissions

When excited by the therapeutic ultrasound pulse, MBs are driven into dynamic oscillatory behavior, whose character is governed by the amplitude and frequency of the excitation wave. The vibrating bubbles in turn radiate waves termed acoustic emissions (AEs). These emissions may be detected noninvasively with acoustic transducers (see Detection Transducer Technology) and serve as the primary proxy for monitoring MB behavior. Broadly, this activity is characterized into two regimes: stable cavitation and inertial cavitation.

Stable cavitation that is induced at lower applied pressures manifests as integer- and half-multiples of the excitation frequency. For instance, for a therapeutic pulse with frequency f_0, the echoes re-radiated by stably oscillating bubbles will contain harmonic content at $0.5f_0$ (subharmonic), nf_0 (harmonics), as well as $(n + 1/2)f_0$ (ultraharmonics) [204]. As summarized in Figure 4, stable cavitation has been associated with safe opening of the BBB.

On the other hand, the onset of inertial cavitation typically occurs at higher applied focal pressures (mechanical index near 0.4), wherein overexpansion and subsequent collapse of the bubble due to the surrounding fluid's inertia gives rise more violent mechanisms such as jetting [205–207] and ablation (i.e., for long pulse durations) [208,209]. In BBB-disruption experiments, the presence of broadband AEs has correlated well with instances of tissue damage (Figure 4). As the collapse events are transient in time (tens of nanoseconds), inertial cavitation increases the baseline broadband frequency content (figure 5), which serves as a reliable indicator for the presence of inertial cavitation [35,210–212].

While the presence of sub- and ultraharmonic emissions in the absence of broadband is a well-established metric of stable cavitation, recent evidence has linked this acoustic signature to tissue damage [32,210]. Indeed, vigorous stable MB vibration can affect cell membrane processes both mechanically (e.g., through sonoporation [213,214]), and biochemically (by affecting endocytosis [215]); however, measurements with more sensitive detection capabilities (see Detection Transducer Technology) to confirm that in these investigations broadband emissions were indeed absent and not simply below the detection limit of the system used, are needed before entertaining these possibilities. Either way, the importance of detecting and characterizing AEs is central to effective therapy, thus

techniques and technologies to this end are of great importance to MB-FUS and its translation to the clinic.

Passive Cavitation Detection

Passive cavitation detection (PCD) is achieved using one or more piezoelectric transducer elements operated in listen-only mode, whose field of view is aligned with the focal region of the therapeutic transducer. Recording the MB emissions during the application of US allows characterization of the cavitation based on the signals' spectra. PCD has several attractive features. Because typical therapeutic pulses have duration on the order of milliseconds, they comprise hundreds of acoustic periods, and thus their harmonic content is well defined. Additionally, the central frequency of these pulses is in the low kilohertz range, such that a receiver with bandwidth of order 1 MHz is sensitive to many harmonics and ultra-harmonics. For these reasons, PCD has been widely adopted as a means for acoustic therapeutic monitoring [216–219]. Additionally, piezoelectric elements are relatively cheap and robust, such that their incorporation into transcranial FUS systems is simplified [220]. A critical component of the detection is the processing of the recorded emissions, such as filtering and spectral analysis of the recorded echoes, including transient cavitation events [221,222]. The latter, the acquired data is implemented in real time using fast Fourier transform (FFTs) with modest computing resources [56] and the data are presented are either as arbitrary units or in decibels (dB) using as reference AE from sonications in the absence of MBs.

Use of PCD for a range of treatment parameters, including MB type and dose [164,165], cavitation thresholds [30,223,224], and pulse durations [225,226], has led to the identification of acoustic signatures (e.g., strong harmonics in the absence of broadband emission) for safe and reversible BBB opening [227] (See Figure 4 and Suppl. Table 2). However, a primary drawback of PCD is the lack of localization; while it may detect the presence of cavitation, it cannot confirm its colocation with the treatment area. This is not a major limitation for preclinical investigations in rodents, but for clinical translation spatial information is critical for minimizing false positives (i.e., from MBs from different locations, including outside the brain).

Passive Acoustic Mapping

Passive acoustic mapping (PAM), also called passive cavitation imaging (PCI) [228], uses a geometrically registered array of receivers to beamform the recorded MB emissions to determine their location. In addition to the valuable spatial information, PAM also benefits from improved sensitivity, as it exploits the coherence between signals, which effectively enlarges the aperture of the receiver [229,230]; such sensitivity is important to reduce false negatives (e.g., cavitation not detectable by PCD). Several techniques have been proposed to combine the individual receivers' signals to form an image (a process termed "beamforming"; see Table 5). In time domain PAM, signals from each array element are delayed in time (corresponding to the time-of-flight between a pixel in the image and the element) and then added, such that pixels containing sources will have strong constructive interference [231–234]. Time domain PAM is a robust technique that may be extended to account for arbitrary array geometry [235,236], skull aberrations (by adjusting

the time-of-flight [237,238]) and to improve resolution (by carefully adjusting the relative amplitude of each channel [234,239–241]), but remains computationally expensive. While real-time implementations have been demonstrated, these require graphical processing units (GPUs) [242,243] and data filtering to isolate different spectral components of the acoustic emissions [244].

To allow for frequency selectivity and improve the computational cost of PAM, methods that operate in the frequency domain [228,245] and spatial frequency domain (or wavenumber domain) [230] have been proposed. These methods offer more efficient calculations (up to a hundredfold reduction in the order of the number of required calculations) by evaluating smaller portions of the spectra or potentially by considering decimation of the time series [246]. While early implementations assumed uniform sound speed, recent investigations have extended these methods to account for skull aberration [247]. Together with their ability to form maps at frequencies pertinent to MB oscillation type make frequency domain PAM ideal for spatiotemporal monitoring and control of MB dynamics (see Detection Transducer Technology). While the systems for PAM (time or frequency domain) come with increased complexity and cost, we anticipate that their high sensitivity and the importance of localizing MB activity, which could happen at different locations concurrently (e.g., outside vs inside the brain), will outweigh the advantages of simpler acoustic emission systems.

A remaining challenge in acoustic emissions based monitoring is the lack of a system-independent method to quantify the emissions and their spectral components [171]. Quantifying the AE in decibels is suboptimal and hinges on the reference data used and their spectral content (e.g., background data often contain harmonics). Moreover, metrics like cavitation dose (i.e., the integrated area under the spectrum compared to the baseline measurement over frequency bands of interest) [248,249], which have been shown to correlate well with intended bioeffects, rely on the instrumentation used and its sensitivity, SNR, etc.. Also, the term dose might be misleading for an emitted quantity. A more universal means of quantifying the acoustic cavitation will be a breakthrough in this field, as it would allow to take MB-FUS away from experts, while facilitating both translational research and clinical implementation of different treatment protocols and across different centers. Advanced calibration methods that will take into account the impulse response function of the receivers, in addition to absolute calibration methods, will likely be critical moving forward.

Real-time Control of Microbubble Dynamics

Despite the enormous potential of MB vibrations to promote mass and drug transport in the brain, an outstanding question in the field is how to control the MB dynamics in the brain. As discussed in the previous section, PCD and PAM methods enable real-time detection, localization, and characterization of the cavitation activity from their acoustic emissions. Based on these inferences, the excitation pressure (i.e., the applied US energy) can then be tuned to reach and maintain a specific level of MB emission correlated with reversible BBB opening, while simultaneously monitoring to limit the presence of damaging inertial cavitation. However, the relatively fast MB clearance, as well as the limits on the number of MBs administrated to patients imposed by FDA, imposes stringent time constraints for

tuning and optimizing the sonication per patient and per target. As such, several approaches have been developed for tuning the excitation pressure, including open and closed-loop controllers of the bubble dynamics, in real time.

Broadly, cavitation controllers use the spectral content of the MB emissions, measured via PCD, as a state observer (i.e., a proxy measurement) to infer the MB dynamics, and then enforce a control law (an algorithm based on the value of the state observer) to change the applied acoustic energy to obtain a desired level of cavitation (Figure 5). The state observer is usually based on harmonic [35,56], subharmonic [250,251], ultraharmonic [252,253], or broadband emissions, or some combination thereof [229,254]. Additionally, metrics such as the stable cavitation dose (SCD) or inertial cavitation dose (ICD), may be state observers [255–257]. The optimal frequency content measurements to use depends on the particular apparatus (e.g., it will be influenced by the detection transducer's sensitivity and bandwidth), but for BBB disruption the aim is achieve robust stable cavitation, while avoiding (and mitigating) the occurrence of damaging inertial cavitation.

The chosen state observer metrics are fed into the control law, which dictates whether to increase or decrease the ultrasound pressure, or even alter sonication pulse length [258]. It was proven that all the aforementioned state observers were strong indicators of BBB-opening. However, when designing a controller (especially for clinical purposes), choosing a frequency band of interest to be used in the state observer is a critical component due to the transcranial energy loss. Although current clinical systems monitor sub-harmonic emission due to its superior transcranial efficiency associated with low losses, different state observer such as harmonics and ultra-harmonics can also be chosen depending on the driven frequency of the FUS and sensitivity of the system. In static law controllers, the control law is prescribed *a priori* to tune the sonication to achieve the target level [35,210,250,255]. Current clinical systems (e.g., ExAblate) employ one such controller proposed by O'Reilly and Hynynen, wherein the pressure continuously increases by fixed increment, and then halves the FUS pressure when ultraharmonic signals are detected [252]. A similar static law controller designed by Kamimura proceeds until broadband content (inertial cavitation) is detected [255]. While this algorithm contains feedback (from broadband emissions), we will consider it as open-loop since the control law does not alter pressure step size. Additionally, a "manual" control approach based on harmonic emission strength measurements was proposed [35]. Harmonics constitute the strongest signal emitted by the oscillating bubbles, as a result they can support controllers with high SNR. This approach also allows tracking of the MB kinetics during the sonication, providing additional information towards treatment monitoring and verification as well as providing important information for activating/deactivating the controller.

Due to the characteristics of static law controllers (e.g., the applied pressure level increases slowly until a certain acoustic emission threshold to avoid overshooting the target), safety is ensured by reducing the preset threshold; this aspect is attractive enough to facilitate the clinical transition of static law controllers [104,259]. Despite these benefits, a major drawback of static law controllers is the long time required to attain the desired state (rise time) associated with the relatively small pressure increments. While the rise time might not be detrimental for a single target, to cover the entire tumor, most treatments involve more

than 30 targets in which the pressure must be adjusted individually. Additionally, because the control law is predetermined (i.e., the pressure step size is small and unchanged), they have limited ability to respond to sudden changes in the acoustic emissions during the sonication (e.g., uptake or washout of the bubbles).

To mitigate the challenges, dynamic controllers have been recently proposed. Dynamic law feedback controllers have a control law that may depend on the observed acoustic emissions. For instance, the pressure increment may depend on the difference between the target level and the last measured level. Typically, the control law adjusts the pressure increment proportionally to the difference between target output state and current output state [229,251,253,254,258]. These methods have resulted in robust BBB opening and effective drug delivery in rodents, supporting further developments [254]. A potential challenge for closed-loop controllers is that their operation might be affected by the fast MB clearance and the associated decay in the acoustic emissions over time. To minimize this effect, a continuous MB infusion is often used [35,253,255,256]. In some controller algorithms, bolus injection [250,254] or bolus and infusion combined [56,252], or bolus injection combined with inactivation of the controller after fixed duration (e.g., 25 seconds) [254] has been adopted. Importantly, both for open and closed-loop controllers, arrival of microbubbles to the brain as well as the decaying concentration after bolus injection should also be accounted for during optimization of the control law (i.e., determining the threshold level of cavitation).

In addition to detecting and controlling the MB emissions, knowing their location is of particular importance due to the high likelihood of emissions from gas trapped on the skin or in the coupling medium to interfere with the acoustic emissions from the targeted region and render the recordings unreliable. Recently, a closed-loop dynamic law controller of MB dynamics that allows for the concurrent detection and local control of the MB dynamics has been proposed [229]. A key finding of this paper was the ability to control locally the MB dynamics in the presence of cavitation activity at multiple regions. They also showed that the controller had very high tolerance (within 10% of target) and was robust across a range of conditions. Demonstrating spatiotemporal control *in vivo* is the next critical step to move this technology to the clinic and towards developing tunable systems for targeted drug delivery in brain tumors. Likewise, identifying ways to link the MB emissions with changes in MB radius to directly control the MB dynamics (radius vs time) [260–262] will allow to better define and refine spatial and temporal treatment windows and potentially move closer to developing universal means of quantifying and controlling the acoustic cavitation *in vivo*.

Detection Transducer Technology

The detectors for monitoring and controlling FUS treatments via PCD or PAM (Table 6) should have high sensitivity and low noise over a broad bandwidth to detect stable and inertial cavitation (Figure 5). Experiments and simulations indicate that in order to detect acoustic emissions from single oscillating MB (stable cavitation) after 15 cm of propagation (i.e., middle of the brain) and through intact skull, one needs to measure pressure levels as low as 0.5 Pa over megahertz bandwidths with reasonable signal to noise ratios [263].

Ideally the detection systems should be sensitive to these levels in addition to providing spatial information [138,264].

While several technologies for detection are currently available, current clinical systems use high power, electrically tuned narrow bandwidth thickness mode piezoceramics that are sharply tuned at the subharmonic emissions. To improve detection at other harmonics, concentric piezoelectric transducers tuned to both subharmonic and harmonics are used to capture the spectral components required to assess stable cavitation with high sensitivity [104,266]. This approach however is not optimal for detection of broadband emissions to determine the onset of inertial cavitation. To overcome this limitation broadband receivers made from thin piezoelectric films like polyvinylidene fluoride (PVDF) or damped piezoelectric ceramics have been proposed, albeit with limited sensitivity [138,252,264].

By integrating diagnostic ultrasound imaging arrays to the FUS system can provide spatial mapping of MB activity with good sensitivity [230]. However, this approach requires imaging arrays to be sensitive to the lower harmonics, which is not always the case. Also, due to the use of ID arrays, it is limited to cross sectional (2D) mapping of cavitation activity. For volumetric mapping, 2-D sparse receiver arrays tuned to harmonic frequencies are integrated either between the transmit elements or collocated with the transmit elements using innovative designs where multiple lateral mode piezoelectric tubes resonating at fundamental and harmonic frequencies [137,138,266]. These systems provide sufficient sensitivity at harmonic and subharmonic frequencies for controller operation. However, a potential limitation of this approach is the lack of sensitivity to broadband acoustic emissions for inertial cavitation detection and complex device construction [137,266]. To overcome the bandwidth limitation, separate highly damped single piezoelectric ceramic transducers are used as broadband detectors with adequate sensitivity, but these approaches do not provide spatial information [252]. In some other implementations, broadband PVDF transducers are integrated as a thin film on piezoceramic transmitters [264,276]. While this approach enables broad bandwidth operation and spatial mapping, the inherent sensitivity limitations of PVDF and complexity of array construction might limit its broader adoption.

Finally, newer microfabricated ultrasound transducer (MUT) technologies such as CMUTs [277,278] and PMUTs [267], and acousto-optics [275] have demonstrated substantial benefits over traditional piezoelectric elements in terms of bandwidth, flexibility, and sensitivity—characteristics crucial for the successful detection of cavitation (Table 6). The wider deployment and refinement of these devices for PCD and PAM may lead to very sensitive systems for both basic research and clinical implementation of MB-FUS.

Biomarkers of BBB Opening and Targeted Drug Delivery

Assessment and quantification of the degree of BBB/BTB opening and correlating this with therapeutic delivery is fundamental to effectively applying MB-FUS for improved brain tumor therapy. This information can also be used to elucidate drug transport mechanisms, reducing false negatives, and, by extension, improving treatment outcomes. As such, several preclinical and clinical methods have been explored to assess NVU permeability and drug delivery. Most notably, intravital microscopy has been utilized to collect quantitative time-

lapse images of drug PK at single cell resolution and study the BBB permeability and interstitial transport of chemotherapeutic agents in the brain TME [279]. This level of detail has allowed to refine our understanding of MB-FUS mediated drug delivery (i.e., improved interstitial fluid flow) and led to new MB-FUS-drug combinations for treating brain cancer [58].

Despite the unique insights gained in the transport dynamics in the brain TME with intravital microscopy, contrast enhanced MR, mostly based on gadolinium-based contrast agents, is the current standard method for assessing BBB opening in both preclinical and clinical investigations. Most notably, digital substruction (at steady state) of pre- and post-contrast T1-weighted MRI has been used extensively for assessing the effect of MB-FUS in the brain and brain TME [65,280,281]; while this is the current standard, for long treatment times, MRI contrast agents with half-lives in the circulation longer than the half-life of gadolinium (90 min, [282]) might allow the assessment of BBB opening under a single administration. While this method is used to assess only the relative difference in BBB permeability, Dynamic Contrast-Enhanced (DCE) MRI and calculated K^{trans} values - a bulk transport parameter that is dependent on both capillary permeability and perfusion - provide a semi-quantitative method to characterize the effectiveness of BBB opening (increase in K^{trans}) [281,283]. Another MRI method that can be useful for quantifying the effect on MB-FUS in the brain TME is based on Dynamic Susceptibility Contrast (DSC; based on T2-weighted) MRI. This method can be used to estimate blood volume and flow, vessel size, and vessel permeability [284,285]. While contrast enhanced MRI has been used to assess BBB opening in most clinical and pre-clinical investigations, when the BBB is already disrupted, this method provides a less specific assessment of FUS-mediated changes in NVU permeability. Moreover, the different pharmacokinetics of MRI contrast agents compared with anticancer drugs may limit their predictive utility as surrogates of therapeutic agents delivery [65,286].

Labeling the drugs with MRI contrast agents (or PET tracers) will likely lead to more specific and effective methods for monitoring MB-FUS drug delivery in brain TME [287]. Unfortunately, these methods cannot discriminate between vascular and perivascular delivery with deep drug penetration ($\gg$20 μm) and cancer cell uptake. However, combining them with ex vivo analysis of drug penetration and function using microscopy may allow to mitigate this limitation. A key advantage of labeling drugs with PET tracers is their superior sensitivity and ability to quantify drug delivery [288]. Moreover, PET imaging, for example, with [18F]-DPA714, which is a biomarker of translocator protein (TSPO) [289], can be used to assess MB-FUS drug delivery and changes in the TME (e.g., for immunomodulation or immunotherapy) [50]. However, PET tracers are short lived and require extended facilities (e.g., cyclotrons), which may limit their widespread use.

Perspective

Next Generation FUS systems

CMUTs have much larger bandwidth as compared to more conventional piezocomposite receivers [277,278], and are ideal for PAM especially when integrated with low noise electronics that can further boost their performance [269–271,290]. While CMUTs present

some challenges with their inherent nonlinearity and DC bias requirement, initial studies indicate that by proper biasing and signal processing these hurdles can be overcome [271]. CMUTs can also be useful for integrated ultrasound imaging of the skull surface for CT registration for FUS. They have also been combined with piezoelectric transducers for high pressure generation at low frequencies [272]. The frequency response of the CMUT array can be adapted by adjusting the DC bias on the device [273,291], potentially supporting the development of therapeutic US systems with multimodal operation (Figure 2). Though their bandwidth is less than that of CMUTs, PMUTs can also be used as PAM receivers and receiver arrays [267].

The possibility of 2-D array implementation with arbitrary geometries, tight electronics integration, and local signal processing/filtering capabilities with CMUTs and PMUTs offers some unique opportunities for FUS and PAM [268,292]. These developments, mainly driven by portable point-of-care ultrasound and wireless technologies for data transmission and control, can have significant impact in this area, especially as the need for portable and conformal systems grows. Given the 3-D imaging performance of most recent CMUT based handheld probes with 9000 elements [274] with a single cable connection, low power FUS treatment while using an array of these probes for full skull surface mapping for CT image registration and MB mapping with PAM is not a stretch of imagination. Similarly, wireless ultrasound imaging, control and data readout can dramatically reduce the size of the FUS systems and make them part of the point-of-care ultrasound arsenal for clinical use (Figure 3) [293].

Evidently, significant progress has been made in targeting brain tumors with FUS with several systems already available in the clinic and many new approaches and systems under evaluation (Table 3). Moving forward it is expected that current aberration correction methods, most likely in combination with sound propagation toolboxes that provide a more complete description of the physics, will be shared among the different systems [294–298]. Due to improved aberration correction, registration errors and estimation of the skull acoustic properties and microstructure will also become increasingly important as will research to correct them. For instance, methods that infer the appropriate phase and amplitude of each element by maximizing the local displacement induced at the targeted location by the radiation force of transmitted ultrasonic signals, as imaged by MR-Acoustic Radiation Force Imaging [129], can help account for these errors. Likewise, echo focusing techniques that rely on the sound scattered by intravenously injected MB can provide an alternative adaptive method to improve focusing [299].

Moreover, identifying new ways to study transcranial sound propagation might also lead to systems with improved performance. For example, an approach that has shown promising results for brain imaging [300], but has not been tested in the context of FUS therapy and aberration correction, is based on wave-equation inversion methods. These methods aim to minimize the mismatch between waveforms propagating through the skull in simulated and experimental data. While this approach it is still in early days, attaining a good match between simulated and experimentally observed waveforms may lead to a very accurate estimation of the required frequency-dependent phase and amplitude of each element for transcranial focusing. To demonstrate the principle, challenges associated with element

location and impulse response function between the experimental data and simulations along with improved computational efficiency need to be addressed.

Finally, targeting of the tumor, microbubble modeling, and control has thus far largely relied on classical physical models, signal processing, and control theory. The recent proliferation of machine learning and deep learning techniques in problems of acoustics [301] and diagnostic ultrasound [302,303] may well find use toward this complex clinical problem. Particularly, optimization of the myriad treatment parameters as well as estimation of cavitation thresholds and control may be enabled by such networks, provided the large sets of labeled training data they require can be made available.

Overall, it is envisioned that improved i) registration accuracy, ii) estimation of the skull properties, and iii) computational efficiency of the different aberration correction methods along with adaptive beam focusing capabilities, potentially based on second order effects, will characterize the next generation systems that aim to attain high targeting precision, large treatment envelope, and cost effectiveness. New transducer technologies may also lead to more integrated and sensitive systems, thereby enabling treatments with large therapeutic windows (spatial and temporal) to increase drug efficacy with minimal side effects.

Next Generation “Bubbles”

As discussed above, FUS-MB studies have largely relied on encapsulated microbubbles whose design was motivated by applications in contrast imaging (Table 4). It is evident that the design of MB formulations for modulating the brain TME, should consider MB’s physical properties (size, distribution, charge, etc.), resonant effects, half-life, and acoustic emissions along with detailed assessment of key biological variables (BBB permeability, Tight Junction expression, inflammatory markers, etc.), Understanding how the MB properties affect their echoes, half-life, and changes in the BBB phenotype is the next critical step towards designing the next generation MBs for MB-FUS with the goal to increase the treatment window for safe and effective drug delivery in brain tumors.

Recently, new classes of acoustic particles have emerged [163,304], including phase change contrast agents [305–307], particles with shell inclusions (such as dyes or magnetic nanoparticles), nanobubbles [253,308,309] and even biologically engineered gas vesicles within the cells themselves [310–312]. In addition to BBB opening, the goal with these nano-formulations is to promote MB-related effects (Figure 1) within the interstitial space and to the cancer cells. While, current formulations are much larger than the average pore size in the brain (typically below 60 nm) [313], more refined designs and sonication schemes may allow to overcome this limitation.

FUS Immunomodulation and Immunotherapy

The distinct immunological characteristics of the CNS and brain tumors, combined with the comparatively limited impact of immunotherapy on intracranial malignancies, highlights the need for new methods to increase the communication and therapeutic trafficking between the brain TME and the immune system [314,315]. Although MB-FUS has been primarily considered as a drug delivery technology, increasing evidence suggests that it can also be used to facilitate these interactions. While many potential mechanisms of FUS-based

immunomodulation and immunotherapy exist [16], current evidence highlights three main avenues.

The first is improvement of penetration of immunotherapeutic agents [50]. As we alluded to, MB-FUS was able to improve the uptake and efficacy of anti-PD1 and anti-CD47 monoclonal Ab in glioma (GL261) mice tumor models [50,51]. Interestingly, more anti-CD47 was delivered to the tumor when it was administrated after the sonication (as compared to pre-MB-FUS). While the reason for the improved uptake is not clear, the specific Ab targets the macrophages in the TME, which are known to be activated post-MB-FUS [31,316–318], potentially implicating MB-FUS and BBB-opening associated priming in anti-CD47 uptake. Considering the strong coupling of cancer cells with the cells of the central nervous system [5,319,320] and the potential therapeutic activity of anti-PD-1 via M1 polarization of the microglia [52], it is expected that combinations that aim to modulate this interaction will be an active area of research over the next years.

The second mechanism is facilitation of the infiltration of immune cells in the brain TME. Early evidence suggests MB-FUS leads to greater accumulation of HER-2 specific NK-92 cells in a model of HER2+ breast cancer brain metastasis (administered prior to MB-FUS) [39]. While this is another mechanism of action that remains poorly understood, recent investigations, primarily in the healthy brains, have implicated downstream effects from mechano-responsive and acute inflammation processes following MB-FUS [316]. It is unclear if the observed responses are provoked directly by MB activity or indirectly by the extravasation of plasma proteins like albumin and immunoglobulins into the brain that in turn can promote immune responses [321]. The observed inflammatory cascade can lead to release of damage-associated molecular patterns (DAMPs), pro-inflammatory cytokines and cell adhesion molecules (CAM) [33,316], followed by the infiltration of immune cells (e.g.e.g., neutrophils) in the brain parenchyma [322], and finally by the activation of astrocytes and microglia, which can last up to several days [289,323]. While recent studies reported similar responses into the brain TME [106], it remains unclear how MB-FUS may change the trafficking of adaptive and innate immune cells as well as alter the expression of cell adhesion molecules. It is also likely that tumor endothelial cells already exist in a more activated state [324], hence the impact of MB-FUS might not be as dramatic as it is in healthy brains or depend on the tumor model and type. These differences are reflected in recent investigations that showed limited homing of activated T cells to melanoma metastasis (B16F1ZsGreenOVA) brain tumors [324], while other investigations using epidermal growth factor receptor variant III (EGFRvIII) chimeric antigen receptor (CAR) T cells have demonstrated both increased homing and improved median survival in NSG mice with EGFRvIII-U87 gliomas [51]. Longitudinal characterization of the impact of MB-FUS on BBB/BTB phenotype and immune cell trafficking and function, across different tumor models will be critical. In addition, leveraging closed-loop control and advanced MB formulations [33,38,325] will help further advance MB-FUS immunotherapy and develop effective therapeutic strategies based on highly tuned immuno-mechano-biological mechanisms.

Third, FUS-immunomodulation may operate by improving antigen presentation either within the brain TME or at the level of the meninges and cervical lymph nodes.

This mechanism is supported by recent studies indicating increased shedding of cancer associated molecules in the circulation [248,326] following MB-FUS. However, using the B16F1ZsGreenOVA melanoma cancer cell line, which are stably transfected to express MHC-restricted peptides derived from OVA in frame with ZsGreen fluorescent protein, Curley et al. found limited evidence of increased antigen drainage to the lymph nodes and associated dendritic cell activation and maturation [324]. Considering that antigen presentation can lead to robust immune response (via DC priming and activation), these findings are consistent with numerous investigations that assessed the impact MB-FUS alone on survival in immunocompetent murine brain tumor models (i.e., the control group in the studies reported in Table 1) and have not reported a statistically significant improvement in survival (Suppl. Table 3). While these findings suggest that this mechanism of action or mode of ultrasound are unlikely to be sufficient to promote robust immune responses, the potential impact of MB-FUS in improving antigen presentation in combination with immunotherapies should be considered.

Looking forward immunotherapeutic combinations with FUS are one of the most promising lines of investigation and potential anti-cancer treatments. Given the complexity of immunotherapeutic delivery in the CNS and the highly immunosuppressive nature of many brain TMEs, accurately modelling and evaluating the biology of treatment responses will be critical. This can be accomplished by leveraging advanced analyses of tumor immune phenotype and immunocompetent brain tumor models [327], conducting experiments to assess the time of administration of the therapeutic relative to the sonication, refining the sonication parameters (amount and type of microbubbles administered, FUS frequency, the duration of the sonication, acoustic emissions etc.), designing pre-clinical FUS systems that closely recapitulate the clinical system(s) to be used, and employing window of opportunity and Phase 0 trial paradigms to identify promising combinations.

Combinational Approaches

MB-FUS treatment can also be combined with the application of FUS-mediated thermal stress in the bran TME. Locally applied thermal stress or local hyperthermia is broadly separated in two different regimes: (1) moderate hyperthermia that utilizes mild temperatures (38 – 42 °C for up to one hour; sub-ablative fibrillar heating) that can promote heat-dependent physiological changes and (2) high temperature focal hyperthermia (>45 °C for a few seconds; ablative heating), which can directly kill cancer cells and reduce tumor burden [328]. Sub-ablative hyperthermic exposures offer the potential to sensitize tumor cells to DNA damaging treatments like radiation [329,330]. This mode of FUS treatment could be combined with current standard of care therapies, temozolomide and/or intensity modulated radiation therapy. Ablative heating is characterized by the ablation zone and the periablative or transition zone (i.e., the penumbra zone between necrotic and viable tissue), where cells experience the sub-ablative effects. In the future, employing thermal ablation strategies with thin transition zones for direct tumor control within the core regions in combination with MB-FUS mediated BBB opening/drug delivery in the infiltrating margin, may offer exciting new therapeutic opportunities for high grade gliomas.

Although local mild hyperthermia and thermosensitive drugs, represent promising strategies to locally enhance drug delivery in solid tumors and improve treatment outcomes, their application in brain tumors remains limited. Recently, Kim et al. by combining closed-loop trans-skull focused ultrasound hyperthermia with thermosensitive liposomes (TSLs) were able to promote effective drug delivery in gliomas [331]. More research to assess this technology using current clinical systems (ExAblate, Sonocloud, etc.) in combination with MB-FUS (e.g., improving TSL – Dox delivery) may further improve these already encouraging findings. Beyond targeted drug release and delivery, combining the FUS thermal and mechanical stresses can also promote the increased trafficking and remote control of T cell activity of genetically engineered T cells with thermal gene switches by localized expression of tumor-targeting receptors, among others [332,333]. More research in this direction is clearly warranted.

FUS-mediated Liquid Biopsy

By recognizing that upon opening the BBB the transport across this biological interface is bidirectional Zhu et al. hypothesized that MB-FUS can enhance the shedding in the circulation of molecules secreted by cancer cells, such as cell-free tumor DNA (ctDNA; average size of 200 pb ~7.5 kDa) [334]. Their investigations in tumor-bearing rodents and pigs confirmed the improvement in the shedding of reported gene messenger RNA (i.e., GFP gene, used to label the cancer cells) and neural proteins (glial fibrillary acidic protein and myelin basic protein), after the application of MB-FUS [334,335]. These findings have also been investigated in the clinic, with early evidence indicating that BBB opening correlates with increases in circulating cell free DNA [326]. Considering the simplicity of this method, the established limitations of liquid biopsy techniques in the brain [336], and the number of ongoing MB-FUS clinical trials (Table 2), this application is expected to grow rapidly. Demonstrating this concept using actual tumor-specific oncogenes and expanding to other biomarkers (e.g., extracellular vesicles) may create unique opportunities for 1) assessing changes and degrees of change in BBB permeability, 2) improving diagnostic information in the setting of various tumor types (e.g., Medulloblastoma), 3) monitoring responses to therapy as well as assessing treatment effects and resistance, and 4) informing precision and personalized therapeutic selections in combination with MB FUS [58].

Predictive Models for MB-FUS drug delivery

Although still in early phase, mathematical modeling can help identify new treatment regimens and drug combinations under MB-FUS. Most notably, physiologically based pharmacokinetics (PBPK) modelling has already been used to characterize the transvascular and interstitial transport of chemotherapeutic agents and, via sensitivity analysis, to refine drug administration protocols for improved uptake. For example, PBPK modeling indicated that chemotherapy infusion can lead to higher drug uptake as compared to bolus administration [43,337]. Although rigorous and prospective validation of the specific PBPK models is critical for reducing extrapolation errors, these predictions seem to be in agreement with recent clinical trials that demonstrated improved efficacy under MB-US followed by carboplatin infusion (45 mins) [71]. PBPK modeling combined with quantitative imaging has also been used to probe the optimal nanoparticle properties, including size and surface charge, for effective delivery of siRNA-based therapeutics in

brain tumors under MB-FUS (i.e., 50 nm weakly cationic, +10 mV, hybrid lipid polymeric NPs) [58]. If these approaches are expanded to incorporate the MB dynamics [338,339] can be powerful in generating hypothesis that can then be used to narrow down the parameter space towards identifying MB (properties), FUS (frequency and sonication characteristics) and drug (PK/PD) combinations for improved drug delivery in brain TME. Incorporating the increasing amount of data and information gathered during preclinical and clinical investigations may allow to identify new ways to promote antitumor immunity, including the type and abundance of immune cell populations that can cross the BBB/BTB under MB-FUS and facilitate the development of rational strategies to deliver drugs and cells in the brain TME and accelerate their translation to the clinic.

Concluding Remarks

Substantial progress has been made in the last decade towards improving the transport of therapeutics across the BBB, through reversible opening via MB-FUS. The groundwork has been laid through the steady investigation of the component biology, biophysics, and pharmacokinetics of these approaches. Simultaneous advancement in transducer technology, signal processing, and controller design have rendered non-invasive, real-time, feedback control of the treatments to optimize efficacy a near term reality. As human clinical trials for using MB-FUS expand, we anticipate the utility and impact of MB-FUS to accelerate towards new therapeutic applications and combinations (e.g., with immune adjuvants) to address significant challenges in effectively treating brain tumors.

Supplementary Material

Refer to Web version on PubMed Central for supplementary material.

Acknowledgments

Scott Schoen Jr., M. Sait Kilinc, Hohyun Lee, Yutong Guo, F. Levent Degertekin, and Costas Arvanitis research in this area is supported by the NIH (National Institutes of Health) Grant R37CA239039 (National Cancer Institute) and the NSF (National Science Foundation) Grant 1933158 (Leading Engineering for America's Prosperity, Health, and Infrastructure). Graeme Woodworth's research in this area is supported by the NIH R21NS113016, R21NS118232, and Focused Ultrasound Foundation Grant 20010533.

References

[1]. Hawkins BT, Davis TP, The Blood-Brain Barrier/Neurovascular Unit in Health and Disease, Pharmacol. Rev 57 (2005) 173–185. 10.1124/pr.57.2.4. [PubMed: 15914466]

[2]. McConnell HL, Kersch CN, Woltjer RL, Neuwelt EA, The Translational Significance of the Neurovascular Unit*, J. Biol. Chem 292 (2017) 762–770. 10.1074/jbc.R116.760215. [PubMed: 27920202]

[3]. Phenix CP, Togtema M, Pichardo S, Zehbe I, Curiel L, High Intensity Focused Ultrasound Technology, its Scope and Applications in Therapy and Drug Delivery, J. Pharm. Pharm. Sci 17 (2014) 136–153. 10.18433/J3ZP5F. [PubMed: 24735765]

[4]. Arvanitis CD, Ferraro GB, Jain RK, The blood-brain barrier and blood-tumour barrier in brain tumours and metastases, Nat. Rev. Cancer 20 (2020) 26–41. 10.1038/s41568-019-0205-x. [PubMed: 31601988]

[5]. Arvanitis CD, Ferraro GB, Jain RK, The blood-brain barrier and blood-tumour barrier in brain tumours and metastases, Nat. Rev. Cancer 20 (2020) 26–41. 10.1038/s41568-019-0205-x. [PubMed: 31601988]

[6]. Sarkaria JN, Hu LS, Parney IF, Pafundi DH, Brinkmann DH, Laack NN, Giannini C, Burns TC, Kizilbash SH, Laramy JK, Swanson KR, Kaufmann TJ, Brown PD, Agar NYR, Galanis E, Buckner JC, Elmquist WF, Is the blood-brain barrier really disrupted in all glioblastomas? A critical assessment of existing clinical data, Neuro-Oncol. 20 (2018) 184–191. 10.1093/neuonc/nox175. [PubMed: 29016900]

[7]. Jain RK, Antiangiogenesis Strategies Revisited: From Starving Tumors to Alleviating Hypoxia, Cancer Cell. 26 (2014) 605–622. 10.1016/j.ccell.2014.10.006. [PubMed: 25517747]

[8]. Nia HT, Munn LL, Jain RK, Physical traits of cancer, Science. 370 (2020). 10.1126/science.aaz0868.

[9]. Li J, Wu J, Bao X, Honea N, Xie Y, Kim S, Sparreboom A, Sanai N, Quantitative and Mechanistic Understanding of AZD1775 Penetration across Human Blood-Brain Barrier in Glioblastoma Patients Using an IVIVE-PBPK Modeling Approach, Clin. Cancer Res. Off. J. Am. Assoc. Cancer Res 23 (2017) 7454–7466. 10.1158/1078-0432.CCR-17-0983.

[10]. Wang D, Wang C, Wang L, Chen Y, A comprehensive review in improving delivery of small-molecule chemotherapeutic agents overcoming the blood-brain/brain tumor barriers for glioblastoma treatment, Drug Deliv. 26 (2019) 551–565. 10.1080/10717544.2019.1616235. [PubMed: 31928355]

[11]. Hersh DS, Wadajkar AS, Roberts N, Perez JG, Connolly NP, Frenkel V, Winkles JA, Woodworth GF, Kim AJ, Evolving Drug Delivery Strategies to Overcome the Blood Brain Barrier, Curr. Pharm. Des 22 (2016) 1177–1193. [PubMed: 26685681]

[12]. Woodworth GF, Dunn GP, Nance EA, Hanes J, Brem H, Emerging Insights into Barriers to Effective Brain Tumor Therapeutics, Front. Oncol 4 (2014). 10.3389/fonc.2014.00126.

[13]. Aryal M, Arvanitis CD, Alexander PM, McDannold N, Ultrasound-mediated blood-brain barrier disruption for targeted drug delivery in the central nervous system, Adv. Drug Deliv. Rev 72 (2014) 94–109. 10.1016/j.addr.2014.01.008. [PubMed: 24462453]

[14]. Meng Y, Hynynen K, Lipsman N, Applications of focused ultrasound in the brain: from thermoablation to drug delivery, Nat. Rev. Neurol (2020) 1–16. 10.1038/s41582-020-00418-z. [PubMed: 31827266]

[15]. Hynynen K, McDannold N, Vykhodtseva N, Jolesz FA, Noninvasive MR Imaging-guided Focal Opening of the Blood-Brain Barrier in Rabbits1, Radiology. 220 (2001) 640–646. 10.1148/radiol.2202001804. [PubMed: 11526261]

[16]. Curley CT, Sheybani ND, Bullock TN, Price RJ, Focused Ultrasound Immunotherapy for Central Nervous System Pathologies: Challenges and Opportunities, Theranostics. 7 (2017) 3608–3623. 10.7150/thno.21225. [PubMed: 29109764]

[17]. Pandit R, Chen L, Götz J, The blood-brain barrier: Physiology and strategies for drug delivery, Adv. Drug Deliv. Rev 165–166 (2020) 1–14. 10.1016/j.addr.2019.11.009.

[18]. Meairs S, Facilitation of Drug Transport across the Blood-Brain Barrier with Ultrasound and Microbubbles, Pharmaceutics. 7 (2015) 275–293. 10.3390/pharmaceutics7030275. [PubMed: 26404357]

[19]. Timbie KF, Mead BP, Price RJ, Drug and gene delivery across the blood-brain barrier with focused ultrasound, J. Controlled Release 219 (2015) 61–75. 10.1016/j.jconrel.2015.08.059.

[20]. Burgess A, Shah K, Hough O, Hynynen K, Focused ultrasound-mediated drug delivery through the blood–brain barrier, Expert Rev. Neurother 15 (2015) 477–491. 10.1586/14737175.2015.1028369. [PubMed: 25936845]

[21]. Stride E, Coussios C, Nucleation, mapping and control of cavitation for drug delivery, Nat. Rev. Phys 1 (2019) 495–509. 10.1038/s42254-019-0074-y.

[22]. Frinking P, Segers T, Luan Y, Tranquart F, Three Decades of Ultrasound Contrast Agents: A Review of the Past, Present and Future Improvements, Ultrasound Med. Biol 46 (2020) 892–908. 10.1016/j.ultrasmedbio.2019.12.008. [PubMed: 31941587]

[23]. Blomley MJK, Cooke JC, Unger EC, Monaghan MJ, Cosgrove DO, Microbubble contrast agents: a new era in ultrasound, BMJ. 322 (2001) 1222–1225. 10.1136/bmj.322.7296.1222. [PubMed: 11358777]

[24]. Sheikov N, McDannold N, Sharma S, Hynynen K, Effect of Focused Ultrasound Applied With an Ultrasound Contrast Agent on the Tight Junctional Integrity of the Brain Microvascular

Endothelium, Ultrasound Med. Biol 34 (2008) 1093–1104. 10.1016/j.ultrasmedbio.2007.12.015. [PubMed: 18378064]

[25]. Alonso A, Reinz E, Jenne JW, Fatar M, Schmidt-Glenewinkel H, Hennerici MG, Meairs S, Reorganization of Gap Junctions after Focused Ultrasound Blood-Brain Barrier Opening in the Rat Brain, J. Cereb. Blood Flow Metab 30 (2010) 1394–1402. 10.1038/jcbfm.2010.41. [PubMed: 20332798]

[26]. Shang X, Wang P, Liu Y, Zhang Z, Xue Y, Mechanism of Low-Frequency Ultrasound in Opening Blood-Tumor Barrier by Tight Junction, J. Mol. Neurosci 43 (2011) 364–369. 10.1007/s12031-010-9451-9. [PubMed: 20852968]

[27]. Jalali S, Huang Y, Dumont DJ, Hynynen K, Focused ultrasound-mediated bbb disruption is associated with an increase in activation of AKT: experimental study in rats, BMC Neurol. 10 (2010) 114. 10.1186/1471-2377-10-114. [PubMed: 21078165]

[28]. Deng J, Huang Q, Wang F, Liu Y, Wang Z, Wang Z, Zhang Q, Lei B, Cheng Y, The Role of Caveolin-1 in Blood-Brain Barrier Disruption Induced by Focused Ultrasound Combined with Microbubbles, J. Mol. Neurosci 46 (2012) 677–687. 10.1007/s12031-011-9629-9. [PubMed: 21861133]

[29]. Xia C, Liu Y, Wang P, Xue Y, Low-Frequency Ultrasound Irradiation Increases Blood-Tumor Barrier Permeability by Transcellular Pathway in a Rat Glioma Model, J. Mol. Neurosci 48 (2012) 281–290. 10.1007/s12031-012-9770-0. [PubMed: 22528460]

[30]. McDannold N, Arvanitis CD, Vykhodtseva N, Livingstone MS, Temporary Disruption of the Blood-Brain Barrier by Use of Ultrasound and Microbubbles: Safety and Efficacy Evaluation in Rhesus Macaques, Cancer Res. 72 (2012) 3652–3663. 10.1158/0008-5472.CAN-12-0128. [PubMed: 22552291]

[31]. Todd N, Angolano C, Ferrari C, Devor A, Borsook D, McDannold N, Secondary effects on brain physiology caused by focused ultrasound-mediated disruption of the blood-brain barrier, J. Controlled Release 324 (2020) 450–459. 10.1016/j.jconrel.2020.05.040.

[32]. McMahon D, O'Reilly MA, Hynynen K, Therapeutic Agent Delivery Across the Blood-Brain Barrier Using Focused Ultrasound, Annu. Rev. Biomed. Eng (2021). 10.1146/annurev-bioeng-062117-121238.

[33]. McMahon D, Hynynen K, Acute Inflammatory Response Following Increased Blood-Brain Barrier Permeability Induced by Focused Ultrasound is Dependent on Microbubble Dose, Theranostics. 7 (2017) 3989–4000. 10.7150/thno.21630. [PubMed: 29109793]

[34]. Kovacs ZI, Kim S, Jikaria N, Qureshi F, Milo B, Lewis BK, Bresler M, Burks SR, Frank JA, Disrupting the blood-brain barrier by focused ultrasound induces sterile inflammation, Proc. Natl. Acad. Sci (2016) 201614777. 10.1073/pnas.1614777114.

[35]. Arvanitis CD, Livingstone MS, Vykhodtseva N, McDannold N, Controlled Ultrasound-Induced Blood-Brain Barrier Disruption Using Passive Acoustic Emissions Monitoring, PLOS ONE. 7 (2012) e45783. 10.1371/journal.pone.0045783. [PubMed: 23029240]

[36]. Baseri B, Choi JJ, Tung Y-S, Konofagou EE, Multi-Modality Safety Assessment of Blood-Brain Barrier Opening Using Focused Ultrasound and Definity Microbubbles: A Short-Term Study, Ultrasound Med. Biol 36 (2010) 1445–1459. 10.1016/j.ultrasmedbio.2010.06.005. [PubMed: 20800172]

[37]. Song K-H, Harvey BK, Borden MA, State-of-the-art of microbubble-assisted blood-brain barrier disruption, Theranostics. 8 (2018) 4393–4408. 10.7150/thno.26869. [PubMed: 30214628]

[38]. McMahon D, Lassus A, Gaud E, Jeannot V, Hynynen K, Microbubble formulation influences inflammatory response to focused ultrasound exposure in the brain, Sci. Rep 10 (2020) 21534. 10.1038/s41598-020-78657-9. [PubMed: 33299094]

[39]. Alkins R, Burgess A, Ganguly M, Francia G, Kerbel R, Weis WS, Hynynen K, Focused Ultrasound Delivers Targeted Immune Cells to Metastatic Brain Tumors, Cancer Res. 73 (2013) 1892–1899. 10.1158/0008-5472.CAN-12-2609. [PubMed: 23302230]

[40]. Alkins R, Burgess A, Kerbel R, Weis WS, Hynynen K, Early treatment of HER2-amplified brain tumors with targeted NK-92 cells and focused ultrasound improves survival, Neuro-Oncol. 18 (2016) 974–981. 10.1093/neuonc/nov318. [PubMed: 26819443]

[41]. Kovacs Z, Werner B, Rassi A, Sass JO, Martin-Fiori E, Bernasconi M, Prolonged survival upon ultrasound-enhanced doxorubicin delivery in two syngenic glioblastoma mouse models, J. Controlled Release 187 (2014) 74–82. 10.1016/j.jconrel.2014.05.033.

[42]. McDannold N, Zhang Y, Supko JG, Power C, Sun T, Peng C, Vykhodtseva N, Golby AJ, Reardon DA, Acoustic feedback enables safe and reliable carboplatin delivery across the blood-brain barrier with a clinical focused ultrasound system and improves survival in a rat glioma model, Theranostics. 9 (2019) 6284–6299. 10.7150/thno.35892. [PubMed: 31534551]

[43]. Arvanitis CD, Askoxylakis V, Guo Y, Datta M, Kloepper J, Ferraro GB, Bernabeu MO, Fukumura D, McDannold N, Jain RK, Mechanisms of enhanced drug delivery in brain metastases with focused ultrasound-induced blood-tumor barrier disruption, Proc. Natl. Acad. Sci 115 (2018) E8717–E8726. 10.1073/pnas.1807105115. [PubMed: 30150398]

[44]. Aryal M, Fischer K, Gentile C, Gitto S, Zhang Y-Z, McDannold N, Effects on P-Glycoprotein Expression after Blood-Brain Barrier Disruption Using Focused Ultrasound and Microbubbles, PLOS ONE. 12 (2017) e0166061. 10.1371/journal.pone.0166061. [PubMed: 28045902]

[45]. Goutal S, Gerstenmayer M, Auvity S, Caillé F, Mériaux S, Buvat I, Larrat B, Tournier N, Physical blood-brain barrier disruption induced by focused ultrasound does not overcome the transporter-mediated efflux of erlotinib, J. Controlled Release 292 (2018) 210–220. 10.1016/j.jconrel.2018.11.009.

[46]. Robey RW, Pluchino KM, Hall MD, Fojo AT, Bates SE, Gottesman MM, Revisiting the role of ABC transporters in multidrug-resistant cancer, Nat. Rev. Cancer 18 (2018) 452–464. 10.1038/s41568-018-0005-8. [PubMed: 29643473]

[47]. Drago JZ, Modi S, Chandarlapaty S, Unlocking the potential of antibody–drug conjugates for cancer therapy, Nat. Rev. Clin. Oncol (2021) 1–18. 10.1038/s41571-021-00470-8. [PubMed: 33060841]

[48]. Mullard A, FDA approves 100th monoclonal antibody product, Nat. Rev. Drug Discov (2021). 10.1038/d41573-021-00079-7.

[49]. Kobus T, Zervantonakis IK, Zhang Y, McDannold NJ, Growth inhibition in a brain metastasis model by antibody delivery using focused ultrasound-mediated blood-brain barrier disruption, J. Control. Release Off. J.Control. Release Soc 238 (2016) 281–288. 10.1016/j.jconrel.2016.08.001.

[50]. Sheybani ND, Breza VR, Paul S, McCauley KS, Berr SS, Miller GW, Neumann KD, Price RJ, ImmunoPET-informed sequence for focused ultrasound-targeted mCD47 blockade controls glioma, J. Controlled Release. 331 (2021) 19–29. 10.1016/j.jconrel.2021.01.023.

[51]. Sabbagh A, Beccaria K, Ling X, Marisetty A, Ott M, Caruso H, Barton E, Kong L-Y, Fang D, Latha K, Zhang DY, Wei J, de Groot JF, Curran MA, Rao G, Hu J, Desseaux C, Bouchoux G, Canney M, Carpentier A, Heimberger AB, Opening of the blood-brain barrier using low-intensity pulsed ultrasound enhances responses to immunotherapy in preclinical glioma models, Clin. Cancer Res (2021). 10.1158/1078-0432.CCR-20-3760.

[52]. Rao G, Latha K, Ott M, Sabbagh A, Marisetty A, Ling X, Zamler D, Doucette TA, Yang Y, Kong L-Y, Wei J, Fuller GN, Benavides F, Sonabend AM, Long J, Li S, Curran M, Heimberger AB, Anti-PD-1 Induces M1 Polarization in the Glioma Microenvironment and Exerts Therapeutic Efficacy in the Absence of CD8 Cytotoxic T Cells, Clin. Cancer Res. Off. J. Am. Assoc. Cancer Res 26 (2020) 4699–4712. 10.1158/1078-0432.CCR-19-4110.

[53]. Hutter G, Theruvath J, Graef CM, Zhang M, Schoen MK, Manz EM, L Bennett M, Olson A, Azad TD, Sinha R, Chan C, Kahn SA, Gholamin S, Wilson C, Grant G, He J, L Weissman I, Mitra SS, Cheshier SH, Microglia are effector cells of CD47-SIRPa antiphagocytic axis disruption against glioblastoma, Proc. Natl. Acad. Sci 116 (2019) 997–1006. 10.1073/pnas.1721434116. [PubMed: 30602457]

[54]. Curley CT, Mead BP, Negron K, Kim N, Garrison WJ, Miller GW, Kingsmore KM, Thim EA, Song J, Munson JM, Klibanov AL, Suk JS, Hanes J, Price RJ, Augmentation of brain tumor interstitial flow via focused ultrasound promotes brain-penetrating nanoparticle dispersion and transfection, Sci. Adv 6 (2020) eaay1344. 10.1126/sciadv.aay1344. [PubMed: 32494662]

[55]. Aryal M, Vykhodtseva N, Zhang Y-Z, McDannold N, Multiple sessions of liposomal doxorubicin delivery via focused ultrasound mediated blood-brain barrier disruption: A safety study, J. Controlled Release 204 (2015) 60–69. 10.1016/j.jconrel.2015.02.033.

[56]. Sun T, Zhang Y, Power C, Alexander PM, Sutton JT, Aryal M, Vykhodtseva N, L Miller E, McDannold NJ, Closed-loop control of targeted ultrasound drug delivery across the blood-brain/tumor barriers in a rat glioma model, Proc. Natl. Acad. Sci (2017) 201713328. 10.1073/pnas.1713328114.

[57]. Timbie KF, Afzal U, Date A, Zhang C, Song J, Wilson Miller G, Suk JS, Hanes J, Price RJ, MR image-guided delivery of cisplatin-loaded brain-penetrating nanoparticles to invasive glioma with focused ultrasound, J. Controlled Release 263 (2017) 120–131. 10.1016/j.jconrel.2017.03.017.

[58]. Guo Y, Lee H, Fang Z, Velalopoulou A, Kim J, Thomas MB, Liu J, Abramowitz RG, Kim Y, Coskun AF, Krummel DP, Sengupta S, MacDonald TJ, Arvanitis C, Single-cell analysis reveals effective siRNA delivery in brain tumors with microbubble-enhanced ultrasound and cationic nanoparticles, Sci. Adv 7 (2021) eabf7390. 10.1126/sciadv.abf7390. [PubMed: 33931452]

[59]. Wilhelm S, Tavares AJ, Dai Q, Ohta S, Audet J, Dvorak HF, Chan WCW, Analysis of nanoparticle delivery to tumours, Nat. Rev. Mater 1(2016) 1–12. 10.1038/natrevmats.2016.14.

[60]. Pellow C, O'Reilly MA, Hynynen K, Zheng G, Goertz DE, Simultaneous Intravital Optical and Acoustic Monitoring of Ultrasound-Triggered Nanobubble Generation and Extravasation, Nano Lett. (2020). 10.1021/acs.nanolett.0c01310.

[61]. Chen P-Y, Liu H-L, Hua M-Y, Yang H-W, Huang C-Y, Chu P-C, Lyu L-A, Tseng l.-C., Feng L-Y, Tsai H-C, Chen S-M, Lu Y-J, Wang J-J, Yen T-C, Ma Y-H, Wu T, Chen J-P, Chuang J-I, Shin J-W, Hsueh C, Wei K-C, Novel magnetic/ultrasound focusing system enhances nanoparticle drug delivery for glioma treatment, Neuro-Oncol. 12 (2010) 1050–1060. 10.1093/neuonc/noq054. [PubMed: 20663792]

[62]. Liu H-L, Hua M-Y, Yang H-W, Huang C-Y, Chu P-C, Wu J-S, Tseng I-C, Wang J-J, Yen T-C, Chen P-Y, Wei K-C, Magnetic resonance monitoring of focused ultrasound/magnetic nanoparticle targeting delivery of therapeutic agents to the brain, Proc. Natl. Acad. Sci. U. S. A 107 (2010) 15205–15210. 10.1073/pnas.1003388107. [PubMed: 20696897]

[63]. Fan C-H, Cheng Y-H, Ting C-Y, Ho Y-J, Hsu P-H, Liu H-L, Yeh C-K, Ultrasound/Magnetic Targeting with SPIO-DOX-Microbubble Complex for Image-Guided Drug Delivery in Brain Tumors, Theranostics. 6 (2016) 1542–1556. 10.7150/thno.15297. [PubMed: 27446489]

[64]. Kovacs Z, Werner B, Rassi A, Sass JO, Martin-Fiori E, Bernasconi M, Prolonged survival upon ultrasound-enhanced doxorubicin delivery in two syngenic glioblastoma mouse models, J. Controlled Release 187 (2014) 74–82. 10.1016/j.jconrel.2014.05.033.

[65]. Park J, Aryal M, Vykhodtseva N, Zhang Y-Z, McDannold N, Evaluation of permeability, doxorubicin delivery, and drug retention in a rat brain tumor model after ultrasound-induced blood-tumor barrier disruption, J. Controlled Release 250 (2017) 77–85. 10.1016/j.jconrel.2016.10.011.

[66]. Ishida J, Alii S, Bondoc A, Golbourn B, Sabha N, Mikloska K, Krumholtz S, Srikanthan D, Fujita N, Luck A, Maslink C, Smith C, Hynynen K, Rutka J, MRI-guided focused ultrasound enhances drug delivery in experimental diffuse intrinsic pontine glioma, J. Controlled Release 330 (2021) 1034–1045. 10.1016/j.jconrel.2020.11.010.

[67]. Liu H-L, Hua M-Y, Chen P-Y, Chu P-C, Pan C-H, Yang H-W, Huang C-Y, Wang J-J, Yen T-C, Wei K-C, Blood-Brain Barrier Disruption with Focused Ultrasound Enhances Delivery of Chemotherapeutic Drugs for Glioblastoma Treatment, Radiology. 255 (2010) 415–425. 10.1148/radiol.10090699. [PubMed: 20413754]

[68]. Wei K-C, Chu P-C, Wang H-YJ, Huang C-Y, Chen P-Y, Tsai H-C, Lu Y-J, Lee P-Y, Tseng I-C, Feng L-Y, Hsu P-W, Yen T-C, Liu H-L, Focused Ultrasound-Induced Blood-Brain Barrier Opening to Enhance Temozolomide Delivery for Glioblastoma Treatment: A Preclinical Study, PLOS ONE. 8 (2013) e58995. 10.1371/journal.pone.0058995. [PubMed: 23527068]

[69]. Dong Q, He L, Chen L, Deng Q, Opening the Blood-Brain Barrier and Improving the Efficacy of Temozolomide Treatments of Glioblastoma Using Pulsed, Focused Ultrasound with a Microbubble Contrast Agent, BioMed Res. Int 2018 (2018) e6501508. 10.1155/2018/6501508.

[70]. Liu H-L, Huang C-Y, Chen J-Y, Wang H-YJ, Chen P-Y, Wei K-C, Pharmacodynamic and Therapeutic Investigation of Focused Ultrasound-Induced Blood-Brain Barrier Opening for Enhanced Temozolomide Delivery in Glioma Treatment, PLOS ONE. 9 (2014) ell4311. 10.1371/journal.pone.0114311.

[71]. Dréan A, Lemaire N, Bouchoux G, Goldwirt L, Canney M, Goli L, Bouzidi A, Schmitt C, Guehennec J, Verreault M, Sanson M, Delattre J-Y, Mokhtari K, Sottilini F, Carpentier A, Idbaih A, Temporary blood-brain barrier disruption by low intensity pulsed ultrasound increases carboplatin delivery and efficacy in preclinical models of glioblastoma, J. Neurooncol 144 (2019) 33–41. 10.1007/s11060-019-03204-0. [PubMed: 31197598]

[72]. McDannold N, Zhang Y, Supko JG, Power C, Sun T, Vykhodtseva N, Golby AJ, Reardon DA, Blood-brain barrier disruption and delivery of irinotecan in a rat model using a clinical transcranial MRI-guided focused ultrasound system, Sci. Rep 10 (2020). 10.1038/s41598-020-65617-6.

[73]. Wei H-J, Upadhyayula PS, Pouliopoulos AN, Englander ZK, Zhang X, Jan C.-l., Guo J, Mela A, Zhang Z, Wang TJC, Bruce JN, Canoll PD, Feldstein NA, Zacharoulis S, Konofagou EE, Wu C-C, Focused Ultrasound-Mediated Blood-Brain Barrier Opening Increases Delivery and Efficacy of Etoposide for Glioblastoma Treatment, Int. J. Radiat. Oncol (2020). 10.1016/j.ijrobp.2020.12.019.

[74]. Englander ZK, Wei H-J, Pouliopoulos AN, Bendau E, Upadhyayula P, Jan C-I, Spinazzi EF, Yoh N, Tazhibi M, McQuillan NM, Wang TJC, Bruce JN, Canoll P, Feldstein NA, Zacharoulis S, Konofagou EE, Wu C-C, Focused ultrasound mediated blood-brain barrier opening is safe and feasible in a murine pontine glioma model, Sci. Rep 11 (2021) 6521. 10.1038/s41598-021-85180-y. [PubMed: 33753753]

[75]. Park E-J, Zhang Y-Z, Vykhodtseva N, McDannold N, Ultrasound-mediated blood-brain/blood-tumor barrier disruption improves outcomes with trastuzumab in a breast cancer brain metastasis model, J. Control. Release Off. J. Control. Release Soc 163 (2012) 277–284. 10.1016/j.jconrel.2012.09.007.

[76]. Chen P-Y, Hsieh H-Y, Huang C-Y, Lin C-Y, Wei K-C, Liu H-L, Focused ultrasound-induced blood-brain barrier opening to enhance interleukin-12 delivery for brain tumor immunotherapy: a preclinical feasibility study, J. Transl. Med 13 (2015). 10.1186/s12967-015-0451-y.

[77]. Liu H-L, Hsu P-H, Lin C-Y, Huang C-W, Chai W-Y, Chu P-C, Huang C-Y, Chen P-Y, Yang L-Y, Kuo JS, Wei K-C, Focused Ultrasound Enhances Central Nervous System Delivery of Bevacizumab for Malignant Glioma Treatment, Radiology. 281 (2016) 99–108. 10.1148/radiol.2016152444. [PubMed: 27192459]

[78]. Brighi C, Reid L, White AL, Genovesi LA, Kojic M, Millar A, Bruce Z, Day BW, Rose S, Whittaker AK, Puttick S, MR-guided focused ultrasound increases antibody delivery to nonenhancing high-grade glioma, Neuro-Oncol. Adv 2 (2020). 10.1093/noajnl/vdaa030.

[79]. Sabbagh A, Beccaria K, Ling X, Marisetty A, Ott M, Caruso H, Barton E, Kong L-Y, Fang D, Latha K, Zhang DY, Wei J, de Groot JF, Curran MA, Rao G, Hu J, Desseaux C, Bouchoux G, Canney M, Carpentier A, Heimberger AB, Opening of the blood-brain barrier using low-intensity pulsed ultrasound enhances responses to immunotherapy in preclinical glioma models, Clin. Cancer Res. Off. J. Am. Assoc. Cancer Res (2021). 10.1158/1078-0432.CCR-20-3760.

[80]. Treat LH, McDannold N, Zhang Y, Vykhodtseva N, Hynynen K, Improved Anti-Tumor Effect of Liposomal Doxorubicin After Targeted Blood-Brain Barrier Disruption by MRI-Guided Focused Ultrasound in Rat Glioma, Ultrasound Med. Biol 38(2012) 1716–1725. 10.1016/j.ultrasmedbio.2012.04.015. [PubMed: 22818878]

[81]. Yang F-Y, Wang H-E, Liu R-S, Teng M-C, Li J-J, Lu M, Wei M-C, Wong T-T, Pharmacokinetic Analysis of 111ln-Labeled Liposomal Doxorubicin in Murine Glioblastoma after Blood-Brain Barrier Disruption by Focused Ultrasound, PLOS ONE. 7 (2012) e45468. 10.1371/journal.pone.0045468. [PubMed: 23029030]

[82]. Yang F-Y, Teng M-C, Lu M, Liang H-F, Lee Y-R, Yen C-C, Liang M-L, Wong T-T, Treating glioblastoma multiforme with selective high-dose liposomal doxorubicin chemotherapy induced by repeated focused ultrasound, Int. J. Nanomedicine 7 (2012) 965–974. 10.2147/IJN.S29229. [PubMed: 22393293]

[83]. Aryal M, Vykhodtseva N, Zhang Y-Z, Park J, McDannold N, Multiple treatments with liposomal doxorubicin and ultrasound-induced disruption of blood-tumor and blood-brain barriers improves outcomes in a rat glioma model, J. Control. Release Off. J. Control. Release Soc 169 (2013) 103–111. 10.1016/j.jconrel.2013.04.007.

[84]. Aryal M, Park J, Vykhodtseva N, Zhang Y-Z, McDannold N, Enhancement in blood-tumor barrier permeability and delivery of liposomal doxorubicin using focused ultrasound and microbubbles: evaluation during tumor progression in a rat glioma model, Phys. Med. Biol 60 (2015) 2511–2527. 10.1088/0031-9155/60/6/2511. [PubMed: 25746014]

[85]. Yang F-Y, Wong T-T, Teng M-C, Liu R-S, Lu M, Liang H-F, Wei M-C, Focused ultrasound and interleukin-4 receptor-targeted liposomal doxorubicin for enhanced targeted drug delivery and antitumor effect in glioblastoma multiforme, J. Controlled Release 160 (2012) 652–658. 10.1016/j.jconrel.2012.02.023.

[86]. Shen Y, Pi Z, Yan F, Yeh C-K, Zeng X, Diao X, Hu Y, Chen S, Chen X, Zheng H, Enhanced delivery of paclitaxel liposomes using focused ultrasound with microbubbles for treating nude mice bearing intracranial glioblastoma xenografts, Int. J. Nanomedicine 12 (2017) 5613–5629. 10.2147/IJN.S136401. [PubMed: 28848341]

[87]. Zhao Y-Z, Lin Q, Wong HL, Shen X-T, Yang W, Xu H-L, Mao K-L, Tian F-R, Yang J-J, Xu J, Xiao J, Lu C-T, Glioma-targeted therapy using Cilengitide nanoparticles combined with UTMD enhanced delivery, J. Controlled Release 224 (2016) 112–125. 10.1016/j.jconrel.2016.01.015.

[88]. Diaz RJ, McVeigh PZ, O'Reilly MA, Burrell K, Bebenek M, Smith C, Etame AB, Zadeh G, Hynynen K, Wilson BC, Rutka JT, Focused ultrasound delivery of Raman nanoparticles across the blood-brain barrier: Potential for targeting experimental brain tumors, Nanomedicine Nanotechnol. Biol. Med 10 (2014) e1075–e1087. 10.1016/j.nano.2013.12.006.

[89]. Coluccia D, Figueiredo CA, Wu MY, Riemenschneider AN, Diaz R, Luck A, Smith C, Das S, Ackerley C, O'Reilly M, Hynynen K, Rutka JT, Enhancing Glioblastoma Treatment using Cisplatin-Gold-Nanoparticle Conjugates and Targeted Delivery with Magnetic Resonance-Guided Focused Ultrasound, Nanomedicine Nanotechnol. Biol. Med (2018). 10.1016/j.nano.2018.01.021.

[90]. Zhang DY, Dmello C, Chen L, Arrieta VA, Gonzalez-Buendia E, Kane JR, Magnusson LP, Baran A, James CD, Horbinski C, Carpentier A, Desseaux C, Canney M, Muzzio M, Stupp R, Sonabend AM, Ultrasound-mediated Delivery of Paclitaxel for Glioma: A Comparative Study of Distribution, Toxicity, and Efficacy of Albumin-bound Versus Cremophor Formulations, Clin. Cancer Res 26 (2020) 477–486. 10.1158/1078-0432.CCR-19-2182. [PubMed: 31831565]

[91]. Chen Y-C, Chiang C-F, Wu S-K, Chen L-F, Hsieh W-Y, Lin W-L, Targeting microbubbles-carrying TGFβ1 inhibitor combined with ultrasound sonication induce BBB/BTB disruption to enhance nanomedicine treatment for brain tumors, J. Controlled Release 211 (2015) 53–62. 10.1016/j.jconrel.2015.05.288.

[92]. Wu M, Chen W, Chen Y, Zhang H, Liu C, Deng Z, Sheng Z, Chen J, Liu X, Yan F, Zheng H, Focused Ultrasound-Augmented Delivery of Biodegradable Multifunctional Nanoplatforms for Imaging-Guided Brain Tumor Treatment, Adv. Sci 5 (2018) 1700474. 10.1002/advs.201700474.

[93]. Ting C-Y, Fan C-H, Liu H-L, Huang C-Y, Hsieh H-Y, Yen T-C, Wei K-C, Yeh C-K, Concurrent blood-brain barrier opening and local drug delivery using drug-carrying microbubbles and focused ultrasound for brain glioma treatment, Biomaterials. 33 (2012) 704–712. 10.1016/j.biomaterials.2011.09.096. [PubMed: 22019122]

[94]. Fan C-H, Ting C-Y, Liu H-L, Huang C-Y, Hsieh H-Y, Yen T-C, Wei K-C, Yeh C-K, Antiangiogenic-targeting drug-loaded microbubbles combined with focused ultrasound for glioma treatment, Biomaterials. 34 (2013) 2142–2155. 10.1016/j.biomaterials.2012.11.048. [PubMed: 23246066]

[95]. Zhao G, Huang Q, Wang F, Zhang X, Hu J, Tan Y, Huang N, Wang Z, Wang Z, Cheng Y, Targeted shRNA-loaded liposome complex combined with focused ultrasound for blood brain barrier disruption and suppressing glioma growth, Cancer Lett. 418 (2018) 147–158. 10.1016/j.canlet.2018.01.035. [PubMed: 29339208]

[96]. Baghirov H, Snipstad S, Sulheim E, Berg S, Hansen R, Thorsen F, Mørch Y, de L. Davies C, Åslund AKO, Ultrasound-mediated delivery and distribution of polymeric nanoparticles in the normal brain parenchyma of a metastatic brain tumour model, PLOS ONE. 13 (2018) e0191102. 10.1371/journal.pone.0191102. [PubMed: 29338016]

[97]. Fan C-H, Ting C-Y, Lin H-J, Wang C-H, Liu H-L, Yen T-C, Yeh C-K, SPIO-conjugated, doxorubicin-loaded microbubbles for concurrent MRI and focused-ultrasound enhanced brain-

tumor drug delivery, Biomaterials. 34 (2013) 3706–3715. 10.1016/j.biomaterials.2013.01.099. [PubMed: 23433776]

[98]. Yang Q, Zhou Y, Chen J, Huang N, Wang Z, Cheng Y, Gene Therapy for Drug-Resistant Glioblastoma via Lipid-Polymer Hybrid Nanoparticles Combined with Focused Ultrasound, Int. J. Nanomedicine Volume 16 (2021) 185–199. 10.2147/IJN.S286221. [PubMed: 33447034]

[99]. Yang F-Y, Chang W-Y, Lin W-T, Hwang J-J, Chien Y-C, Wang H-E, Tsai M-L, Focused ultrasound enhanced molecular imaging and gene therapy for multifusion reporter gene in glioma-bearing rat model, Oncotarget. 6 (2015) 36260–36268. [PubMed: 26429860]

[100]. Chang E-L, Ting C-Y, Hsu P-H, Lin Y-C, Liao E-C, Huang C-Y, Chang Y-C, Chan H-L, Chiang C-S, Liu H-L, Wei K-C, Fan C-H, Yeh C-K, Angiogenesis-targeting microbubbles combined with ultrasound-mediated gene therapy in brain tumors, J. Controlled Release 255 (2017) 164–175. 10.1016/j.jconrel.2017.04.010.

[101]. Askoxylakis V, Arvanitis CD, Wong CSF, Ferraro GB, Jain RK, Emerging strategies for delivering antiangiogenic therapies to primary and metastatic brain tumors, Adv. Drug Deliv. Rev 119 (2017) 159–174. 10.1016/j.addr.2017.06.011. [PubMed: 28648712]

[102]. Samson A, Scott KJ, Taggart D, West EJ, Wilson E, Nuovo GJ, Thomson S, Corns R, Mathew RK, Fuller MJ, Kottke TJ, Thompson JM, Ilett EJ, Cockle JV, van Hille P, Sivakumar G, Poison ES, Turnbull SJ, Appleton DS, Migneco G, Rose AS, Coffey MC, Beirne DA, Collinson FJ, Ralph C, Anthoney DA, Twelves CJ, Furness AJ, Quezada SA, Wurdak H, Errington-Mais F, Pandha H, Harrington KJ, Selby PJ, Vile RG, Griffin SD, Stead LF, Short SC, Melcher AA, Intravenous delivery of oncolytic reovirus to brain tumor patients immunologically primes for subsequent checkpoint blockade, Sci. Transl. Med 10 (2018) eaam7577. 10.1126/scitranslmed.aam7577. [PubMed: 29298869]

[103]. Bommareddy PK, Shettigar M, Kaufman HL, Integrating oncolytic viruses in combination cancer immunotherapy, Nat. Rev. Immunol 18 (2018) 498. 10.1038/s41577-018-0014-6. [PubMed: 29743717]

[104]. Mainprize T, Lipsman N, Huang Y, Meng Y, Bethune A, Ironside S, Heyn C, Alkins R, Trudeau M, Sahgal A, Perry J, Hynynen K, Blood-Brain Barrier Opening in Primary Brain Tumors with Non-invasive MR-Guided Focused Ultrasound: A Clinical Safety and Feasibility Study, Sci. Rep 9 (2019) 321. 10.1038/s41598-018-36340-0. [PubMed: 30674905]

[105]. Idbaih A, Canney M, Belin L, Desseaux C, Vignot A, Bouchoux G, Asquier N, Law-Ye B, Leclercq D, Bissery A, Rycke YD, Trosch C, Capelle L, Sanson M, Hoang-Xuan K, Dehais C, Houillier C, Laigle-Donadey F, Mathon B, Andre A, Lafon C, Chapelon J-Y, Delattre J-Y, Carpentier A, Safety and Feasibility of Repeated and Transient Blood-Brain Barrier Disruption by Pulsed Ultrasound in Patients with Recurrent Glioblastoma, Clin. Cancer Res (2019) clincanres.3643.2018. 10.1158/1078-0432.CCR-18-3643.

[106]. Chen K-T, Chai W-Y, Lin Y-J, Lin C-J, Chen P-Y, Tsai H-C, Huang C-Y, Kuo JS, Liu H-L, Wei K-C, Neuronavigation-guided focused ultrasound for transcranial blood-brain barrier opening and immunostimulation in brain tumors, Sci. Adv 7 (2021) eabd0772. 10.1126/sciadv.abd0772. [PubMed: 33547073]

[107]. Wen PY, Weller M, Lee EQ, Alexander BM, Barnholtz-Sloan JS, Barthel FP, Batchelor TT, Bindra RS, Chang SM, Chiocca EA, Cloughesy TF, DeGroot JF, Galanis E, Gilbert MR, Hegi ME, Horbinski C, Huang RY, Lassman AB, Le Rhun E, Lim M, Mehta MP, Mellinghoff IK, Minniti G, Nathanson D, Platten M, Preusser M, Roth P, Sanson M, Schiff D, Short SC, Taphoorn MJB, Tonn J-C, Tsang J, Verhaak RGW, von Deimling A, Wick W, Zadeh G, Reardon DA, Aldape KD, van den Bent MJ, Glioblastoma in adults: a Society for Neuro-Oncology (SNO) and European Society of Neuro-Oncology (EANO) consensus review on current management and future directions, Neuro-Oncol. (2020) noaa106. 10.1093/neuonc/noaa106.

[108]. Gilbert MR, Wang M, Aldape KD, Stupp R, Hegi ME, Jaeckle KA, Armstrong TS, Wefel JS, Won M, Blumenthal DT, Mahajan A, Schultz CJ, Erridge S, Baumert B, Hopkins KI, Tzuk-Shina T, Brown PD, Chakravarti A, Curran WJ, Mehta MP, Dose-Dense Temozolomide for Newly Diagnosed Glioblastoma: A Randomized Phase III Clinical Trial, J. Clin. Oncol 31 (2013) 4085–4091. 10.1200/JCO.2013.49.6968. [PubMed: 24101040]

[109]. Quinn JA, Jiang SX, Reardon DA, Desjardins A, Vredenburgh JJ, Friedman AH, Sampson JH, McLendon RE, Herndon JE, Friedman HS, Phase II trial of temozolomide (TMZ) plus

irinotecan (CPT-11) in adults with newly diagnosed glioblastoma multiforme before radiotherapy, J. Neurooncol 95 (2009) 393–400. 10.1007/s11060-009-9937-x. [PubMed: 19533023]

[110]. Chinot OL, Wick W, Mason W, Henriksson R, Saran F, Nishikawa R, Carpentier AF, Hoang-Xuan K, Kavan P, Cernea D, Brandes AA, Hilton M, Abrey L, Cloughesy T, Bevacizumab plus Radiotherapy–Temozolomide for Newly Diagnosed Glioblastoma, N. Engl. J. Med 370 (2014) 709–722. 10.1056/NEJMoa1308345. [PubMed: 24552318]

[111]. Stupp R, Hegi ME, Gorlia T, Erridge SC, Perry J, Hong Y-K, Aldape KD, Lhermitte B, Pietsch T, Grujicic D, Steinbach JP, Wick W, Tarnawski R, Nam D-H, Hau P, Weyerbrock A, Taphoorn MJB, Shen C-C, Rao N, Thurzo L, Herrlinger U, Gupta T, Kortmann R-D, Adamska K, McBain C, Brandes AA, Tonn JC, Schnell O, Wiegel T, Kim C-Y, Nabors LB, Reardon DA, van den Bent MJ, Hicking C, Markivskyy A, Picard M, Weller M, Cilengitide combined with standard treatment for patients with newly diagnosed glioblastoma with methylated MGMT promoter (CENTRIC EORTC 26071-22072 study): a multicentre, randomised, open-label, phase 3 trial, Lancet Oncol. 15 (2014) 1100–1108. 10.1016/S1470-2045(14)70379-1. [PubMed: 25163906]

[112]. Weller M, Butowski N, Tran DD, Recht LD, Lim M, Hirte H, Ashby L, Mechtler L, Goldlust SA, Iwamoto F, Drappatz J, O'Rourke DM, Wong M, Hamilton MG, Finocchiaro G, Perry J, Wick W, Green J,He Y, Turner CD, Yellin MJ, Keler T, Davis TA, Stupp R, Sampson JH, Butowski N, Campian J, Recht L, Lim M, Ashby L, Drappatz J, Hirte H, Iwamoto F, Mechtler L, Goldlust S, Becker K, Barnett G, Nicholas G, Desjardins A, Benkers T, Wagle N, Groves M, Kesari S, Horvath Z, Merrell R, Curry R, O'Rourke J, Schuster D, Wong M, Mrugala M, Jensen R, Trusheim J, Lesser G, Belanger K, Sloan A, Purow B, Fink K, Raizer J, Schulder M, Nair S, Peak S, Perry J, Brandes A, Weller M, Mohile N, Landolfi J, Olson J, Finocchiaro G, Jennens R, DeSouza P, Robinson B, Crittenden M, Shih K, Flowers A, Ong S, Connelly J, Hadjipanayis C, Giglio P, Mott F, Mathieu D, Lessard N, Sepulveda SJ, Lövey J, Wheeler H, Inglis P-L, Hardie C, Bota D, Lesniak M, Portnow J, Frankel B, Junck L, Thompson R, Berk L, McGhie J, Macdonald D, Saran F, Soffietti R, Blumenthal D, André de SBCM, Nowak A, Singhal N, Hottinger A, Schmid A, Srkalovic G, Baskin D, Fadul C, Nabors L, LaRocca R, Villano J, Paleologos N, Kavan P, Pitz M, Thiessen B, Idbaih A, Frenel JS, Domont J, Grauer O, Hau P, Marosi C, Sroubek J, Hovey E, Sridhar PS, Cher L, Dunbar E, Coyle T, Raymond J, Barton K, Guarino M, Raval S, Stea B, Dietrich J, Hopkins K, Erridge S, Steinbach J-P, Pineda LE, Balana QC, Sonia del BB, Wenczl M, Molnár K, Hideghéty K, Lossos A, Myra van L, Levy A, Harrup R, Patterson W, Lwin Z, Sathornsumetee S, Lee E-J, Ho J-T, Emmons S, Duic JP, Shao S, Ashamalla H, Weaver M, Lutzky J, Avgeropoulos N, Hanna W, Nadipuram M, Cecchi G, O'Donnell R, Pannullo S, Carney J, Hamilton M, MacNeil M, Beaney R, Fabbro M, Schnell O, Fietkau R, Stockhammer G, Malinova B, Odrazka K, Sames M, Miguel Gil G, Razis E, Lavrenkov K, Castro G, Ramirez F, Baldotto C, Viola F, Malheiros S, Lickliter J, Gauden S, Dechaphunkul A, Thaipisuttikul I, Thotathil Z, Ma H.-l., Cheng W-Y, Chang C-H, Salas F, Dietrich P-Y, Mamot C, Nayak L, Nag S, Rindopepimut with temozolomide for patients with newly diagnosed, EGFRvIII-expressing glioblastoma (ACT IV): a randomised, double-blind, international phase 3 trial, Lancet Oncol. 18 (2017) 1373–1385. 10.1016/S1470-2045(17)30517-X. [PubMed: 28844499]

[113]. Anastasiadis P, Gandhi D, Guo Y, Ahmed A-K, Bentzen SM, Arvanitis C, Woodworth GF, Localized blood–brain barrier opening in infiltrating gliomas with MRI-guided acoustic emissions–controlled focused ultrasound, Proc. Natl. Acad. Sci 118 (2021). 10.1073/pnas.2103280118.

[114]. Idbaih A, Canney M, Belin L, Desseaux C, Vignot A, Bouchoux G, Asquier N, Law-Ye B, Leclercq D, Bissery A, Rycke YD, Trosch C, Capelle L, Sanson M, Hoang-Xuan K, Dehais C, Houillier C, Laigle-Donadey F, Mathon B, André A, Lafon C, Chapelon J-Y, Delattre J-Y, Carpentier A, Safety and Feasibility of Repeated and Transient Blood-Brain Barrier Disruption by Pulsed Ultrasound in Patients with Recurrent Glioblastoma, Clin. Cancer Res (2019) clincanres.3643.2018. 10.1158/1078-0432.CCR-18-3643.

[115]. Fry FJ, Barger JE, Acoustical properties of the human skull, J Acoust Soc Am. 63 (1978) 1576–90. [PubMed: 690336]

[116]. Pinton G, Aubry J-F, Bossy E, Muller M, Pernot M, Tanter M, Attenuation, scattering, and absorption of ultrasound in the skull bone, Med. Phys 39 (2012) 299–307. 10.1118/1.3668316. [PubMed: 22225300]

[117]. Pichardo S, Sin VW, Hynynen K, Multi-frequency characterization of the speed of sound and attenuation coefficient for longitudinal transmission of freshly excised human skulls, Phys. Med. Biol 56 (2011) 219. 10.1088/0031-9155/56/1/014. [PubMed: 21149950]

[118]. Chang WS, Jung HH, Zadicario E, Rachmilevitch I, Tlusty T, Vitek S, Chang JW, Factors associated with successful magnetic resonance-guided focused ultrasound treatment: efficiency of acoustic energy delivery through the skull, J. Neurosurg 124 (2016) 411–416. 10.3171/2015.3.JNS142592. [PubMed: 26361280]

[119]. Escoffre J-M, Bouakaz A, eds., Therapeutic Ultrasound, Springer International Publishing, Cham, 2016. 10.1007/978-3-319-22536-4.

[120]. Jagannathan J, Sanghvi NT, Crum LA, Yen C-P, Medel R, Dumont AS, Sheehan JP, Steiner L, Jolesz F, Kassell NF, HIGH-INTENSITY FOCUSED ULTRASOUND SURGERY OF THE BRAIN: PART 1–A HISTORICAL PERSPECTIVE WITH MODERN APPLICATIONS, Neurosurgery. 64 (2009) 201–211. 10.1227/01.NEU.0000336766.18197.8E. [PubMed: 19190451]

[121]. Elias WJ, Huss D, Voss T, Loomba J, Khaled M, Zadicario E, Frysinger RC, Sperling SA, Wylie S, Monteith SJ, Druzgal J, Shah BB, Harrison M, Wintermark M, A Pilot Study of Focused Ultrasound Thalamotomy for Essential Tremor, N. Engl. J. Med 369 (2013) 640–648. 10.1056/NEJMoa1300962. [PubMed: 23944301]

[122]. Elias WJ, Lipsman N, Ondo WG, Ghanouni P, Kim YG, Lee W, Schwartz M, Hynynen K, Lozano AM, Shah BB, Huss D, Dallapiazza RF, Gwinn R, Witt J, Ro S, Eisenberg HM, Fishman PS, Gandhi D, Halpern CH, Chuang R, Butts Pauly K, Tierney TS, Hayes MT, Cosgrove GR, Yamaguchi T, Abe K, Taira T, Chang JW, A Randomized Trial of Focused Ultrasound Thalamotomy for Essential Tremor, N. Engl. J. Med 375 (2016) 730–739. 10.1056/NEJMoa1600159. [PubMed: 27557301]

[123]. Martínez-Fernández R, Máñez-Miró JU, Rodríguez-Rojas R, del Álamo M, Shah BB, Hernández-Fernández F, Pineda-Pardo JA, Monje MHG, Fernández-RodrÍguez B, Sperling SA, Mata-MarÍn D, Guida P, Alonso-Frech F, Obeso I, Gasca-Salas C, Vela-Desojo L, Elias WJ, Obeso JA, Randomized Trial of Focused Ultrasound Subthalamotomy for Parkinson's Disease, N. Engl. J. Med 383 (2020) 2501–2513. 10.1056/NEJMoa2016311. [PubMed: 33369354]

[124]. Aubry JF, Tanter M, Pernot M, Thomas JL, Fink M, Experimental demonstration of noninvasive transskull adaptive focusing based on prior computed tomography scans, J. Acoust. Soc. Am 113 (2003) 84–93. [PubMed: 12558249]

[125]. Clement GT, Hynynen K, A non-invasive method for focusing ultrasound through the human skull, Phys. Med. Biol 47 (2002) 1219. 10.1088/0031-9155/47/8/301. [PubMed: 12030552]

[126]. Marquet F, Pernot M, Aubry J-F, Montaldo G, Marsac L, Tanter M, Fink M, Non-invasive transcranial ultrasound therapy based on a 3D CT scan: protocol validation andin vitroresults, Phys. Med. Biol 54 (2009) 2597–2613. 10.1088/0031-9155/54/9/001. [PubMed: 19351986]

[127]. Schoen S, Arvanitis CD, Heterogeneous Angular Spectrum Method for Trans-Skull Imaging and Focusing, IEEE Trans. Med. Imaging 39 (2020) 1605–1614. 10.1109/TMI.2019.2953872. [PubMed: 31751231]

[128]. Thomas JL, Fink MA, Ultrasonic beam focusing through tissue inhomogeneities with a time reversal mirror: application to transskull therapy, IEEE Trans. Ultrason. Ferroelectr. Freq. Control 43 (1996) 1122–1129. 10.1109/58.542055.

[129]. Vyas U, Kaye E, Pauly KB, Transcranial phase aberration correction using beam simulations and MR-ARFI: Phase aberration correction using beam simulations and MR-ARFI, Med. Phys 41 (2014) 032901. 10.1118/1.4865778. [PubMed: 24593740]

[130]. Bancel T, Houdouin A, Annic P, Rachmilevitch I, Shapira Y, Tanter M, Aubry J-F, Comparison Between Ray-Tracing and Full-Wave Simulation for Transcranial Ultrasound Focusing on a Clinical System Using the Transfer Matrix Formalism, IEEE Trans. Ultrason. Ferroelectr. Freq. Control 68 (2021) 2554–2565. 10.1109/TUFFC.2021.3063055. [PubMed: 33651688]

[131]. Kyriakou A, Neufeld E, Werner B, Paulides MM, Szekely G, Kuster N, A review of numerical and experimental compensation techniques for skull-induced phase aberrations in transcranial focused ultrasound, Int. J. Hyperthermia 30 (2014) 36–46. 10.3109/02656736.2013.861519. [PubMed: 24325307]

[132]. McDannold N, Clement GT, Black P, Jolesz F, Hynynen K, Transcranial magnetic resonance imaging-guided focused ultrasound surgery of brain tumors: initial findings in 3 patients, Neurosurgery. 66 (2010) 323–32. [PubMed: 20087132]

[133]. Meng Y, Jones RM, Davidson B, Huang Y, Pople CB, Surendrakumar S, Hamani C, Hynynen K, Lipsman N, Technical Principles and Clinical Workflow of Transcranial MR-Guided Focused Ultrasound, Stereotact. Funct. Neurosurg 99 (2021) 329–342. 10.1159/000512111.

[134]. Jones RM, Deng L, Leung K, McMahon D, O'Reilly MA, Hynynen K, Three-dimensional transcranial microbubble imaging for guiding volumetric ultrasound-mediated blood-brain barrier opening, Theranostics. 8 (2018) 2909–2926. 10.7150/thno.24911. [PubMed: 29896293]

[135]. Wu S-Y, Aurup C, Sanchez CS, Grondin J, Zheng W, Kamimura H, Ferrera VP, Konofagou EE, Efficient Blood-Brain Barrier Opening in Primates with Neuronavigation-Guided Ultrasound and Real-Time Acoustic Mapping, Sci. Rep 8 (2018) 7978. 10.1038/s41598-018-25904-9. [PubMed: 29789530]

[136]. Wei K-C, Tsai H-C, Lu Y-J, Yang H-W, Hua M-Y, Wu M-F, Chen P-Y, Huang C-Y, Yen T-C, Liu H-L, Neuronavigation-Guided Focused Ultrasound-Induced Blood-Brain Barrier Opening: A Preliminary Study in Swine, Am. J. Neuroradiol 34 (2013) 115–120. 10.3174/ajnr.A3150. [PubMed: 22723060]

[137]. Adams C, Jones RM, Yang SD, Kan WM, Leung K, Zhou Y, Lee KU, Huang Y, Hynynen K, Implementation of a Skull-Conformal Phased Array for Transcranial Focused Ultrasound Therapy, IEEE Trans. Biomed. Eng (2021) 1–1. 10.1109/TBME.2021.3077802.

[138]. Crake C, Brinker ST, Coviello CM, Livingstone MS, McDannold NJ, A dual-mode hemispherical sparse array for 3D passive acoustic mapping and skull localization within a clinical MRI guided focused ultrasound device, Phys. Med. Biol 63 (2018) 065008. 10.1088/1361-6560/aab0aa. [PubMed: 29459494]

[139]. Carpentier A, Canney M, Vignot A, Reina V, Beccaria K, Horodyckid C, Karachi C, Leclercq D, Lafon C, Chapelon J-Y, Capelle L, Cornu P, Sanson M, Hoang-Xuan K, Delattre J-Y, Idbaih A, Clinical trial of blood-brain barrier disruption by pulsed ultrasound, Sci. Transl. Med 8 (2016) 343re2–343re2. 10.1126/scitranslmed.aaf6086.

[140]. Maimbourg G, Houdouin A, Deffieux T, Tanter M, Aubry J-F, 3D-printed adaptive acoustic lens as a disruptive technology for transcranial ultrasound therapy using single-element transducers, Phys. Med. Biol 63 (2018) 025026. 10.1088/1361-6560/aaa037. [PubMed: 29219124]

[141]. Ferri M, Bravo JM, Redondo J, Sánchez-Pérez JV, Enhanced Numerical Method for the Design of 3-D-Printed Holographic Acoustic Lenses for Aberration Correction of Single-Element Transcranial Focused Ultrasound, Ultrasound Med. Biol 45 (2019) 867–884. 10.1016/j.ultrasmedbio.2018.10.022. [PubMed: 30600128]

[142]. Jiménez-GambÍn S, Jiménez N, Benlloch JM, Camarena F, Holograms to Focus Arbitrary Ultrasonic Fields through the Skull, Phys. Rev. Appl 12 (2019) 014016. 10.1103/PhysRevApplied.12.014016.

[143]. Melde K, Mark AG, Qiu T, Fischer P, Holograms for acoustics, Nature. 537 (2016) 518–522. 10.1038/nature19755. [PubMed: 27652563]

[144]. Firouzi K, Ghanouni P, Khuri-Yakub BT, Efficient transcranial ultrasound delivery via excitation of Lamb waves, in: 2017 IEEE Int. Ultrason. Symp. IUS, 2017: pp. 1–1. 10.1109/ULTSYM.2017.8092792.

[145]. White PJ, Clement GT, Hynynen K, Longitudinal and shear mode ultrasound propagation in human skull bone, Ultrasound Med Biol. 32 (2006) 1085–96. [PubMed: 16829322]

[146]. Khuri-Yakub BT, Firouzi K, Efficient acoustic energy transfer through skull via excitation of Lamb waves, US20180280735A1, 2018. https://patents.google.com/patent/US20180280735A1/en (accessed March 12, 2021).

[147]. Rezai AR, Ranjan M, D'Haese P-F, Haut MW, Carpenter J, Najib U, Mehta R.l., Chazen JL, Zibly Z, Yates JR, Hodder SL, Kaplitt M, Noninvasive hippocampal blood–brain barrier opening in Alzheimer's disease with focused ultrasound, Proc. Natl. Acad. Sci 117 (2020) 9180–9182. 10.1073/pnas.2002571117. [PubMed: 32284421]

[148]. Pouliopoulos AN, Kwon N, Jensen G, Meaney A, Niimi Y, Burgess MT, Ji R, McLuckie AJ, Munoz FA, Kamimura HAS, Teich AF, Ferrera VP, Konofagou EE, Safety evaluation of a clinical

focused ultrasound system for neuronavigation guided blood-brain barrier opening in non-human primates, Sci. Rep 11 (2021) 15043. 10.1038/s41598-021-94188-3. [PubMed: 34294761]

[149]. Chen K-T, Lin Y-J, Chai W-Y, Lin C-J, Chen P-Y, Huang C-Y, Kuo JS, Liu H-L, Wei K-C, Neuronavigation-guided focused ultrasound (NaviFUS) for transcranial blood-brain barrier opening in recurrent glioblastoma patients: clinical trial protocol, Ann. Transl. Med 8 (2020) 673. 10.21037/atm-20-344. [PubMed: 32617293]

[150]. Maimbourg G, Houdouin A, Deffieux T, Tanter M, Aubry J-F, Steering Capabilities of an Acoustic Lens for Transcranial Therapy: Numerical and Experimental Studies, IEEE Trans. Biomed. Eng 67 (2020) 27–37. 10.1109/TBME.2019.2907556. [PubMed: 30932823]

[151]. Di Mascolo D, Palange AL, Primavera R, Macchi F, Catelani T, Piccardi F, Spanò R, Ferreira M, Marotta R, Armirotti A, Gallotti AL, Galli R, Wilson C, Grant GA, Decuzzi P, Conformable hierarchically engineered polymeric micromeshes enabling combinatorial therapies in brain tumours, Nat. Nanotechnol 16 (2021) 820–829. 10.1038/s41565-021-00879-3. [PubMed: 33795849]

[152]. Clement GT, White PJ, Hynynen K, Enhanced ultrasound transmission through the human skull using shear mode conversion, J. Acoust. Soc. Am 115 (2004) 1356–1364. 10.1121/1.1645610. [PubMed: 15058357]

[153]. Pichardo S, Hynynen K, Treatment of near-skull brain tissue with a focused device using shear-mode conversion: a numerical study, Phys. Med. Biol 52 (2007) 7313–7332. 10.1088/0031-9155/52/24/008. [PubMed: 18065841]

[154]. Legon W, Ai L, Bansal P, Mueller JK, Neuromodulation with single-element transcranial focused ultrasound in human thalamus, Hum Brain Mapp. 39 (2018) 1995–2006. 10.1002/hbm.23981. [PubMed: 29380485]

[155]. Park TY, Pahk KJ, Kim H, Method to optimize the placement of a single-element transducer for transcranial focused ultrasound, Comput Methods Programs Biomed. 179 (2019) 104982. 10.1016/j.cmpb.2019.104982. [PubMed: 31443869]

[156]. Fan C-H, Yeh C-K, Microbubble-enhanced Focused Ultrasound-induced Blood–brain Barrier Opening for Local and Transient Drug Delivery in Central Nervous System Disease, J. Med. Ultrasound 22 (2014) 183–193. 10.1016/j.jmu.2014.11.001.

[157]. Lee J-H, Cho I-J, Ko K, Yoon E-S, Park H-H, Kim TS, Flexible piezoelectric micromachined ultrasonic transducer (pMUT) for application in brain stimulation, Microsyst. Technol 23 (2017) 2321–2328.

[158]. Seok C, Adelegan O, Biliroglu AO, Yamaner FY, Oralkan Ö, A 2D Ultrasonic Transmit Phased Array Based on a 32x32 CMUT Array Flip-Chip Bonded to an ASIC for Neural Stimulation, 2020 IEEE Int. Ultrason. Symp. IUS (n.d.) 1–4.

[159]. Jung G, Pirouz A, Tekes C, Carpenter T, Rashid MW, Revanitabar A, Cowell D, Freear S, Ghovanloo M, Degertekin FL, Single-chip reduced-wire CMUT-on-CMOS system for intracardiac echocardiography, 2018 IEEE Int. Ultrason. Symp. IUS (n.d.) 1–4.

[160]. Hyvelin J-M, Gaud E, Costa M, Helbert A, Bussat P, Bettinger T, Frinking P, Characteristics and Echogenicity of Clinical Ultrasound Contrast Agents: An In Vitro and In Vivo Comparison Study, J. Ultrasound Med 36 (2017) 941–953. 10.7863/ultra.16.04059. [PubMed: 28240842]

[161]. Prada F, Gennari AG, Linville IM, Mutersbaugh ME, Chen Z, Sheybani N, DiMeco F, Padilla F, Hossack JA, Quantitative analysis of in-vivo microbubble distribution in the human brain, Sci. Rep 11 (2021) 11797. 10.1038/s41598-021-91252-w. [PubMed: 34083642]

[162]. Dauba A, Delalande A, Kamimura HAS, Conti A, Larrat B, Tsapis N, Novell A, Recent Advances on Ultrasound Contrast Agents for Blood-Brain Barrier Opening with Focused Ultrasound, Pharmaceutics. 12 (2020) 1125. 10.3390/pharmaceutics12111125.

[163]. Stride E, Segers T, Lajoinie G, Cherkaoui S, Bettinger T, Versluis M, Borden M, Microbubble Agents: New Directions, Ultrasound Med. Biol 46 (2020) 1326–1343. 10.1016/j.ultrasmedbio.2020.01.027. [PubMed: 32169397]

[164]. Vlachos F, Tung Y-S, Konofagou E, Permeability dependence study of the focused ultrasound-induced blood-brain barrier opening at distinct pressures and microbubble diameters using DCE-MRI, Magn. Reson. Med 66 (2011) 821–830. 10.1002/mrm.22848. [PubMed: 21465543]

[165]. Samiotaki G, Vlachos F, Tung Y-S, Konofagou EE, A quantitative pressure and microbubble-size dependence study of focused ultrasound-induced blood-brain barrier opening reversibility in vivo using MRI, Magn. Reson. Med 67 (2012) 769–777. 10.1002/mrm.23063. [PubMed: 21858862]

[166]. Choi JJ, Feshitan JA, Baseri B, Wang S, Tung Y-S, Borden MA, Konofagou EE, Microbubble-Size Dependence of Focused Ultrasound-Induced Blood–Brain Barrier Opening in Mice In Vivo, IEEE Trans. Biomed. Eng 57 (2010) 145–154. 10.1109/TBME.2009.2034533. [PubMed: 19846365]

[167]. Wang S, Samiotaki G, Olumolade O, Feshitan JA, Konofagou EE, Microbubble Type and Distribution Dependence of Focused Ultrasound-Induced Blood–Brain Barrier Opening, Ultrasound Med. Biol 40 (2014) 130–137. 10.1016/j.ultrasmedbio.2013.09.015. [PubMed: 24239362]

[168]. Marmottant P, van der Meer S, Emmer M, Versluis M, de Jong N, Hilgenfeldt S, Lohse D, A model for large amplitude oscillations of coated bubbles accounting for buckling and rupture, J. Acoust. Soc. Am 118 (2005) 3499–3505. 10.1121/1.2109427.

[169]. Sun Y, Kruse DE, Dayton PA, Ferrara KW, High-frequency dynamics of ultrasound contrast agents, IEEE Trans. Ultrason. Ferroelectr. Freq. Control 52 (2005) 1981–1991. 10.1109/TUFFC.2005.1561667. [PubMed: 16422410]

[170]. McDannold N, Vykhodtseva N, Hynynen K, Blood-brain barrier disruption induced by focused ultrasound and circulating preformed microbubbles appears to be characterized by the mechanical index, Ultrasound Med. Biol 34 (2008) 834–840. 10.1016/j.ultrasmedbio.2007.10.016. [PubMed: 18207311]

[171]. Song K-H, Harvey BK, Borden MA, State-of-the-art of microbubble-assisted blood-brain barrier disruption, Theranostics. 8 (2018) 4393–4408. 10.7150/thno.26869. [PubMed: 30214628]

[172]. Song K-H, Fan AC, Hinkle JJ, Newman J, Borden MA, Harvey BK, Microbubble gas volume: A unifying dose parameter in blood-brain barrier opening by focused ultrasound, Theranostics. 7 (2017) 144–152. 10.7150/thno.15987. [PubMed: 28042323]

[173]. Borden MA, Lipid-Coated Nanodrops and Microbubbles, in: Ashokkumar M (Ed.), Handb. Ultrason. Sonochemistry, Springer, Singapore, 2015: pp. 1–26. 10.1007/978-981-287-470-2_26-1.

[174]. King DA, Malloy MJ, Roberts AC, Haak A, Yoder CC, O'Brien WD, Determination of postexcitation thresholds for single ultrasound contrast agent microbubbles using double passive cavitation detection, J. Acoust. Soc. Am 127 (2010) 3449–3455. 10.1121/1.3373405. [PubMed: 20550244]

[175]. McDannold N, Vykhodtseva N, Hynynen K, Use of Ultrasound Pulses Combined with Definity for Targeted Blood-Brain Barrier Disruption: A Feasibility Study, Ultrasound Med. Biol 33 (2007) 584–590. 10.1016/j.ultrasmedbio.2006.10.004. [PubMed: 17337109]

[176]. Bing C, Hong Y, Hernandez C, Rich M, Cheng B, Munaweera I, Szczepanski D, Xi Y, Bolding M, Exner A, Chopra R, Characterization of different bubble formulations for blood-brain barrier opening using a focused ultrasound system with acoustic feedback control, Sci. Rep 8 (2018) 7986. 10.1038/s41598-018-26330-7. [PubMed: 29789589]

[177]. Wu S-K, Chu P-C, Chai W-Y, Kang S-T, Tsai C-H, Fan C-H, Yeh C-K, Liu H-L, Characterization of Different Microbubbles in Assisting Focused Ultrasound-Induced Blood-Brain Barrier Opening, Sci. Rep 7 (2017) 46689. 10.1038/srep46689. [PubMed: 28425493]

[178]. Lentacker I, De Geest BG, Vandenbroucke RE, Peeters L, Demeester J, De Smedt SC, Sanders NN, Ultrasound-Responsive Polymer-Coated Microbubbles That Bind and Protect DNA, Langmuir. 22 (2006) 7273–7278. 10.1021/la0603828. [PubMed: 16893226]

[179]. Wang DS, Panje C, Pysz MA, Paulmurugan R, Rosenberg J, Gambhir SS, Schneider M, Willmann JK, Cationic versus Neutral Microbubbles for Ultrasound-mediated Gene Delivery in Cancer, Radiology. 264 (2012) 721–732. 10.1148/radiol.12112368. [PubMed: 22723497]

[180]. Tan J-KY, Pham B, Zong Y, Perez C, Maris DO, Hemphill A, Miao CH, Matula TJ, Mourad PD, Wei H, Sellers DL, Horner PJ, Pun SH, Microbubbles and ultrasound increase intraventricular polyplex gene transfer to the brain, J. Controlled Release 231 (2016) 86–93. 10.1016/j.jconrel.2016.02.003.

[181]. Tu J, Swalwell JE, Giraud D, Cui W, Chen W, Matula TJ, Microbubble Sizing and Shell Characterization Using Flow Cytometry, IEEE Trans. Ultrason. Ferroelectr. Freq. Control 58 (2011) 955–963. 10.1109/TUFFC.2011.1896. [PubMed: 21622051]

[182]. Goertz DE, de Jong N, van der Steen AFW, Attenuation and Size Distribution Measurements of Definity™ and Manipulated Definity™ Populations, Ultrasound Med. Biol 33 (2007) 1376–1388. 10.1016/j.ultrasmedbio.2007.03.009. [PubMed: 17521801]

[183]. Helfield BL, Goertz DE, Nonlinear resonance behavior and linear shell estimates for Definity™ and MicroMarker™ assessed with acoustic microbubble spectroscopy, J. Acoust. Soc. Am 133 (2013) 1158–1168. 10.1121/1.4774379. [PubMed: 23363132]

[184]. Kimmel E, Krasovitski B, Hoogi A, Razansky D, Adam D, Subharmonic Response of Encapsulated Microbubbles: Conditions for Existence and Amplification, Ultrasound Med. Biol 33 (2007) 1767–1776. 10.1016/j.ultrasmedbio.2007.05.011. [PubMed: 17720301]

[185]. Wu S-K, Chu P-C, Chai W-Y, Kang S-T, Tsai C-H, Fan C-H, Yeh C-K, Liu H-L, Characterization of Different Microbubbles in Assisting Focused Ultrasound-Induced Blood-Brain Barrier Opening, Sci. Rep 7 (2017) 46689. 10.1038/srep46689. [PubMed: 28425493]

[186]. Ja'afar F, Leow CH, Garbin V, Sennoga CA, Tang M-X, Seddon JM, Surface Charge Measurement of SonoVue, Definity and Optison: A Comparison of Laser Doppler Electrophoresis and Micro-Electrophoresis, Ultrasound Med. Biol 41 (2015) 2990–3000. 10.1016/j.ultrasmedbio.2015.07.001. [PubMed: 26318559]

[187]. Tu J, Guan J, Qiu Y, Matula TJ, Estimating the shell parameters of SonoVue® microbubbles using light scattering, J. Acoust. Soc. Am 126 (2009) 2954–2962. 10.1121/1.3242346. [PubMed: 20000908]

[188]. Gorce J-M, Arditi M, Schneider M, Influence of Bubble Size Distribution on the Echogenicity of Ultrasound Contrast Agents: A Study of SonoVue™, Invest. Radiol 35 (2000) 661. [PubMed: 11110302]

[189]. Podell S, Burrascano C, Gaal M, Golec B, Maniquis J, Mehlhaff P, Physical and biochemical stability of Optison®, an injectable ultrasound contrast agent, Biotechnol. Appl. Biochem 30 (1999) 213–223. 10.1111/j.1470-8744.1999.tb00773.x. [PubMed: 10574690]

[190]. Dayton PA, Morgan KE, Klibanov AL, Brandenburger GH, Ferrara KW, Optical and acoustical observations of the effects of ultrasound on contrast agents, IEEE Trans. Ultrason. Ferroelectr. Freq. Control 46 (1999) 220–232. 10.1109/58.741536. [PubMed: 18238417]

[191]. Chomas JE, Dayton P, Allen J, Morgan K, Ferrara KW, Mechanisms of contrast agent destruction, IEEE Trans. Ultrason. Ferroelectr. Freq. Control 48 (2001) 232–248. 10.1109/58.896136. [PubMed: 11367791]

[192]. Shi WT, Forsberg F, Ultrasonic characterization of the nonlinear properties of contrast microbubbles, Ultrasound Med. Biol 26 (2000) 93–104. 10.1016/S0301-5629(99)00117-9. [PubMed: 10687797]

[193]. Kamaev PP, Hutcheson JD, Wilson ML, Prausnitz MR, Quantification of Optison bubble size and lifetime during sonication dominant role of secondary cavitation bubbles causing acoustic bioeffects, J. Acoust. Soc. Am 115 (2004) 1818–1825. 10.1121/1.1624073. [PubMed: 15101659]

[194]. Chatterjee D, Sarkar K, A Newtonian rheological model for the interface of microbubble contrast agents, Ultrasound Med. Biol 29 (2003) 1749–1757. 10.1016/S0301-5629(03)01051-2. [PubMed: 14698342]

[195]. Schneider M, Anantharam B, Arditi M, Bokor D, Broillet A, Bussat P, Fouillet X, Frinking P, Tardy I, Terrettaz J, Senior R, Tranquart F, BR38, a New Ultrasound Blood Pool Agent, Invest. Radiol 46 (2011) 486–494. 10.1097/RLI.0b013e318217b821. [PubMed: 21487303]

[196]. Kovacs Z, Werner B, Rassi A, Sass JO, Martin-Fiori E, Bernasconi M, Prolonged survival upon ultrasound-enhanced doxorubicin delivery in two syngenic glioblastoma mouse models, J. Controlled Release 187 (2014) 74–82. 10.1016/j.jconrel.2014.05.033.

[197]. Sarkar K, Shi WT, Chatterjee D, Forsberg F, Characterization of ultrasound contrast microbubbles using in vitro experiments and viscous and viscoelastic interface models for encapsulation, J. Acoust. Soc. Am 118 (2005) 539–550. 10.1121/1.1923367. [PubMed: 16119373]

[198]. Sontum PC, Physicochemical Characteristics of Sonazoid™, A New Contrast Agent for Ultrasound Imaging, Ultrasound Med. Biol 34 (2008) 824–833. 10.1016/j.ultrasmedbio.2007.11.006. [PubMed: 18255220]

[199]. Garg S, Thomas AA, Borden MA, The effect of lipid monolayer in-plane rigidity on in vivo microbubble circulation persistence, Biomaterials. 34 (2013) 6862–6870. 10.1016/j.biomaterials.2013.05.053. [PubMed: 23787108]

[200]. Ferrara K, Pollard R, Borden M, Ultrasound Microbubble Contrast Agents: Fundamentals and Application to Gene and Drug Delivery, Annu. Rev. Biomed. Eng 9 (2007) 415–447. 10.1146/annurev.bioeng.8.061505.095852. [PubMed: 17651012]

[201]. Kooiman K, Vos HJ, Versluis M, de Jong N, Acoustic behavior of microbubbles and implications for drug delivery, Adv. Drug Deliv. Rev 72 (2014) 28–48. 10.1016/j.addr.2014.03.003. [PubMed: 24667643]

[202]. Omata D, Maruyama T, Unga J, Hagiwara F, Munakata L, Kageyama S, Shima T, Suzuki Y, Maruyama K, Suzuki R, Effects of encapsulated gas on stability of lipid-based microbubbles and ultrasound-triggered drug delivery, J. Controlled Release 311–312 (2019) 65–73. 10.1016/j.jconrel.2019.08.023.

[203]. McMahon D, Hynynen K, Acute Inflammatory Response Following Increased Blood-Brain Barrier Permeability Induced by Focused Ultrasound is Dependent on Microbubble Dose, Theranostics. 7 (2017) 3989–4000. 10.7150/thno.21630. [PubMed: 29109793]

[204]. Ilyichev V.l., Koretz VL, Melnikov NP, Spectral characteristics of acoustic cavitation, Ultrasonics. 27 (1989) 357–361. 10.1016/0041-624X(89)90034-6. [PubMed: 2815406]

[205]. Miller MW, Miller DL, Brayman AA, A review of in vitro bioeffects of inertial ultrasonic cavitation from a mechanistic perspective, Ultrasound Med. Biol 22 (1996) 1131–1154. 10.1016/S0301-5629(96)00089-0. [PubMed: 9123638]

[206]. Cleve S, Inserra C, Prentice P, Contrast Agent Microbubble Jetting during Initial Interaction with 200-kHz Focused Ultrasound, Ultrasound Med. Biol 45 (2019) 3075–3080. 10.1016/j.ultrasmedbio.2019.08.005. [PubMed: 31477370]

[207]. Chen H, Kreider W, Brayman AA, Bailey MR, Matula TJ, Blood Vessel Deformations on Microsecond Time Scales by Ultrasonic Cavitation, Phys. Rev. Lett 106 (2011) 034301. 10.1103/PhysRevLett.106.034301. [PubMed: 21405276]

[208]. Arvanitis CD, Vykhodtseva N, Jolesz F, Livingstone M, McDannold N, Cavitation-enhanced nonthermal ablation in deep brain targets: feasibility in a large animal model, J. Neurosurg 124 (2016) 1450–1459. 10.3171/2015.4JNS142862. [PubMed: 26381252]

[209]. Huang Y, Vykhodtseva N.l., Hynynen K, Creating brain lesions with low-intensity focused ultrasound with microbubbles: a rat study at half a megahertz, Ultrasound Med. Biol 39 (2013) 1420–1428. 10.1016/j.ultrasmedbio.2013.03.006. [PubMed: 23743099]

[210]. O'Reilly MA, Hynynen K, Blood-Brain Barrier: Real-time Feedback-controlled Focused Ultrasound Disruption by Using an Acoustic Emissions-based Controller, Radiology. 263 (2012) 96–106. 10.1148/radiol.11111417. [PubMed: 22332065]

[211]. Chen H, Konofagou EE, The Size of Blood-Brain Barrier Opening Induced by Focused Ultrasound is Dictated by the Acoustic Pressure, J. Cereb. Blood Flow Metab 34 (2014) 1197–1204. 10.1038/jcbfm.2014.71. [PubMed: 24780905]

[212]. Leighton TG, The Acoustic Bubble, Academic Press, Inc., San Diego, 1994.

[213]. Frenkel V, Ultrasound mediated delivery of drugs and genes to solid tumors, Adv. Drug Deliv. Rev 60 (2008) 1193–1208. 10.1016/j.addr.2008.03.007. [PubMed: 18474406]

[214]. Meng L, Liu X, Wang Y, Zhang W, Zhou W, Cai F, Li F, Wu J, Xu L, Niu L, Zheng H, Sonoporation of Cells by a Parallel Stable Cavitation Microbubble Array, Adv. Sci 6 (2019) 1900557. 10.1002/advs.201900557.

[215]. Meijering Bernadet D.M., Juffermans Lynda J.M., van Wamel Annemieke, Henning Rob H., Zuhorn Inge S., Emmer Marcia, Versteilen Amanda M.G., Paulus Walter J., van Gilst Wiek H., Kooiman Klazina, de Jong Nico, Musters Rene J.P., Deelman Leo E., Kamp Otto, Ultrasound and Microbubble-Targeted Delivery of Macromolecules Is Regulated by Induction of Endocytosis and Pore Formation, Circ. Res 104 (2009) 679–687. 10.1161/CIRCRESAHA.108.183806. [PubMed: 19168443]

[216]. McDannold N, Vykhodtseva N, Hynynen K, Targeted disruption of the blood–brain barrier with focused ultrasound: association with cavitation activity, Phys. Med. Biol 51 (2006) 793–807. 10.1088/0031-9155/51/4/003. [PubMed: 16467579]

[217]. Wu S, Tung Y, Marquet F, Downs ME, Sanchez CS, Chen CC, Ferrera V, Konofagou E, Transcranial cavitation detection in primates during blood-brain barrier opening-a performance assessment study, IEEE Trans. Ultrason. Ferroelectr. Freq. Control 61 (2014) 966–978. 10.1109/TUFFC.2014.2992. [PubMed: 24859660]

[218]. Tung Y-S(童耀生), Marquet F, Teichert T, Ferrera V, Konofagou EE, Feasibility of noninvasive cavitation-guided blood-brain barrier opening using focused ultrasound and microbubbles in nonhuman primates, Appl. Phys. Lett 98 (2011) 163704. 10.1063/1.3580763. [PubMed: 21580802]

[219]. Chu P-C, Chai W-Y, Tsai C-H, Kang S-T, Yeh C-K, Liu H-L, Focused Ultrasound-Induced Blood-Brain Barrier Opening: Association with Mechanical Index and Cavitation Index Analyzed by Dynamic Contrast-Enhanced Magnetic-Resonance Imaging, Sci. Rep 6 (2016) 33264. 10.1038/srep33264. [PubMed: 27630037]

[220]. Harary M, Segar DJ, Huang KT, Tafel IJ, Valdes PA, Cosgrove GR, Focused ultrasound in neurosurgery: a historical perspective, Neurosurg. Focus 44 (2018) E2. 10.3171/2017.11.FOCUS17586.

[221]. Novell A, Kamimura H. a. S., Cafarelli A, Gerstenmayer M, Flament J, Valette J, Agou P, Conti A, Selingue E, Aron Badin R, Hantraye P, Larrat B, A new safety index based on intrapulse monitoring of ultraharmonic cavitation during ultrasound-induced blood-brain barrier opening procedures, Sci. Rep 10 (2020) 10088. 10.1038/s41598-020-66994-8. [PubMed: 32572103]

[222]. Haqshenas SR, Saffari N, Multi-resolution analysis of passive cavitation detector signals, J. Phys. Conf. Ser 581 (2015) 012004. 10.1088/1742-6596/581/1/012004.

[223]. Sun T, Samiotaki G, Wang S, Acosta C, Chen CC, Konofagou EE, Acoustic cavitation-based monitoring of the reversibility and permeability of ultrasound-induced blood-brain barrier opening, Phys. Med. Biol 60 (2015) 9079–9094. 10.1088/0031-9155/60/23/9079. [PubMed: 26562661]

[224]. Tung Y-S, Vlachos F, Choi JJ, Deffieux T, Selert K, Konofagou EE, In vivo transcranial cavitation threshold detection during ultrasound-induced blood–brain barrier opening in mice, Phys. Med. Biol 55 (2010) 6141–6155. 10.1088/0031-9155/55/20/007. [PubMed: 20876972]

[225]. Guo X, Li Q, Zhang Z, Zhang D, Tu J, Investigation on the inertial cavitation threshold and shell properties of commercialized ultrasound contrast agent microbubbles, J. Acoust. Soc. Am 134 (2013) 1622–1631. 10.1121/1.4812887. [PubMed: 23927202]

[226]. Hynynen K, McDannold N, Sheikov NA, Jolesz FA, Vykhodtseva N, Local and reversible blood–brain barrier disruption by noninvasive focused ultrasound at frequencies suitable for trans-skull sonications, Neuroimage. 24 (2005) 12–20. 10.1016/j.neuroimage.2004.06.046. [PubMed: 15588592]

[227]. Chen K-T, Wei K-C, Liu H-L, Theranostic Strategy of Focused Ultrasound Induced Blood-Brain Barrier Opening for CNS Disease Treatment, Front. Pharmacol 10 (2019). 10.3389/fphar.2019.00086.

[228]. Haworth KJ, Bader KB, Rich KT, Holland CK, Mast TD, Quantitative Frequency-Domain Passive Cavitation Imaging, IEEE Trans. Ultrason. Ferroelectr. Freq. Control 64 (2017) 177–191. 10.1109/TUFFC.2016.2620492. [PubMed: 27992331]

[229]. Patel A, Schoen SJ, Arvanitis CD, Closed-Loop Spatial and Temporal Control of Cavitation Activity With Passive Acoustic Mapping, IEEE Trans. Biomed. Eng 66 (2019) 2022–2031. 10.1109/TBME.2018.2882337.

[230]. Arvanitis CD, Crake C, McDannold N, Clement GT, Passive Acoustic Mapping with the Angular Spectrum Method, IEEE Trans. Med. Imaging. 36 (2017) 983–993. 10.1109/TMI.2016.2643565. [PubMed: 28026755]

[231]. Norton SJ, Won IJ, Time exposure acoustics, IEEE Trans. Geosci. Remote Sens 38 (2000) 1337–1343. 10.1109/36.843027.

[232]. Gyongy M, Coussios C, Passive Spatial Mapping of Inertial Cavitation During HIFU Exposure, IEEE Trans. Biomed. Eng 57 (2010) 48–56. 10.1109/TBME.2009.2026907. [PubMed: 19628450]

[233]. Gyöngy M, Coussios C-C, Passive cavitation mapping for localization and tracking of bubble dynamics, J. Acoust. Soc. Am 128 (2010) EL175–EL180. 10.1121/1.3467491. [PubMed: 20968322]

[234]. Burgess MT, Apostolakis I, Konofagou EE, Power cavitation-guided blood-brain barrier opening with focused ultrasound and microbubbles, Phys. Med. Biol 63 (2018) 065009. 10.1088/1361-6560/aab05c. [PubMed: 29457587]

[235]. Liu H-L, Jan C-K, Chu P-C, Hong J-C, Lee P-Y, Hsu J-D, Lin C-C, Huang C-Y, Chen P-Y, Wei K-C, Design and experimental evaluation of a 256-channel dual-frequency ultrasound phased-array system for transcranial blood-brain barrier opening and brain drug delivery, IEEE Trans. Biomed. Eng 61 (2014) 1350–1360. 10.1109/TBME.2014.2305723. [PubMed: 24658258]

[236]. Liu H-L, Tsai C-H, Jan C-K, Chang H-Y, Huang S-M, Li M-L, Qiu W, Zheng H, Design and Implementation of a Transmit/Receive Ultrasound Phased Array for Brain Applications, IEEE Trans. Ultrason. Ferroelectr. Freq. Control 65 (2018) 1756–1767. 10.1109/TUFFC.2018.2855181. [PubMed: 30010555]

[237]. Jones RM, O'Reilly MA, Hynynen K, Experimental demonstration of passive acoustic imaging in the human skull cavity using CT-based aberration corrections, Med. Phys 42 (2015) 4385–4400. 10.1118/1.4922677. [PubMed: 26133635]

[238]. Jones RM, Hynynen K, Comparison of analytical and numerical approaches for CT-based aberration correction in transcranial passive acoustic imaging, Phys. Med. Biol 61 (2015) 23–36. 10.1088/0031-9155/61/1/23. [PubMed: 26605827]

[239]. Coviello C, Kozick R, Choi J, Gyöngy M, Jensen C, Smith PP, Coussios C-C, Passive acoustic mapping utilizing optimal beamforming in ultrasound therapy monitoring, J. Acoust. Soc. Am 137 (2015) 2573–2585. 10.1121/1.4916694. [PubMed: 25994690]

[240]. Lu S, Hu H, Yu X, Long J, Jing B, Zong Y, Wan M, Passive acoustic mapping of cavitation using eigenspace-based robust Capon beamformer in ultrasound therapy, Ultrason. Sonochem 41 (2018) 670–679. 10.1016/j.ultsonch.2017.10.017. [PubMed: 29137800]

[241]. O'Reilly MA, Hynynen K, A super-resolution ultrasound method for brain vascular mapping, Med. Phys 40 (2013) 110701. 10.1118/1.4823762. [PubMed: 24320408]

[242]. Kamimura HAS, Wu S-Y, Grondin J, Ji R, Aurup C, Zheng W, Heidmann M, Pouliopoulos AN, Konofagou EE, Real-Time Passive Acoustic Mapping Using Sparse Matrix Multiplication, IEEE Trans. Ultrason. Ferroelectr. Freq. Control 68 (2021) 164–177. 10.1109/TUFFC.2020.3001848. [PubMed: 32746182]

[243]. Wu S-Y, Aurup C, Sanchez CS, Grondin J, Zheng W, Kamimura H, Ferrera VP, Konofagou EE, Efficient Blood-Brain Barrier Opening in Primates with Neuronavigation-Guided Ultrasound and Real-Time Acoustic Mapping, Sci. Rep 8 (2018) 7978. 10.1038/s41598-018-25904-9. [PubMed: 29789530]

[244]. Jones RM, Hynynen K, Advances in acoustic monitoring and control of focused ultrasound-mediated increases in blood-brain barrier permeability, Br. J. Radiol (2018) . 10.1259/bjr.20180601. [PubMed: 20180601]

[245]. Haworth KJ, Raymond JL, Radhakrishnan K, Moody MR, Huang S-L, Peng T, Shekhar H, Klegerman ME, Kim H, McPherson DD, Holland CK, Trans-Stent B-Mode Ultrasound and Passive Cavitation Imaging, Ultrasound Med. Biol 42 (2016) 518–527. 10.1016/j.ultrasmedbio.2015.08.014. [PubMed: 26547633]

[246]. Kim P, Song JH, Song T-K, A new frequency domain passive acoustic mapping method using passive Hilbert beamforming to reduce the computational complexity of fast Fourier transform, Ultrasonics. 102 (2020) 106030. 10.1016/j.ultras.2019.106030. [PubMed: 31785584]

[247]. Schoen S, Arvanitis CD, Heterogeneous Angular Spectrum Method for Trans-Skull Imaging and Focusing, IEEE Trans. Med. Imaging. 39 (2020) 1605–1614. 10.1109/TMI.2019.2953872. [PubMed: 31751231]

[248]. Yang Y, Zhang X, Ye D, Laforest R, Williamson J, Liu Y, Chen H, Cavitation dose painting for focused ultrasound-induced blood-brain barrier disruption, Sci. Rep 9 (2019) 2840. 10.1038/s41598-019-39090-9. [PubMed: 30808897]

[249]. Xu S, Ye D, Wan L, Shentu Y, Yue Y, Wan M, Chen H, Correlation Between Brain Tissue Damage and Inertial Cavitation Dose Quantified Using Passive Cavitation Imaging, Ultrasound Med. Biol 45 (2019) 2758–2766. 10.1016/j.ultrasmedbio.2019.07.004. [PubMed: 31378549]

[250]. Tsai C-H, Zhang J-W, Liao Y-Y, Liu H-L, Real-time monitoring of focused ultrasound blood-brain barrier opening via subharmonic acoustic emission detection: implementation of confocal dual-frequency piezoelectric transducers, Phys. Med. Biol 61 (2016) 2926–2946. 10.1088/0031-9155/61/7/2926. [PubMed: 26988240]

[251]. Cornu C, Guédra M, Béra J-C, Liu H-L, Chen W-S, Inserra C, Ultrafast monitoring and control of subharmonic emissions of an unseeded bubble cloud during pulsed sonication, Ultrason. Sonochem 42 (2018) 697–703. 10.1016/j.ultsonch.2017.12.026. [PubMed: 29429720]

[252]. O'Reilly MA, Hynynen K, Blood-Brain Barrier: Real-time Feedback-controlled Focused Ultrasound Disruption by Using an Acoustic Emissions–based Controller, Radiology. 263 (2012) 96–106. 10.1148/radiol.11111417. [PubMed: 22332065]

[253]. Bing C, Hong Y, Hernandez C, Rich M, Cheng B, Munaweera I, Szczepanski D, Xi Y, Bolding M, Exner A, Chopra R, Characterization of different bubble formulations for blood-brain barrier opening using a focused ultrasound system with acoustic feedback control, Sci. Rep 8 (2018) 7986. 10.1038/s41598-018-26330-7. [PubMed: 29789589]

[254]. McDannold N, Zhang Y, Supko JG, Power C, Sun T, Peng C, Vykhodtseva N, Golby AJ, Reardon DA, Acoustic feedback enables safe and reliable carboplatin delivery across the blood-brain barrier with a clinical focused ultrasound system and improves survival in a rat glioma model, Theranostics. 9 (2019) 6284–6299. 10.7150/thno.35892. [PubMed: 31534551]

[255]. Kamimura HA, Flament J, Valette J, Cafarelli A, Aron Badin R, Hantraye P, Larrat B, Feedback control of microbubble cavitation for ultrasound-mediated blood–brain barrier disruption in non-human primates under magnetic resonance guidance, J. Cereb. Blood Flow Metab 39 (2019) 1191–1203. 10.1177/0271678X17753514. [PubMed: 29381130]

[256]. Çavuşoğlu M, Zhang J, lelacqua GD, Pellegrini G, Signorell RD, Papachristodoulou A, Brambilla D, Roth P, Weller M, Rudin M, Martin E, Leroux J-C, Werner B, Closed-loop cavitation control for focused ultrasound-mediated blood–brain barrier opening by long-circulating microbubbles, Phys. Med. Biol 64 (2019) 045012. 10.1088/1361-6560/aafaa5. [PubMed: 30577029]

[257]. Tan C, Yan B, Han T, Yu ACH, Qin P, A Real-time Proportional Feedback Controller for Sustaining Uniform Inertial Cavitation Dynamics of Flowing Bubbles, in: 2020 IEEE Int. Ultrason. Symp. IUS, 2020: pp. 1–4. 10.1109/IUS46767.2020.9251638.

[258]. Tan C, Li Y, Han T, Yu ACH, Qin P, Control of Temporal Dynamics of Stable Cavitation by a Real-time Proportional Feedback Method, in: 2019 IEEE Int. Ultrason. Symp. IUS, IEEE, Glasgow, United Kingdom, 2019: pp. 2295–2298. 10.1109/ULTSYM.2019.8925608.

[259]. Lipsman N, Meng Y, Bethune AJ, Huang Y, Lam B, Masellis M, Herrmann N, Heyn C, Aubert I, Boutet A, Smith GS, Hynynen K, Black SE, Blood–brain barrier opening in Alzheimer's disease using MR-guided focused ultrasound, Nat. Commun 9 (2018) 2336. 10.1038/s41467-018-04529-6. [PubMed: 30046032]

[260]. Dadok V, Szeri AJ, Adaptive control of contrast agent microbubbles for shell parameter identification, J. Acoust. Soc. Am 131 (2012) 2579–2586. 10.1121/1.3689555. [PubMed: 22501039]

[261]. Carroll JM, Lauderbaugh LK, Calvisi ML, Application of nonlinear sliding mode control to ultrasound contrast agent microbubbles, J. Acoust. Soc. Am 134 (2013) 216–222. 10.1121/1.4803902. [PubMed: 23862799]

[262]. Renaud G, Bosch JG, van der Steen AFW, de Jong N, An "acoustical camera" for in vitro characterization of contrast agent microbubble vibrations, Appl. Phys. Lett 100 (2012) 101911. 10.1063/1.3693522.

[263]. Sijl J, Vos HJ, Rozendal T, de Jong N, Lohse D, Versluis M, Combined optical and acoustical detection of single microbubble dynamics, J. Acoust. Soc. Am 130 (2011) 3271–3281. 10.1121/1.3626155. [PubMed: 22087999]

[264]. O'Reilly MA, Hynynen K, A PVDF receiver for ultrasound monitoring of transcranial focused ultrasound therapy, IEEE Trans. Biomed. Eng 57 (2010) 2286–2294. [PubMed: 20515709]

[265]. O'Reilly MA, Jones RM, Hynynen K, Three-dimensional transcranial ultrasound imaging of microbubble clouds using a sparse hemispherical array, IEEE Trans. Biomed. Eng 61 (2014) 1285–1294. [PubMed: 24658252]

[266]. Deng L, O'Reilly MA, Jones RM, An R, Hynynen K, A multi-frequency sparse hemispherical ultrasound phased array for microbubble-mediated transcranial therapy and simultaneous cavitation mapping, Phys. Med. Biol 61 (2016) 8476. [PubMed: 27845920]

[267]. Lu Y, Rozen O, Tang H-Y, Smith GL, Fung S, Boser BE, Polcawich RG, Horsley DA, Broadband piezoelectric micromachined ultrasonic transducers based on dual resonance modes, 2015 28th IEEE Int. Conf. Micro Electro Mech. Syst. MEMS. (n.d.) 146–149.

[268]. Jiang X, Tang H-Y, Lu Y, Ng EJ, Tsai JM, Boser BE, Horsley DA, Ultrasonic fingerprint sensor with transmit beamforming based on a PMUT array bonded to CMOS circuitry, IEEE Trans. Ultrason. Ferroelectr. Freq. Control 64 (2017) 1401–1408. [PubMed: 28504937]

[269]. Gurun G, Hochman M, Hasler P, Degertekin FL, Thermal-mechanical-noise-based CMUT characterization and sensing, IEEE Trans. Ultrason. Ferroelectr. Freq. Control 59 (2012) 1267–1275. [PubMed: 22718877]

[270]. Warshavski O, Meynier C, Sénégond N, Chatain P, Rebling J, Razansky D, Felix N, Nguyen-Dinh A, Experimental evaluation of cMUT and PZT transducers in receive only mode for photoacoustic imaging, Photons Plus Ultrasound Imaging Sens. 2016. 9708 (n.d.) 970830.

[271]. Dauba A, Goulas J, Colin L, Jourdain L, Larrat B, Gennisson J-L, Certon D, Novell A, Evaluation of capacitive micromachined ultrasonic transducers for passive monitoring of microbubble-assisted ultrasound therapies, J. Acoust. Soc. Am 148 (2020) 2248–2255. [PubMed: 33138521]

[272]. Savoia AS, Mauti B, Manh T, Hoff L, Lanteri F, Geliy J-F, Eggen T, Design, Fabrication and Characterization of a Hybrid Piezoelectric-CMUT Dual-Frequency Ultrasonic Transducer, 2018 IEEE Int. Ultrason. Symp. IUS. (n.d.) 1–4.

[273]. Pekař M, Dittmer WU, Mihajlović N, van Soest G, de Jong N, Frequency tuning of collapse-mode capacitive micromachined ultrasonic transducer, Ultrasonics. 74 (2017) 144–152. [PubMed: 27780034]

[274]. Sanchez N, Chen K, Chen C, McMahill D, Hwang S, Lutsky J, Yang J, Bao L, Chiu LK, Peyton G, An 8960-Element Ultrasound-on-Chip for Point-of-Care Ultrasound, 2021 IEEE Int. Solid-State Circuits Conf. ISSCC. 64 (n.d.) 480–482.

[275]. Shnaiderman R, Wissmeyer G, Ülgen O, Mustafa Q, Chmyrov A, Ntziachristos V, A submicrometre silicon-on-insulator resonator for ultrasound detection, Nature. 585 (2020) 372–378. [PubMed: 32939068]

[276]. Jiang Z, Dickinson RJ, Hall TL, Choi JJ, A PZT-PVDF Stacked Transducer for Short-pulse Ultrasound Therapy and Monitoring, IEEE Trans. Ultrason. Ferroelectr. Freq. Control (2021).

[277]. Matsumoto Y, Asao Y, Sekiguchi H, Yoshikawa A, Ishii T, Nagae K, Kobayashi S, Tsuge I, Saito S, Takada M, Ishida Y, Kataoka M, Sakurai T, Yagi T, Kabashima K, Suzuki S, Togashi K, Shiina T, Toi M, Visualising peripheral arterioles and venules through high-resolution and large-area photoacoustic imaging, Sci. Rep 8 (2018) 14930. 10.1038/s41598-018-33255-8. [PubMed: 30297721]

[278]. Nagae K, Asao Y, Sudo Y, Murayama N, Tanaka Y, Ohira K, Ishida Y, Otsuka A, Matsumoto Y, Saito S, Furu M, Murata K, Sekiguchi H, Kataoka M, Yoshikawa A, Ishii T, Togashi K, Shiina T, Kabashima K, Toi M, Yagi T, Real-time 3D Photoacoustic Visualization System with a Wide Field of View for Imaging Human Limbs, F1000Research. 7 (2018) 1813. 10.12688/f1000research.16743.2. [PubMed: 30854189]

[279]. Jain RK, Munn LL, Fukumura D, Dissecting tumour pathophysiology using intravital microscopy, Nat. Rev. Cancer. 2 (2002) 266–276. 10.1038/nrc778. [PubMed: 12001988]

[280]. Ellingson BM, Abrey LE, Nelson SJ, Kaufmann TJ, Garcia J, Chinot O, Saran F, Nishikawa R, Henriksson R, Mason WP, Wick W, Butowski N, Ligon KL, Gerstner ER, Colman H, de Groot J, Chang S, Mellinghoff I, Young RJ, Alexander BM, Colen R, Taylor JW, Arrillaga-Romany I, Mehta A, Huang RY, Pope WB, Reardon D, Batchelor T, Prados M, Galanis E,

Wen PY, Cloughesy TF, Validation of postoperative residual contrast-enhancing tumor volume as an independent prognostic factor for overall survival in newly diagnosed glioblastoma, Neuro-Oncol. 20 (2018) 1240–1250. 10.1093/neuonc/noy053. [PubMed: 29660006]

[281]. Chai W-Y, Chu P-C, Tsai M-Y, Lin Y-C, Wang J-J, Wei K-C, Wai Y-Y, Liu H-L, Magnetic-resonance imaging for kinetic analysis of permeability changes during focused ultrasound-induced blood-brain barrier opening and brain drug delivery, J. Controlled Release. 192 (2014) 1–9. 10.1016/j.jconrel.2014.06.023.

[282]. Turyanskaya A, Rauwolf M, Pichler V, Simon R, Burghammer M, Fox OJL, Sawhney K, Hofstaetter JG, Roschger A, Roschger P, Wobrauschek P, Streli C, Detection and imaging of gadolinium accumulation in human bone tissue by micro- and submicro-XRF, Sci. Rep 10 (2020) 6301. 10.1038/s41598-020-63325-9. [PubMed: 32286449]

[283]. Park J, Aryal M, Vykhodtseva N, Zhang Y-Z, McDannold N, Evaluation of permeability, doxorubicin delivery, and drug retention in a rat brain tumor model after ultrasound-induced blood-tumor barrier disruption, J. Controlled Release. 250 (2017) 77–85. 10.1016/j.jconrel.2016.10.011.

[284]. Leu K, Boxerman JL, Cloughesy TF, Lai A, Nghiemphu PL, Liau LM, Pope WB, Ellingson BM, Improved Leakage Correction for Single-Echo Dynamic Susceptibility Contrast Perfusion MRI Estimates of Relative Cerebral Blood Volume in High-Grade Gliomas by Accounting for Bidirectional Contrast Agent Exchange, Am. J. Neuroradiol 37 (2016) 1440–1446. 10.3174/ajnr.A4759. [PubMed: 27079371]

[285]. Chakhoyan A, Yao J, Leu K, Pope WB, Salamon N, Yong W, Lai A, Nghiemphu PL, Everson RG, Prins RM, Liau LM, Nathanson DA, Cloughesy TF, Ellingson BM, Validation of vessel size imaging (VSI) in high-grade human gliomas using magnetic resonance imaging, image-guided biopsies, and quantitative immunohistochemistry, Sci. Rep 9 (2019) 2846. 10.1038/s41598-018-37564-w. [PubMed: 30808879]

[286]. Miller MA, Gadde S, Pfirschke C, Engblom C, Sprachman MM, Kohler RH, Yang KS, Laughney AM, Wojtkiewicz G, Kamaly N, Bhonagiri S, Pittet M, Farokhzad OC, Weissleder R, Predicting therapeutic nanoparticle efficacy using a companion MR imaging nanoparticle, Sci. Transl. Med 7 (2015) 314ra183. 10.1126/scitranslmed.aac6522.

[287]. Gerstner ER, Emblem KE, Chang K, Vakulenko-Lagun B, Yen Y-F, Beers AL, Dietrich J, Plotkin SR, Catana C, Hooker JM, Duda DG, Rosen B, Kalpathy-Cramer J, Jain RK, Batchelor T, Bevacizumab Reduces Permeability and Concurrent Temozolomide Delivery in a Subset of Patients with Recurrent Glioblastoma, Clin. Cancer Res 26 (2020) 206–212. 10.1158/1078-0432.CCR-19-1739. [PubMed: 31558474]

[288]. Chakravarty R, Hong H, Cai W, Positron Emission Tomography Image-Guided Drug Delivery: Current Status and Future Perspectives, Mol. Pharm 11 (2014) 3777–3797. 10.1021/mp500173s. [PubMed: 24865108]

[289]. Sinharay S, Tu T-W, Kovacs ZI, Schreiber-Stainthorp W, Sundby M, Zhang X, Papadakis GZ, Reid WC, Frank JA, Hammoud DA, In vivo imaging of sterile microglial activation in rat brain after disrupting the blood-brain barrier with pulsed focused ultrasound: [18F]DPA-714 PET study, J. Neuroinflammation. 16 (2019) 155. 10.1186/s12974-019-1543-z. [PubMed: 31345243]

[290]. Vallet M, Varray F, Boutet J, Dinten J-M, Caliano G, Savoia AS, Vray D, Quantitative comparison of PZT and CMUT probes for photoacoustic imaging: Experimental validation, Photoacoustics. 8 (2017) 48–58. [PubMed: 29034168]

[291]. Oralkan O, Bayram B, Yaralioglu GG, Ergun AS, Kupnik M, Yeh DT, Wygant IO, Khuri-Yakub BT, Experimental characterization of collapse-mode CMUT operation, leee Trans. Ultrason. Ferroelectr. Freq. Control 53 (2006) 1513–1523.

[292]. Gurun G, Hasler P, Degertekin FL, Front-end receiver electronics for high-frequency monolithic CMUT-on-CMOS imaging arrays, IEEE Trans. Ultrason. Ferroelectr. Freq. Control 58 (2011) 1658–1668. [PubMed: 21859585]

[293]. Moussaoui G, Zakaria AS, Negrean C, Nguyen D-D, Couture F, Tholomier C, Sadri I, Arezki A, Schwartz RN, Elterman DS, Accuracy of Clarius, Handheld Wireless Point-of-Care Ultrasound, in Evaluating Prostate Morphology and Volume Compared to Radical Prostatectomy Specimen Weight: Is There a Difference between Transabdominal vs Transrectal Approach?, J. Endourol (2021).

[294]. Gu J, Jing Y, mSOUND: An Open Source Toolbox for Modeling Acoustic Wave Propagation in Heterogeneous Media, IEEE Trans. Ultrason. Ferroelectr. Freq. Control (2021) 1–1. 10.1109/TUFFC.2021.3051729.

[295]. Treeby BE, Cox BT, k-Wave: MATLAB toolbox for the simulation and reconstruction of photoacoustic wave fields, J. Biomed. Opt 15 (2010) 021314. 10.1117/1.3360308. [PubMed: 20459236]

[296]. Maimbourg G, Guilbert J, Bancel T, Houdouin A, Raybaud G, Tanter M, Aubry J-F, Computationally Efficient Transcranial Ultrasonic Focusing: Taking Advantage of the High Correlation Length of the Human Skull, IEEE Trans. Ultrason. Ferroelectr. Freq. Control 67 (2020) 1993–2002. 10.1109/TUFFC.2020.2993718. [PubMed: 32396081]

[297]. Leung SA, Moore D, Webb TD, Snell J, Ghanouni P, Butts Pauly K, Transcranial focused ultrasound phase correction using the hybrid angular spectrum method, Sci. Rep 11 (2021) 6532. 10.1038/s41598-021-85535-5. [PubMed: 33753771]

[298]. Top CB, A Generalized Split-Step Angular Spectrum Method for Efficient Simulation of Wave Propagation in Heterogeneous Media, IEEE Trans. Ultrason. Ferroelectr. Freq. Control (2021) 1–1. 10.1109/TUFFC.2021.3075367.

[299]. Jones RM, Huang Y, Meng Y, Scantlebury N, Schwartz ML, Lipsman N, Hynynen K, Echo-Focusing in Transcranial Focused Ultrasound Thalamotomy for Essential Tremor: A Feasibility Study, Mov. Disord 35 (2020) 2327–2333. 10.1002/mds.28226. [PubMed: 32815611]

[300]. Guasch L, Calderón Agudo O, Tang M-X, Nachev P, Warner M, Full-waveform inversion imaging of the human brain, Npj Digit. Med 3 (2020) 1–12. 10.1038/s41746-020-0240-8. [PubMed: 31934645]

[301]. Bianco MJ, Gerstoft P, Traer J, Ozanich E, Roch MA, Gannot S, Deledalle C-A, Machine learning in acoustics: Theory and applications, J. Acoust. Soc. Am 146 (2019) 3590–3628. 10.1121/1.5133944. [PubMed: 31795641]

[302]. Brattain LJ, Telfer BA, Dhyani M, Grajo JR, Samir AE, Machine learning for medical ultrasound: status, methods, and future opportunities, Abdom. Radiol 43 (2018) 786–799. 10.1007/s00261-018-1517-0.

[303]. Luijten B, Cohen R, de Bruijn FJ, Schmeitz HAW, Mischi M, Eldar YC, van Sloun RJG, Adaptive Ultrasound Beamforming Using Deep Learning, IEEE Trans. Med. Imaging. 39 (2020) 3967–3978. 10.1109/TMI.2020.3008537. [PubMed: 32746139]

[304]. Exner AA, Kolios MC, Bursting Microbubbles: How Nanobubble Contrast Agents Can Enable the Future of Medical Ultrasound Molecular Imaging and Image-Guided Therapy, Curr. Opin. Colloid Interface Sci (2021) 101463. 10.1016/j.cocis.2021.101463. [PubMed: 34393610]

[305]. Sheeran PS, Luois S, Dayton PA, Matsunaga TO, Formulation and Acoustic Studies of a New Phase-Shift Agent for Diagnostic and Therapeutic Ultrasound, Langmuir ACS J. Surf. Colloids 27 (2011) 10412–10420. 10.1021/la2013705.

[306]. Sheeran PS, Dayton PA, Phase-change contrast agents for imaging and therapy, Curr. Pharm. Des 18 (2012) 2152–2165. 10.2174/138161212800099883. [PubMed: 22352770]

[307]. Mountford PA, Thomas AN, Borden MA, Thermal activation of superheated lipid-coated perfluorocarbon drops, Langmuir ACS J. Surf. Colloids. 31 (2015) 4627–4634. 10.1021/acs.langmuir.5b00399.

[308]. Åslund AKO, Berg S, Hak S, Mørch Ý, Torp SH, Sandvig A, Widerøe M, Hansen R, de Lange Davies C, Nanoparticle delivery to the brain — By focused ultrasound and self-assembled nanoparticle-stabilized microbubbles, J. Controlled Release. 220 (2015) 287–294. 10.1016/j.jconrel.2015.10.047.

[309]. Burke CW, Alexander E, Timbie K, Kilbanov AL, Price RJ, Ultrasound-activated Agents Comprised of 5FU-bearing Nanoparticles Bonded to Microbubbles Inhibit Solid Tumor Growth and Improve Survival, Mol. Ther 22 (2014) 321–328. 10.1038/mt.2013.259. [PubMed: 24172867]

[310]. Maresca D, Lakshmanan A, Lee-Gosselin A, Melis JM, Ni Y-L, Bourdeau RW, Kochmann DM, Shapiro MG, Nonlinear ultrasound imaging of nanoscale acoustic biomolecules, Appl. Phys. Lett 110 (2017) 073704. 10.1063/1.4976105. [PubMed: 28289314]

[311]. Cherin E, Melis JM, Bourdeau RW, Yin M, Kochmann DM, Foster FS, Shapiro MG, Acoustic Behavior of Halobacterium salinarum Gas Vesicles in the High-Frequency Range: Experiments and Modeling, Ultrasound Med. Biol 43 (2017) 1016–1030. 10.1016/j.ultrasmedbio.2016.12.020. [PubMed: 28258771]

[312]. Farhadi A, Ho GH, Sawyer DP, Bourdeau RW, Shapiro MG, Ultrasound imaging of gene expression in mammalian cells, Science. 365 (2019) 1469–1475. 10.1126/science.aax4804. [PubMed: 31604277]

[313]. Thorne RG, Nicholson C, In vivo diffusion analysis with quantum dots and dextrans predicts the width of brain extracellular space, Proc. Natl. Acad. Sci. U. S. A 103 (2006) 5567–5572. 10.1073/pnas.0509425103. [PubMed: 16567637]

[314]. Quail DF, Joyce JA, The Microenvironmental Landscape of Brain Tumors, Cancer Cell. 31 (2017) 326–341. 10.1016/j.ccell.2017.02.009. [PubMed: 28292436]

[315]. Lim M, Xia Y, Bettegowda C, Weller M, Current state of immunotherapy for glioblastoma, Nat. Rev. Clin. Oncol 15 (2018) 422–442. 10.1038/s41571-018-0003-5. [PubMed: 29643471]

[316]. Kovacs ZI, Kim S, Jikaria N, Qureshi F, Milo B, Lewis BK, Bresler M, Burks SR, Frank JA, Disrupting the blood–brain barrier by focused ultrasound induces sterile inflammation, Proc. Natl. Acad. Sci. U. S. A 114 (2017) E75–E84. 10.1073/pnas.1614777114. [PubMed: 27994152]

[317]. McCabe JT, Moratz C, Liu Y, Burton E, Morgan A, Budinich C, Lowe D, Rosenberger J, Chen H, Liu J, Myers M, Application of High-Intensity Focused Ultrasound to the Study of Mild Traumatic Brain Injury, Ultrasound Med. Biol 40 (2014) 965–978. 10.1016/j.ultrasmedbio.2013.11.023. [PubMed: 24462152]

[318]. Morse SV, Boltersdorf T, Harriss BI, Chan TG, Baxan N, Jung HS, Pouliopoulos AN, Choi JJ, Long NJ, Neuron labeling with rhodamine-conjugated Gd-based MRI contrast agents delivered to the brain via focused ultrasound, Theranostics. 10 (2020) 2659–2674. 10.7150/thno.42665. [PubMed: 32194827]

[319]. Venkataramani V, Tanev DI, Strahle C, Studier-Fischer A, Fankhauser L, Kessler T, Körber C, Kardorff M, Ratliff M, Xie R, Horstmann H, Messer M, Paik SP, Knabbe J, Sahm F, Kurz FT, Acikgöz AA, Herrmannsdörfer F, Agarwal A, Bergles DE, Chalmers A, Miletic H, Turcan S, Mawrin C, Hänggi D, Liu H-K, Wick W, Winkler F, Kuner T, Glutamatergic synaptic input to glioma cells drives brain tumour progression, Nature. 573 (2019) 532–538. 10.1038/s41586-019-1564-x. [PubMed: 31534219]

[320]. Venkatesh HS, Morishita W, Geraghty AC, Silverbush D, Gillespie SM, Arzt M, Tam LT, Espenel C, Ponnuswami A, Ni L, Woo PJ, Taylor KR, Agarwal A, Regev A, Brang D, Vogel H, Hervey-Jumper S, Bergles DE, Suvà ML, Malenka RC, Monje M, Electrical and synaptic integration of glioma into neural circuits, Nature. 573 (2019) 539–545. 10.1038/s41586-019-1563-y. [PubMed: 31534222]

[321]. Ransohoff RM, Perry VH, Microglial Physiology: Unique Stimuli, Specialized Responses, Annu. Rev. Immunol 27 (2009) 119–145. 10.1146/annurev.immunol.021908.132528. [PubMed: 19302036]

[322]. Poon C, Pellow C, Hynynen K, Neutrophil recruitment and leukocyte response following focused ultrasound and microbubble mediated blood-brain barrier treatments, Theranostics. 11 (2021) 1655–1671. 10.7150/thno.52710. [PubMed: 33408773]

[323]. Todd N, Angolano C, Ferran C, Devor A, Borsook D, McDannold N, Secondary effects on brain physiology caused by focused ultrasound-mediated disruption of the blood–brain barrier, J. Controlled Release. 324 (2020) 450–459. 10.1016/j.jconrel.2020.05.040.

[324]. Curley CT, Stevens AD, Mathew AS, Stasiak K, Garrison WJ, Miller GW, Sheybani ND, Engelhard VH, Bullock TNJ, Price RJ, Immunomodulation of intracranial melanoma in response to blood-tumor barrier opening with focused ultrasound, Theranostics. 10 (2020) 8821–8833. 10.7150/thno.47983. [PubMed: 32754281]

[325]. Kovacs ZI, Burks SR, Frank JA, Focused ultrasound with microbubbles induces sterile inflammatory response proportional to the blood brain barrier opening: Attention to experimental conditions, Theranostics. 8 (2018) 2245–2248. 10.7150/thno.24181. [PubMed: 29722362]

[326]. Meng Y, Pople CB, Suppiah S, Llinas M, Huang Y, Sahgal A, Perry J, Keith J, Davidson B, Hamani C, Amemiya Y, Seth A, Leong H, Heyn CC, Aubert I, Hynynen K, Lipsman N,

MR-guided focused ultrasound liquid biopsy enriches circulating biomarkers in patients with brain tumors, Neuro-Oncol. (2021). 10.1093/neuonc/noab057.

[327]. Kanvinde PP, Malla AP, Connolly NP, Szulzewsky F, Anastasiadis P, Ames HM, Kim AJ, Winkles JA, Holland EC, Woodworth GF, Leveraging the replication-competent avian-like sarcoma virus/tumor virus receptor-A system for modeling human gliomas, Glia. n/a (n.d.). 10.1002/glia.23984.

[328]. Dewhirst MW, Lee C-T, Ashcraft KA, The future of biology in driving the field of hyperthermia, Int. J. Hyperthermia. 32 (2016) 4–13. 10.3109/02656736.2015.1091093. [PubMed: 26850697]

[329]. Dewey WC, Hopwood LE, Sapareto SA, Gerweck LE, Cellular Responses to Combinations of Hyperthermia and Radiation, Radiology. 123 (1977)463–474. 10.1148/123.2.463. [PubMed: 322205]

[330]. Sneed PK, Stauffer PR, McDermott MW, Diederich CJ, Lamborn KR, Prados MD, Chang S, Weaver KA, Spry L, Malec MK, Lamb SA, Voss B, Davis RL, Wara WM, Larson DA, Phillips TL, Gutin PH, Survival benefit of hyperthermia in a prospective randomized trial of brachytherapy boost ± hyperthermia for glioblastoma multiforme, Int. J. Radiat. Oncol 40 (1998) 287–295. 10.1016/S0360-3016(97)00731-1.

[331]. Kim C, Guo Y, Velalopoulou A, Leisen J, Motamarry A, Ramajayam K, Aryal M, Haemmerich D, Arvanitis CD, Closed-loop trans-skull ultrasound hyperthermia leads to improved drug delivery from thermosensitive drugs and promotes changes in vascular transport dynamics in brain tumors, Theranostics. 11 (2021) 7276–7293. 10.7150/thno.54630. [PubMed: 34158850]

[332]. Gamboa L, Zamat AH, Kwong GA, Synthetic immunity by remote control, Theranostics. 10 (2020) 3652–3667. 10.7150/thno.41305. [PubMed: 32206114]

[333]. Wu Y, Liu Y, Huang Z, Wang X, Jin Z, Li J, Limsakul P, Zhu L, Allen M, Pan Y, Bussell R, Jacobson A, Liu T, Chien S, Wang Y, Control of the activity of CAR-T cells within tumours via focused ultrasound, Nat. Biomed. Eng (2021) 1–12. 10.1038/s41551-021-00779-w. [PubMed: 33483712]

[334]. Zhu L, Cheng G, Ye D, Nazeri A, Yue Y, Liu W, Wang X, Dunn GP, Petti AA, Leuthardt EC, Chen H, Focused Ultrasound-enabled Brain Tumor Liquid Biopsy, Sci. Rep 8 (2018) 6553. 10.1038/s41598-018-24516-7. [PubMed: 29700310]

[335]. Pacia CP, Zhu L, Yang Y, Yue Y, Nazeri A, Michael Gach H, Talcott MR, Leuthardt EC, Chen H, Feasibility and safety of focused ultrasound-enabled liquid biopsy in the brain of a porcine model, Sci. Rep 10 (2020) 7449. 10.1038/s41598-020-64440-3. [PubMed: 32366915]

[336]. Bettegowda C, Sausen M, Leary RJ, Kinde I, Wang Y, Agrawal N, Bartlett BR, Wang H, Luber B, Alani RM, Antonarakis ES, Azad NS, Bardelli A, Brem H, Cameron JL, Lee CC, Fecher LA, Gallia GL, Gibbs P, Le D, Giuntoli RL, Goggins M, Hogarty MD, Holdhoff M, Hong S-M, Jiao Y, Juhl HH, Kim JJ, Siravegna G, Laheru DA, Lauricella C, Lim M, Lipson EJ, Marie SKN, Netto GJ, Oliner KS, Olivi A, Olsson L, Riggins GJ, Sartore-Bianchi A, Schmidt K, Shih le-M., Oba-Shinjo SM, Siena S, Theodorescu D, Tie J, Harkins TT, Veronese S, Wang T-L, Weingart JD, Wolfgang CL, Wood LD, Xing D, Hruban RH, Wu J, Allen PJ, Schmidt CM, Choti MA, Velculescu VE, Kinzler KW, Vogelstein B, Papadopoulos N, Diaz LA, Detection of Circulating Tumor DNA in Early- and Late-Stage Human Malignancies, Sci. Transl. Med 6 (2014) 224ra24–224ra24. 10.1126/scitranslmed.3007094.

[337]. Nhan T, Burgess A, Lilge L, Hynynen K, Modeling localized delivery of Doxorubicin to the brain following focused ultrasound enhanced blood-brain barrier permeability, Phys. Med. Biol 59 (2014) 5987. 10.1088/0031-9155/59/20/5987. [PubMed: 25230100]

[338]. Hosseinkhah N, Goertz DE, Hynynen K, Microbubbles and Blood #x2013;Brain Barrier Opening: A Numerical Study on Acoustic Emissions and Wall Stress Predictions, IEEE Trans. Biomed. Eng 62 (2015) 1293–1304. 10.1109/TBME.2014.2385651. [PubMed: 25546853]

[339]. Khodabakhshi Z, Hosseinkhah N, Ghadiri H, Pulsating Microbubble in a Micro-vessel and Mechanical Effect on Vessel Wall: A Simulation Study, J. Biomed. Phys. Eng 0 (2020). https://jbpe.sums.ac.ir/article_46519.html (accessed May 30, 2021).

Box:

Key definitions

Neurovascular Unit is the specialized complex of blood vessel and brain cells which together create the blood brain barrier

Blood Brain Barrier represents the unique interface between the blood stream and the central nervous system that limits and controls the influx and efflux of most substances, particulates, and cells.

Diffusive Transport is the net movement of molecules from a region of higher concentration to a region of lower concentration.

Convective Transport is mass transport mediated by bulk fluid flow that is driven by a pressure gradient.

Cavitation, in the field of enhanced therapy, refers to the oscillations and dynamic behavior of stabilized microbubbles. Note its use in this context differs from the phenomena of nucleated cavitation (i.e., the creation of holes in the fluid due to large negative pressures) employed, e.g., for histotripsy.

Mechanical Index is a parameter to defined as the peak negative pressure in megapascals, divided by the square root of frequency in megahertz ($MI = P_{-}/\sqrt{f}$).

Stable Cavitation refers to the small-amplitude vibrations of MBs, which radiate harmonic, ultraharmonic, and subharmonic acoustic emissions.

Inertial Cavitation is the transient collapse of the MBs, giving rise to impulsive (broadband) acoustic emissions.

Passive Cavitation Detection is the recording of MB emissions with one or several elements to detect the occurrence of acoustic cavitation and discern its nature.

Passive Cavitation Mapping is use of a registered array of PCD elements and beamforming to detect, localize, and characterize the occurrence and nature of acoustic cavitation.

Static Law Controllers have control laws that are predetermined prior to any measurement of the system's output.

Dynamic Law Controllers have control laws that depend on the measured output of the system.

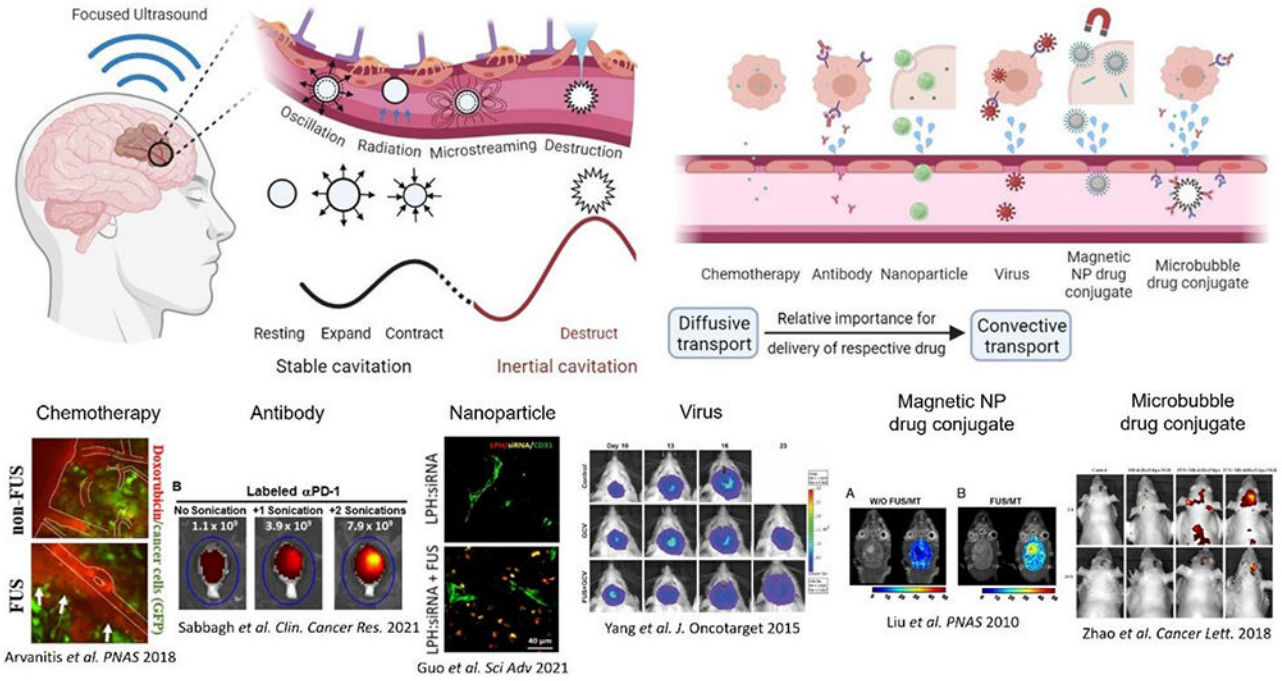

Figure 1:

Circulating microbubble contrast agents are excited by transcranial focused ultrasound. The resulting oscillations give rise to various mechanical effects including microstreaming, radiation forces, and destruction via shockwaves and jetting during bubble collapse. Such effects alter the permeability of the blood brain barrier and enable more convective transport of larger therapeutic agents.

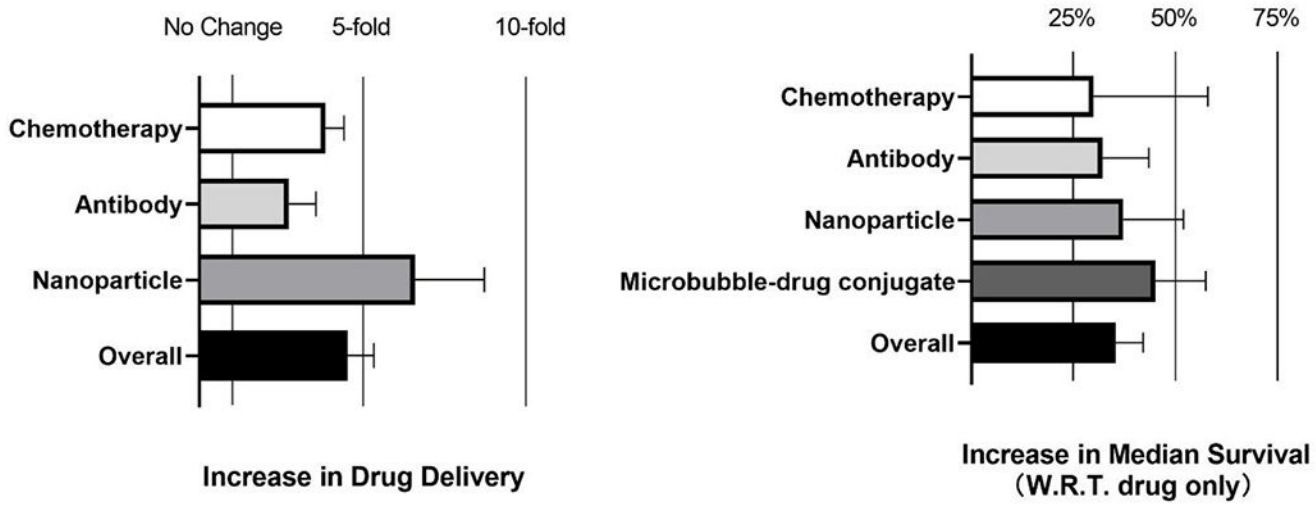

Figure 2.

Analysis of increase in drug delivery (left) and percentage increase in median survival time (IST) (right) after MB-FUS delivery of anticancer agents in murine brain tumor models. Reported increase is with respect to drug only group. All data and citations used to create the plots are provided in Suppl. Table 1.

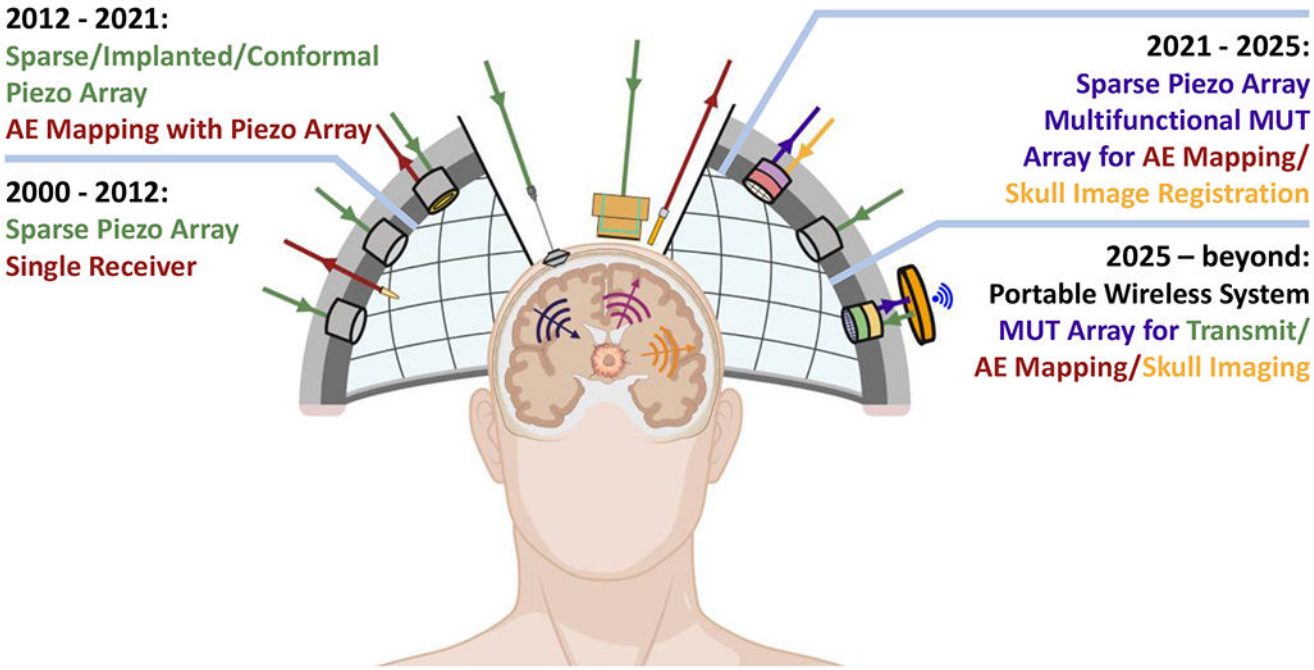

Figure 3.

Evolution of FUS and emissions monitoring transducer technology and potential future implementations. Color Coding: Green: Incident ultrasound, Red: Recorded acoustic emissions (AE), Gold: Skull imaging with ultrasound, Purple: Recorded AE and skull imaging with the same transducer.

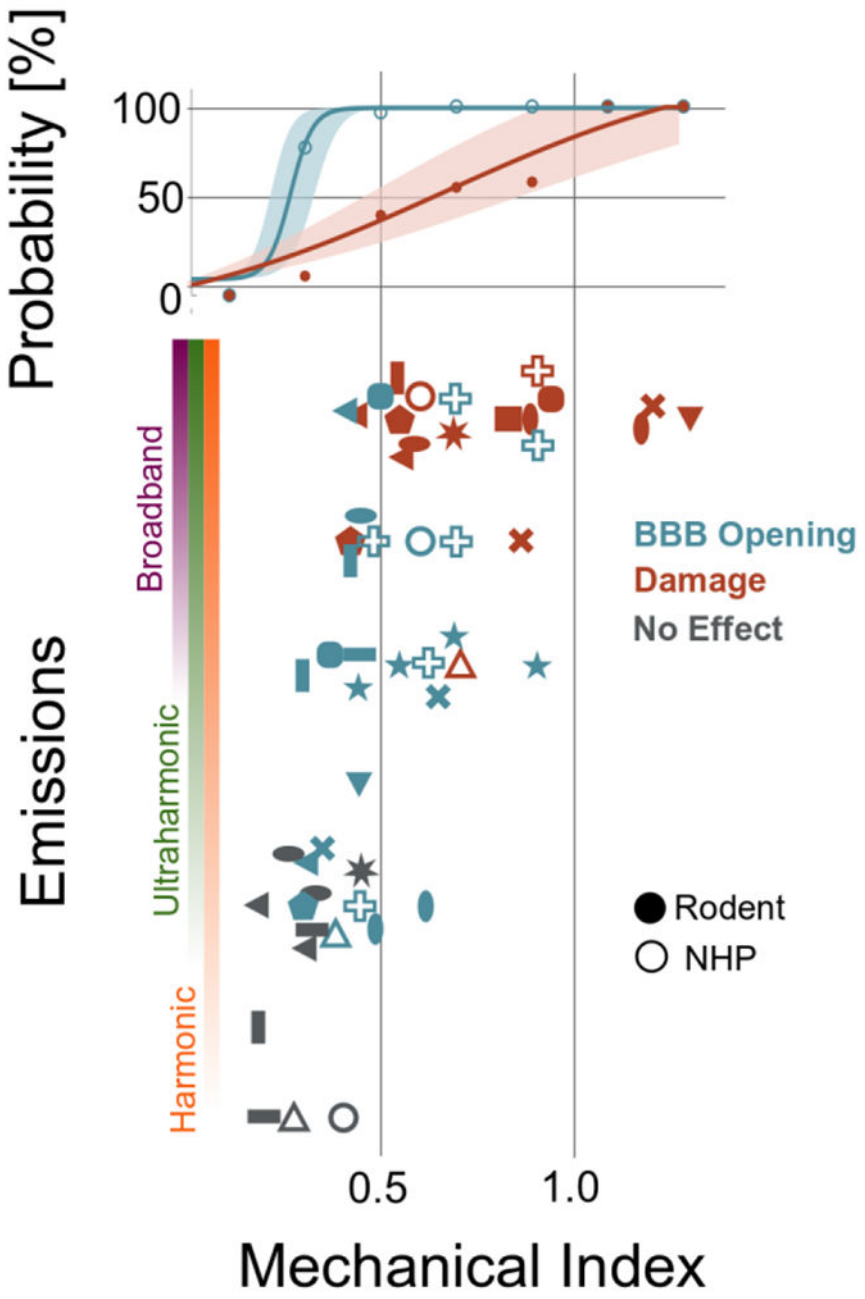

Figure 4.

Emissions and bioeffects reported during MB-FUS for BBB opening. Vertical axis quantifies the type of emissions observed at the given mechanical index (horizontal axis). Blue markers indicate BBB-opening while orange indicate observed tissue damage; the colored bars indicate the probability of no effect, BBB opening, and damage among the studies at that particular MI. Solid markers represent measurements for rodents (mouse, rat, or rabbit) while hollow markers indicate non-human primate studies. Full data provided in Suppl. Table 2.

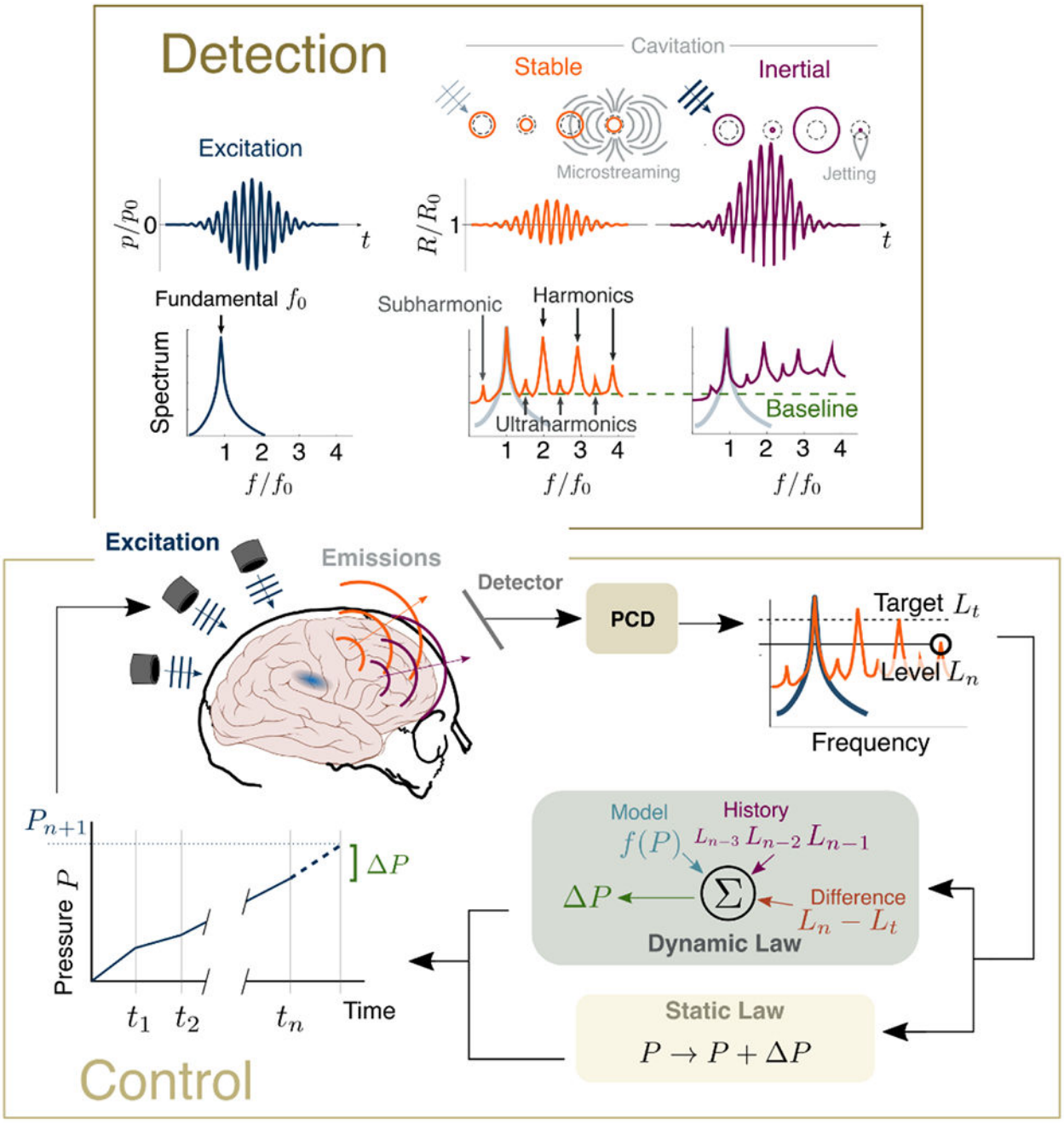

Figure 5.

Detection and control of cavitation. (Top) The therapeutic ultrasound pulse has fundamental frequency f_0. The circulating microbubbles are excited and undergo stable oscillations (inducing microstreaming and radiating harmonic, ultraharmonic, and subharmonic emissions) or, at higher applied pressure magnitudes, transient inertial cavitation (resulting in jetting and broadband emissions). (Bottom) These emissions can be monitored by a

passive detector, which adjusts the applied pressure P based on the type and level L of these emissions relative to a target.

Table 1.

Summary of studies reporting MB-FUS delivery of anticancer agents in murine brain tumor models.

	Type	Therapeutic agent	Tumor model [a]
Diffusive transport	Chemotherapy (194–590 Da)	Doxorubicin	GL261 glioma[64], SMA-560 glioma[64], 9L Gliosarcoma[65], SU-DIPG-17 (PDX) [b] [66], Human HER2$^+$ BT474 breast metastasis[43]
		BCNU	C6 Glioma[67]
		Temozolomide	9L Gliosarcoma[68,69], U87 glioma[70]
		Carboplatin	F98 glioma[42], U87 glioma[71], 6240 PDX glioma[71]
		Irinotecan	F98 glioma[72]
		Etoposide	MGPP3 glioma[73], High-grade glioma (DIPG)[74]
	Antibody (Ab) (75–148 kDa)	Trastuzumab (Herceptin)	Human HER2$^+$ BT474[75]
		Trastuzumab Emtansine	Human HER2$^+$ BT474[43]
		Pertuzumab	Human MDA-MB-361[49]
		Interleukin-12	C6 glioma[76]
		Bevacizumab	U87 glioma[77]
		IgG2a	High-grade glioma (PDX) [b] [78]
		Anti-mCD47	GL261 glioma[50]
		Anti-PD-1	GL261 glioma[79]
Convective transport	Nanoparticle (NP) drug conjugate (7 – 130 nm)	Liposomal (anionic) NP (Doxorubicin[55,56,80–85], Paclitaxel[86]) [c]	9L Gliosarcoma[55,80,83,84], glioma 8401[81,82,85], U87 glioma[86], F98 glioma [56]
		Brain-Penetrating (anionic) NPs (Cisplatin[57], DNA[54])	9L Gliosarcoma[57], F98 glioma[57], U87 glioma[54], B16F1 melanoma[54]
		Cilengitide NP (Peptide)	C6 glioma[87]
		Gold NPs (αEGFR-SERS440[88], cisplatin[89])	9L Gliosarcoma[88], U251 glioma[89]
		Albumin-bound paclitaxel	MES83[90], GBM12[90], 6240 PDXs [b] [90]
		Folate-conjugated polymersomal (Doxorubicin)	C6 glioma[91]
		Mesoporous organosilica NPs (Doxorubicin)	U87 glioma[92]
		Hybrid polymer liposomes (cationic) NPs (siRNA)[58]	GL261 glioma[58], SMO-medulloblastoma[58]
External forces	Magnetic NP drug conjugate [d] (10-40 nm)	BCNU[61]	C6 glioma[61–63]
		Epirubicin[62]	
		Doxorubicin (SPIO)[63]	
	Microbubble drug conjugate (1-2 μm)	BCNU[93]	C6 glioma[93–97]
		VEGFR2-BCNU[94]	
		Doxorubicin (SPIO)[97]	
		shRNA[95]	

	Type	Therapeutic agent	Tumor model [a]
		poly(2-ethyl-butyl cyanoacrylate) (PEBCA)[96]	
		LPHNs-cRGD-CRISPR/Cas9 plasmids	T98G glioma[98]
	Virus (120 – 260 nm)	Herpes Virus (HSV1)	F98[99] and C6 glioma[100]

Table 2.

Completed and ongoing MB-FUS clinical trials in brain tumor patients.

Tumor type	Drug/Molecule	FUS Device	Phase	ClinicalTrials.gov Identifier
Low Grade Glioma	MR-Contrast Agent	Brainsonix	N/A	NCT04063514 (Pending)
GBM	MR-Contrast Agent	ExAblate	N/A	NCT03322813 (Completed)
Brain Tumor	Doxorubicin	ExAblate	N/A	NCT02343991 (Active)
GBM	Fluorescein	ExAblate	N/A	NCT04667715 (Enrolling)
GBM	Temozolomide	ExAblate	N/A	NCT03551249 (Enrolling)
GBM	Temozolomide / Lipodox	ExAblate	N/A	NCT03616860 (Enrolling)
GBM	Temozolomide	ExAblate	N/A	NCT03712293 (Enrolling)
Recurrent GBM	Carboplatin	ExAblate	I/II	NCT04417088 (Enrolling)
Recurrent GBM	Carboplatin	SonoCloud	I/II	NCT02253212 (Completed)
Recurrent GBM	Carboplatin	SonoCloud	I/II	NCT03744026 (Enrolling)
Recurrent GBM	Abraxane	SonoCloud	I/II	NCT04528680 (Enrolling)
GBM	Temozolomide	SonoCloud	II	NCT04614493 (Enrolling)
Recurrent GBM	MR-Contrast Agent	NaviFUS	N/A	NCT03626896 (Completed)
Recurrent GBM	Avastin	NaviFUS	N/A	NCT04446416 (Enrolling)
Breast Brain Met.	Trastuzumab	ExAblate	N/A	NCT03714243 (Enrolling)
Melanoma Brain Met.	Nivolumab / ipilimumab	SonoCloud	I/II	NCT04021420 (Enrolling)
DIPG	Panobinostat	FUS-Navigator	I	NCT04804709 (Pending)

Table 3:

Therapeutic US systems for treating brain tumors.

System	Targeting precision	Aberration Correction	Beam Steering	Cost	Clinic	Advantages, Challenges & Limitations
MRgFUS (ExAblate) [147]	Excellent (<1 mm)	★★★	★★★	$$$	Yes	Unique capabilities for treatment guidance and monitoring. Requires MRI and it is not portable.
Neuro-navigation FUS (NaviFUS and FUS neuro-navigator) [148,149]	Fair (2.3 ± 0.9 mm)	★★☆	★★☆	$$	Yes	Exploits existing neuro-surgery workflow. Portable. It can be challenging to maintain the registration during the treatment.
USgFUS [138]	Not assessed	Not assessed	Not assessed	N/A	No	Potentially high-performance system. Registration errors, aberration correction and beam steering capabilities need rigorous assessment.
US Implant (SonoCloud) [139]	Good	None	★☆☆	$	Yes	Extremely simple and portable system. Invasive (requires surgery); no treatment guidance or monitoring is currently available.
Acoustic lens US system [140,150]	Good (≈1 mm)	★★★	None	$	No	Simple system that could account for aberration. Requires precise positioning of the lens/US system. Potentially useful only for low power applications
US Conformal System [151]	Good	★★☆	★★☆	$$$	No	Adapts to patient head. Rigid system, registration issues might limit performance
Mode Conversion [152,153]	Not assessed	★★☆	Not assessed	-	No	At proof-of-concept stage.

Table 4.

Properties of commercial contrast agents used in MB-FUS delivery of anticancer agents in murine brain tumor models.

Name	Shell	Core	Diameter [μm]	Surface charge [mV]	Half-life [min]	Mechanical properties	Citation
Definity	lipid	C_3F_8	1.1-3.3	−1 ~ −4	6.88 ± 4.88	Resonance Frequency: 2-6 MHz Shell elasticity: 0.38 N/m	[180–186]
SonoVue/ Lumason	lipid	SF_6	2.5	−28.3	1.04 ± 0.15	Resonance Frequency: 1.5-2 MHz Shell elasticity: 0.2-0.3 N/m	[185–188]
Optison	protein	C_3F_8	3-4.5	−10 ~ −25	1.3 ± 0.69	Resonance Frequency: 1.5-4 MHz Shell elasticity: 0.9 N/m Destruction threshold 0.3 MPa	[180,186, 189–194]
BR-38 (BG6895)	lipid	C_4F_{10}	1.4	neutral	-	Resonance Frequency: 4 MHz	[195,196]
USphere	lipid	C_3F_8	0.85	cationic	4.98 ± 0.83	-	[185]
Sonazoid	lipid	C_4F_{10}	2.6	−76 ~ −82	0.67 ± 0.33	Resonance Frequency: 4-6 MHz Shell elasticity: 0.6 N/m	[197,198]

Table 5.

Overview of methods for passive acoustic monitoring of cavitation activity

Method		Sensitivity	Reliability	Complexity	Challenges and Limitations
Single Detector		Medium	Low	Very Low	Does not provide spatial information.
Passive Mapping	Time Domain	High	Very High	High	Large number of required computations.
	Freq. Domain	Very High	Medium	Low	Has not been extended to account for aberration
	Angular Spectrum	Very High	High	Very Low	Restrictive receiver geometry

Table 6 –

Transducer Technologies for Acoustic Emissions Monitoring

Type	Advantages	Challenges and limitations	Key Citations
Piezoelectric Ceramic	• High sensitivity • Already used as FUS transmitter	• Narrow bandwidth • Difficult to integrate with electronics for dense arrays	[15,154–156,230,265,266]
Piezoelectric Thin Film Polymer	• Broad bandwidth • Can be integrated with piezoelectric ceramic transmitters	• Low sensitivity • Difficult to integrate with electronics for dense arrays for mapping acoustic emissions	[252,264]
Micromachined Piezoelectric on Silicon (PMUT)	• Ease of electronics integration for dense arrays for mapping acoustic emissions and aberration correction	• Narrow bandwidth • Low pressure output as potential transmitter	[267,268]
Micromachined Capacitive on Silicon (CMUT)	• Broad and tunable bandwidth • Ability to build dense arrays • Potential for use as transmitter	• Requires integrated electronics • Inherent nonlinearity can impact MB detection	[269–274]
Acousto-optical FiberReadout	• Broadest bandwidth • High sensitivity	• Complex detection and array setup • At proof-of-concept stage	[275]